

# ornl

OAK  
RIDGE  
NATIONAL  
LABORATORY

UNION  
CARBIDE

OPERATED BY  
UNION CARBIDE CORPORATION  
FOR THE UNITED STATES  
DEPARTMENT OF ENERGY

MARTIN MARIETTA ENERGY SYSTEMS LIBRARIES



3 4456 0050052 6

NUREG/CR-0722  
(ORNL/NUREG/TM-287/R2)

## Fission Product Release from Highly Irradiated LWR Fuel

R. A. Lorenz  
J. L. Collins  
A. P. Malinauskas  
O. L. Kirkland  
R. L. Towns

OAK RIDGE NATIONAL LABORATORY

CENTRAL RESEARCH LIBRARY

CIRCULATION SECTION

4500N ROOM 175

**LIBRARY LOAN COPY**

DO NOT TRANSFER TO ANOTHER PERSON

If you wish someone else to see this  
report, send in name with report and  
the library will arrange a loan.

UCN-7969 (3-9-77)

Prepared for the U.S. Nuclear Regulatory Commission  
Office of Nuclear Regulatory Research  
Under Interagency Agreements DOE 40-551-75 and 40-552-75

Printed in the United States of America. Available from  
National Technical Information Service  
U.S. Department of Commerce  
5285 Port Royal Road, Springfield, Virginia 22161

This report was prepared as an account of work sponsored by an agency of the United States Government. Neither the United States Government nor any agency thereof, nor any of their employees, makes any warranty, express or implied, or assumes any legal liability or responsibility for the accuracy, completeness, or usefulness of any information, apparatus, product, or process disclosed, or represents that its use would not infringe privately owned rights. Reference herein to any specific commercial product, process, or service by trade name, trademark, manufacturer, or otherwise, does not necessarily constitute or imply its endorsement, recommendation, or favoring by the United States Government or any agency thereof. The views and opinions of authors expressed herein do not necessarily state or reflect those of the United States Government or any agency thereof.

NUREG/CR-0722  
ORNL/NUREG/TM-287/R2  
Dist. Category R3

Contract No. W-7405-eng-26

CHEMICAL TECHNOLOGY DIVISION

FISSION PRODUCT RELEASE FROM HIGHLY IRRADIATED LWR FUEL

R. A. Lorenz  
J. L. Collins  
A. P. Malinauskas  
O. L. Kirkland  
R. L. Towns

Manuscript Completed: June 1979

Date Published: February 1980

Prepared for the  
U.S. Nuclear Regulatory Commission  
Office of Nuclear Regulatory Research  
Washington, D.C. 20555  
Under Interagency Agreements 40-551-75 and 40-552-75  
NRC FIN No. B0127

Prepared by the  
OAK RIDGE NATIONAL LABORATORY  
Oak Ridge, Tennessee 37830  
operated by  
UNION CARBIDE CORPORATION  
for the  
DEPARTMENT OF ENERGY



3 4456 0050052 6

## CONTENTS

	<u>Page</u>
ABSTRACT .....	1
1. INTRODUCTION .....	1
2. FUEL FOR THE HIGH BURNUP FUEL TEST SERIES .....	2
2.1 Description of H. B. Robinson Fuel .....	2
2.2 Description of Fuel-Rod Test Segments .....	3
2.2.1 Marking and sectioning .....	3
2.2.2 Packaging and shipping .....	6
2.3 Fission Product Inventory .....	7
2.4 Fission Gas Release While in the Robinson Reactor .....	7
3. EXPERIMENTAL APPARATUS AND EQUIPMENT .....	13
4. RESULTS OF HIGH BURNUP FUEL TESTS .....	18
4.1 High Burnup Fuel Test 1 (700°C) .....	18
4.2 High Burnup Fuel Test 2 (900°C) .....	22
4.3 High Burnup Fuel Test 4 (500°C) .....	26
4.4 High Burnup Fuel Test 5 (500°C, Dry air).....	30
4.5 High Burnup Fuel Test 6 (700°C, Dry air).....	38
4.6 High Burnup Fuel Test 7 (900°C) .....	48
4.7 High Burnup Fuel Test 8 (900°C) .....	54
4.8 High Burnup Fuel Test 9 (900 to 1100°C) .....	63
4.9 High Burnup Fuel Test 10 (900 to 1200°C) .....	73
4.10 High Burnup Fuel Test 11 (1200°C) .....	80
4.11 High Burnup Fuel Test 12 (Gap Purge Test).....	90
4.11.1 Experimental results .....	90
4.11.2 Diffusion of cesium from the UO <sub>2</sub> pellet matrix ....	96
4.12 Summary of Release Data .....	100
4.12.1 Cesium, iodine, antimony, and ruthenium release in steam .....	102
4.12.2 Cesium, iodine, and ruthenium releases in dry air compared with those obtained in steam .....	104
4.12.3 Fuel particles ejected at time of rupture .....	105
4.12.4 Fission gas release .....	106



	<u>Page</u>
5. DISCUSSION OF FACTORS AFFECTING FISSION PRODUCT RELEASE .....	107
5.1 Chemical Behavior of Releasable Fission Products .....	107
5.1.1 Behavior of iodine .....	109
5.1.2 Behavior of cesium .....	113
5.1.3 Behavior of ruthenium .....	116
5.1.4 Behavior of antimony .....	120
5.2 Hydrogen Formation and Removal of Oxidizing Contaminants by Steam-Zircaloy Reaction .....	122
5.3 Discussion of Blowdown (Burst) Release .....	124
5.3.1 Mechanism of release .....	124
5.3.2 Concentration of cesium and iodine in the vented gas .....	125
5.3.3 Effect of gap inventory on burst release .....	127
5.3.4 Effect of temperature on burst release .....	128
5.3.5 Rupture characteristics and the rate of blowdown .....	128
5.3.6 Size of hole formed at rupture .....	131
5.3.7 Amount of cladding expansion (ballooning) .....	132
5.4 Discussion of Diffusional Release from the Gap Space .....	132
5.4.1 Effect of gap width .....	132
5.4.2 Effect of hole size .....	133
5.4.3 Effect of gap inventory .....	133
5.4.4 Effect of fuel rod length .....	134
5.4.5 Effect of fragmented cladding .....	134
6. CONCLUSIONS .....	134
7. APPENDIXES .....	139
7.1 Appendix A. Gap Size Measurements for High Burnup Fuel Test Series .....	141
7.2 Appendix B. Low Burnup Fuel Test Results and Comparison with Similar HBU Tests .....	144
7.3 Appendix C. Examination of Fuel Particles Ejected from Ruptured Rods .....	152
8. ACKNOWLEDGMENTS.....	155
9. REFERENCES.....	156

FISSION PRODUCT RELEASE FROM HIGHLY IRRADIATED LWR FUEL

R. A. Lorenz  
J. L. Collins  
A. P. Malinauskas  
O. L. Kirkland  
R. L. Towns

## ABSTRACT

A series of experiments was conducted with highly irradiated light-water reactor fuel rod segments to investigate fission products released in steam in the temperature range 500 to 1200°C. (Two additional release tests were conducted in dry air.) The primary objectives were to quantify and characterize fission product release under conditions postulated for a spent-fuel transportation accident and for a successfully terminated loss-of-coolant accident (LOCA). In simulated, controlled LOCA-type tests, release at the time of rupture proved to be more significant than the diffusional release that followed. Comparison of the release data for the dry-air tests with the release data of similarly conducted tests in steam indicated significant increases in the releases of iodine, ruthenium, and cesium in air. Diffusional releases of cesium and iodine from low burnup (~1000 MWd/MT) fuel irradiated at high-heat ratings (17 to 20 kW/ft) were larger than those obtained from high burnup (~30,000 MWd/MT) fuel irradiated at low-heat ratings (6 to 10 kW/ft). By purging the "gap" space, the gap inventories for cesium and iodine in the low-heat-rated fuel rod segments were experimentally determined to be about 0.30% of the total segment inventory.

Various parameters that affect fission product release are discussed, and experimental observations and analysis of the chemical behavior of releasable fission products in inert, steam, and dry-air atmospheres are examined.

## 1. INTRODUCTION

The primary objective of this experimental program has been to determine the extent and the forms of volatile fission products if they should be released from ruptured or defective fuel rods during a successfully terminated loss-of-coolant (LOCA) or a spent-fuel-transportation accident (SFTA). Thus, a series of experiments with highly irradiated fuel was conducted in steam in the temperature range 500 to 1200°C. (Two tests

were conducted in dry air.) In addition, three other experimental series and a parallel study have been conducted and reported. The first of these, the Control Test Series,<sup>1</sup> was designed to study the behavior of known fission product-type compounds and to develop the most effective arrangement of apparatus for their collection. The second, the Implant Test Series,<sup>2</sup> involved studies of the release of selected fission product species (radioactively traced) that were coated on the surfaces of pellets of unirradiated  $UO_2$  and encapsulated in Zircaloy-4 cladding. In the third series, the Low Burnup Fuel Test Series, tests with capsules irradiated to 1000 MWd/MT at a high-heat rating (560 to 660 W/cm) were conducted in steam at 700 and 900°C. (Additional information about those tests is provided in Appendix A.) In the parallel study, a Knudsen cell--mass spectrometer was used to investigate cesium-uranium interactions.<sup>3</sup>

The High Temperature Test Series, using high burnup H. B. Robinson fuel in the temperature range 1200 to 1600°C to determine fission product release, is now being performed. Finally, a Boiling Water Reactor Fuel Test Series will be conducted with fuel from the Peach Bottom-2 Reactor.

## 2. FUEL FOR THE HIGH BURNUP FUEL TEST SERIES

### 2.1 Description of H. B. Robinson Fuel

Fuel rod segments for the high burnup fission product release experiments were cut from rods D-12 and H-15 of bundle B05, which operated in the Carolina Power and Light Company's H. B. Robinson-2 power plant from October 1971 to May 6, 1974.<sup>4</sup> The peak linear heat rating, 32.6 kW/m (9.95 kW/ft), occurred in December 1971 when the burnup reached 5872 MWd/MT and the average heat rating was 23.3 kW/m (7.10 kW/ft). By May 1974, the peak heat rating had decreased to 21.2 kW/m (6.45 kW/ft) and the average was 17.5 kW/m (5.34 kW/ft).

The fuel rods and the arrangement of the rods in the bundle have been described by Perkins.<sup>5</sup> The cladding is Zircaloy-4, 1.072 cm (0.422 in.) diam, with 0.0617-cm (0.0243-in.) wall thickness. The original diametral pellet-to-clad gap was 0.0165 cm (0.0065 in.), the plenum length was 17.35 cm (6.83 in.), and the overall rod length was 387.0 cm (152.36 in.).

From the total core loading, it can be calculated that each fuel rod originally contained 2495.4 g of  $\text{UO}_2$ , or 2199.6 g of uranium, if it is assumed that the molecular weight of the enriched uranium was 237.92 g/mole.

The two fuel rods utilized in this experimental series were sectioned at Battelle Columbus Laboratories (BCL), as depicted in Fig. 1. A scan of gamma activity in rod F-7, which was obtained by Argonne National Laboratory,<sup>6</sup> is also displayed in Fig. 1. Gamma activity distributions of other rods from bundle B05 were determined by BCL and indicated similar profiles.<sup>7</sup> Fairly regular activity depressions between pellets indicated that the pellets were generally intact and that no significant concentration of fission product cesium or ruthenium occurred during the in-reactor irradiation. The observed axial gamma distributions were very similar to the burnup distribution obtained from in-core flux measurements.<sup>4</sup>

## 2.2 Description of Fuel-Rod Test Segments

A detailed sketch of a typical segment employed in this series is shown in Fig. 2. A description of the cutting and capping operations performed at BCL follows.<sup>8</sup>

### 2.2.1 Marking and sectioning

The two subject rods were received at the BCL Hot Laboratory as part of a shipment of 20 H. B. Robinson-2 fuel rods from Aerojet Nuclear Company (ANC) in Idaho. These rods were removed from the fuel assembly at the ANC facility in Idaho.

Overall dimensions of the fuel rods examined were 152 in. long by 0.422 in. OD. Starting from the bottom, each rod was marked ( $\pm 1/16$  in.) at 12, 24, 48, 60, 72, 84, 96, 120, and 132 in. The area 1 in. on either side of each mark was cleaned with a wire brush. Visual inspection of each cleaned area confirmed the absence of any debris that would hinder Swagelok sealing. A tubing cutter was used to section the rods at each of the marks. Ten pieces (in order, from the bottom), 12, 12, 24, 12, 12, 12, 12, 24, 12, and 20 in. long, were obtained from each rod. In each case, the cutting operation resulted in a negligible amount of fuel falling from any of the cut surfaces.

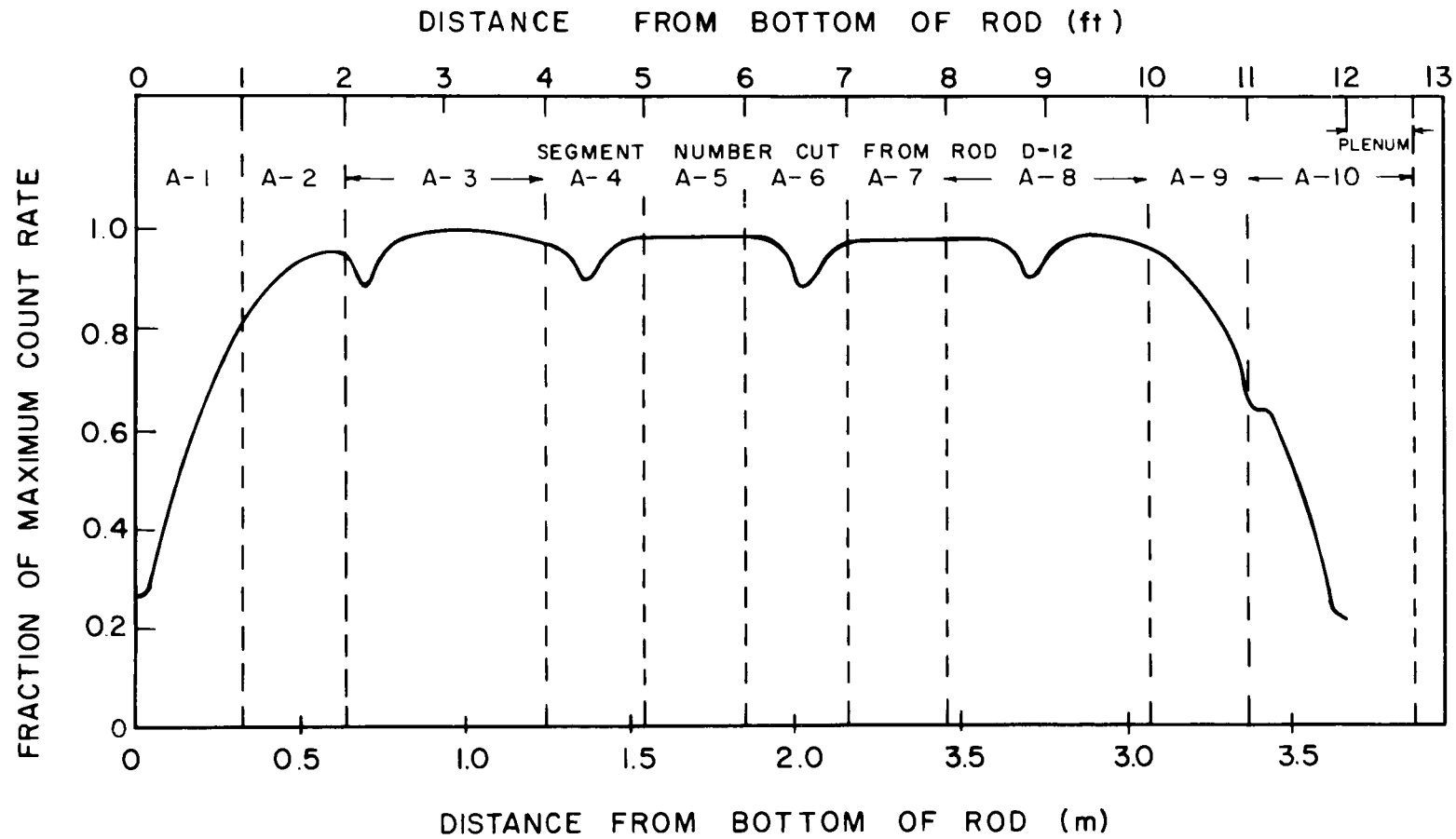
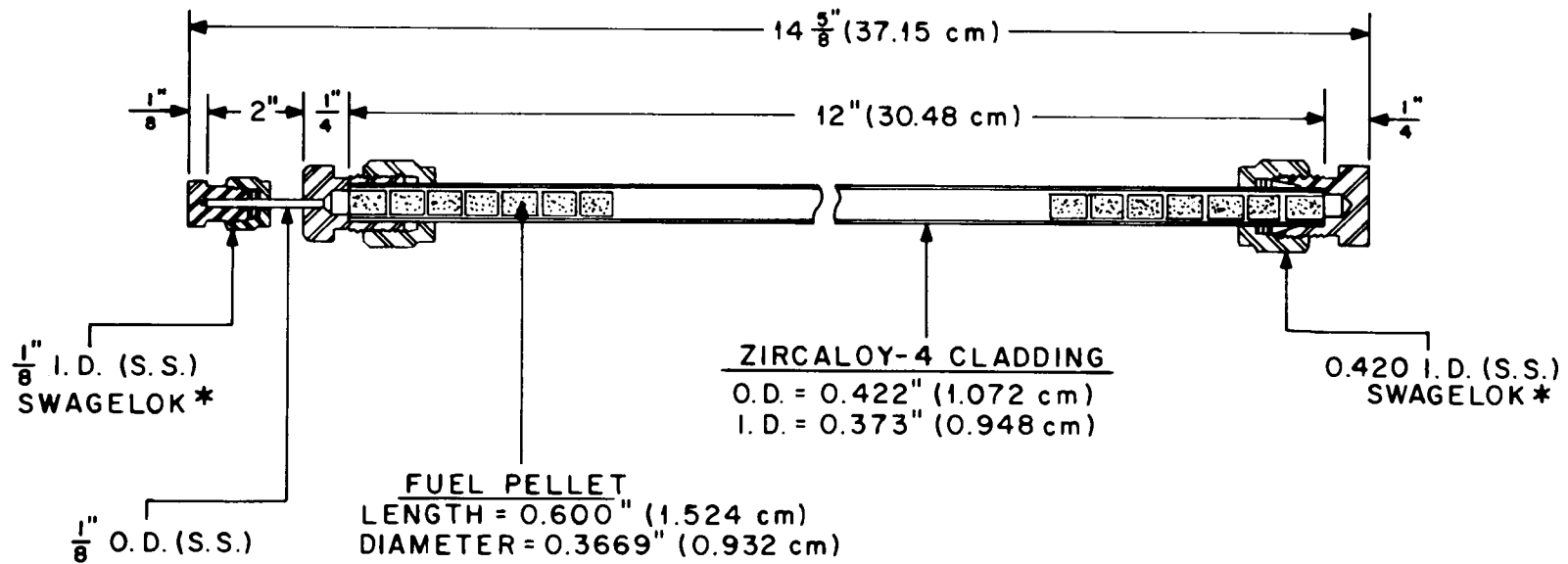


Fig. 1. Identification of fuel rod segments and gamma scan of rod F-7.



\*CRAWFORD FITTING CO.

Fig. 2. Detailed sketch of H. B. Robinson fuel rod segments A-7 and A-4.

Immediately after cutting, the exposed fuel ends of each section were sealed with stainless steel Swagelok fittings. The upper end of each section was sealed with a Swagelok cap fitting, which had a 2-in. length of 1/8-in.-OD stainless steel tubing welded into a hole through the cap. A 1/8-in. Swagelok cap fitting was used to seal the 1/8-in. tube. The lower end of each section was sealed with fittings that had the 1/8-in. tube attachment. Special stainless steel ferrules, made to fit the measured diameter of 0.418 in.,<sup>9</sup> were fabricated for these fittings to ensure a positive seal to the 0.422-in.-diam rod. This method of sealing was verified by performing a helium leak check at 80 psi on a sample system.

For identification purposes, Rod D-12 is designated "A" and Rod H-15 is designated "B." Sections from each rod were numbered 1 through 10, starting at the bottom end of the fuel rod. Thus the sections are identified as A-1 and B-1 through B-10. These identification marks were etched on each of the Swagelok fittings.

Approximately 90 days elapsed between the time the rods were punctured for fission gas analysis and the sectioning procedure. During this interval, an air-tight seal was placed over the small puncture hole in the clad. Note that the interior of Rod A (D-12) was exposed to air through the gas vent hole for about 72 hr before the hole was sealed. Rod B (H-15) was similarly exposed for about 48 hr.

### 2.2.2 Packaging and shipping

The rod sections were individually placed in stainless steel tubes, which were, in turn, placed in larger stainless steel tubes that were tack-welded together into a cluster to form a shipping basket. Spring-loaded stainless steel cylinders were placed into each of the shipping-basket tubes to constrain movement of the fuel rod sections during transport. The entire shipping basket assembly was then positioned in a stainless steel, water-tight shipping canister and transported in this configuration.

All of the rod sections were received in good condition.

### 2.3 Fission Product Inventory

Fuel rods F-7<sup>10</sup> and P-8<sup>7</sup> have been analyzed for burnup. The results, summarized in Table 1, indicate that burnups of 30,000 to 30,900 MWd/MT for the high burnup region are in good agreement with the calculated peak burnup of 31,360 MWd/MT.<sup>4</sup> The detailed operational history of the H. B. Robinson reactor has been used<sup>11</sup> as input to the ORIGEN<sup>12</sup> computer program to calculate fission product inventory, assuming a burnup of 30,745 MWd/MT. This ORIGEN-calculated inventory was then compared with experimental results from the dissolution of portions of fuel from the high burnup region of several fuel rods from bundle B05; generally good agreement was observed, but the ORIGEN-calculated amount of <sup>137</sup>Cs was approximately 10% higher than that determined experimentally.<sup>11</sup>

Because no burnup determinations are planned for rods D-12 and H-15, the ORIGEN calculation has been used to determine the inventory. Masses of important elements calculated with this program are presented in Table 2, whereas Table 3 is a listing of the masses and radioactivities of the principal radionuclides. We assumed that the length of the fuel column was 144 in., and the original uranium content was calculated as 183.3 g per 12-in segment. The fuel column height of 15 fuel rods from bundle B05 was measured while it was being gamma scanned, and the median was determined to be 143.6 in.<sup>7</sup>

### 2.4 Fission Gas Release While in the Robinson Reactor

Rods D-12 and H-15 were punctured and analyzed for fission gas release at BCL. The results indicated that 372 cm<sup>3</sup> (STP) of gas containing 95.2% He (from prepressurization), 0.14% Kr, and 1.1% Xe was present in each rod. Slightly lower fission gas release results were obtained by BCL for six other rods from bundle B05; also, the observed amounts of N<sub>2</sub> and O were much lower in these rods.<sup>13</sup> The median krypton content was 0.10%, and the median xenon content was 0.88%.

Calculated fission gas releases based on the inventory calculated by ORIGEN are presented in Tables 4 and 5; these results, as well as those determined for the other six rods mentioned above, indicate a greater

Table 1. Burnup measurements on H. B. Robinson rods

Rod No.	Distance from rod bottom		Burnup		Comments
	m	ft	at. %	MWd/MT <sup>a</sup>	
F-7	0.006	0.02	1.26	12,100	
P-8	0.31	1.01	2.559	24,570	Below high burnup region
F-8	0.57	1.87	3.14	30,140	
F-7	0.93	3.05	3.12	29,950	
P-8	1.76	5.73	3.221	30,920	
P-8	2.02	6.61	2.877	27,620	At grid spacer location

<sup>a</sup>Assumes that 1 at. % is equivalent to 9600 MWd/MT.

Table 2. Amounts of principal fission product elements in  
H. B. Robinson fuel after 911 days decay<sup>a</sup>

Element	Mass		Element	Mass	
	g/MT	mg/12 in.		g/MT	mg/12 in.
Br	21.04	3.857	Te	468.4	85.86
Kr	321.7	58.97	I	235.4	43.15
Rb	309.4	56.71	Xe	5,188.0	951.0
Sr	777.5	142.5	Cs	2,558.0	468.9
Y	414.5	75.98	Ba	1,509.0	276.6
Zr <sup>b</sup>	3,332.0	610.8	La	1,170.0	214.5
Mo	3,272.0	599.8	Ce	2,365.0	433.5
Tc	711.6	130.4	Pr	1,090.0	199.8
Ru	2,274.0	416.8	Nd	3,827.0	701.5
Rh	436.7	80.05	Sm	739.2	135.5
Pd	1,516.0	277.9	Eu	183.1	33.56
Sn <sup>b</sup>	50.51	9.258	U	956,600.0	175,340.0 <sup>c</sup>
Sb	14.12	2.588	Pu	9,527.0	1,746.0

<sup>a</sup>Calculated by ORIGEN computer program on Nov. 9, 1976 for a burnup of 31,360 MWd/MT. Decay time, 911 days (Nov. 2, 1976).

<sup>b</sup>Calculated amounts in the cladding are  $2.086 \times 10^5$  g of zirconium per MT and 2.480 g of tin per MT of initial uranium.

<sup>c</sup>Initial uranium content of 12 in. of fuel rod was calculated to be 183.3 g.

Table 3. Principal radioactive components of H. B. Robinson  
fuel after 911 days decay<sup>a</sup>

Isotope	Amount per MT of initial uranium		Amount per 12-in. length of fuel rod	
	Ci	g	Ci	mg
<sup>85</sup> Kr	7,440	18.97	1.364	3.477
<sup>90</sup> Sr	65,640	464.2	12.03	85.09
<sup>90</sup> Y	65,640	0.121	12.03	2.22 x 10 <sup>-2</sup>
<sup>95</sup> Zr <sup>b</sup>	95.85	4.56 x 10 <sup>-3</sup>	1.757 x 10 <sup>-2</sup>	8.36 x 10 <sup>-4</sup>
<sup>95</sup> Nb <sup>b</sup>	207.7	5.30 x 10 <sup>-3</sup>	3.807 x 10 <sup>-2</sup>	9.71 x 10 <sup>-4</sup>
<sup>106</sup> Ru	108,000	32.34	19.80	5.928
<sup>106</sup> Rh	108,000	3.03 x 10 <sup>-5</sup>	19.80	5.55 x 10 <sup>-6</sup>
<sup>113m</sup> Cd	32.5	0.150	5.95 x 10 <sup>-1</sup>	0.027
<sup>125</sup> Sb <sup>b</sup>	5,660	5.400	1.037	0.9898
<sup>125m</sup> Te	1,382	7.67 x 10 <sup>-2</sup>	2.533 x 10 <sup>-1</sup>	1.41 x 10 <sup>-2</sup>
<sup>127</sup> Te	48.85	1.85 x 10 <sup>-5</sup>	8.954 x 10 <sup>-3</sup>	3.39 x 10 <sup>-6</sup>
<sup>129</sup> I	0.03237	185.5	5.933 x 10 <sup>-6</sup>	34.00
<sup>134</sup> Cs <sup>c</sup>	62,960	48.60	11.54	8.908
<sup>137</sup> Cs	98,680	1138	18.09	208.6
<sup>137m</sup> Ba	93,350	1.73 x 10 <sup>-4</sup>	17.11	3.17 x 10 <sup>-5</sup>
<sup>144</sup> Ce	122,200	38.30	22.40	7.020
<sup>144</sup> Pr	122,200	1.62 x 10 <sup>-3</sup>	22.40	2.97 x 10 <sup>-4</sup>
<sup>144m</sup> Pr	1,466	8.08 x 10 <sup>-6</sup>	2.687 x 10 <sup>-1</sup>	1.48 x 10 <sup>-6</sup>
<sup>147</sup> Pm	62,550	67.43	11.47	12.36
<sup>154</sup> Eu	13,050	48.28	2.392	8.850

<sup>a</sup>Calculated by ORIGEN computer program on Nov. 9, 1976 for a burnup of 31,360 MWd/MT and 911 days of decay.

<sup>b</sup>Fission product activity only. Activation of cladding components produced per MT of initial uranium: 2.32 Ci of <sup>95</sup>Zr, 5.03 Ci of <sup>95</sup>Nb, 71.0 Ci of <sup>119m</sup>Sn, 1.91 Ci of <sup>123</sup>Sn, 606 Ci of <sup>125</sup>Sb, and 148 Ci of <sup>125m</sup>Te. Experimental results of D. O. Campbell (personal communication) show a <sup>60</sup>Co content of 7.1 Ci/MT.

<sup>c</sup>Based on experimentally measured ratio of <sup>134</sup>Cs: <sup>137</sup>Cs in dissolved Robinson fuel, because ORIGEN apparently overcalculated the amount of <sup>134</sup>Cs (see ref. 11 in this report).

Table 4. Fission gas released to plenum of rod D-12 while in reactor

Isotope	Amount found in plenum <sup>a</sup>			Total produced; ORIGEN calculation <sup>b</sup> (g-atoms/MT)	Amount released to plenum (%)
	Percent of element	cc (STP)	g-atoms/MT		
<sup>83</sup> Kr	13.7	0.0678	$1.376 \times 10^{-3}$	0.385	0.357
<sup>84</sup> Kr	31.1	0.1539	$3.123 \times 10^{-3}$	1.100	0.284
<sup>85</sup> Kr	7.17	0.0355	$7.200 \times 10^{-4}$	0.217	0.332
<sup>86</sup> Kr	48.0	0.2375	$4.820 \times 10^{-3}$	1.754	0.275
Total krypton		0.4948	$1.004 \times 10^{-2}$	3.456	0.291
<sup>128</sup> Xe				0.024	
<sup>130</sup> Xe				0.058	
<sup>131</sup> Xe	7.86	0.3041	$6.172 \times 10^{-3}$	2.598	0.238
<sup>132</sup> Xe	21.0	0.8124	$1.649 \times 10^{-2}$	7.710	0.214
<sup>134</sup> Xe	28.9	1.1180	$2.269 \times 10^{-2}$	9.653	0.235
<sup>136</sup> Xe	42.2	1.6326	$3.314 \times 10^{-2}$	15.196	0.218
Total xenon		3.8688	$7.852 \times 10^{-2}$	35.239	0.223

<sup>a</sup>Measured after 549 days of decay (Aug. 22, 1975).

<sup>b</sup>Calculated by ORIGEN computer program on Nov. 9, 1976 for 28,580 MWd/MT and 549 days of decay.

Table 5. Fission gas released to plenum of rod H-15 while in reactor

Isotope	Amount found in plenum <sup>a</sup>			Total produced; ORIGEN calculation <sup>b</sup> (g-atoms/MT)	Amount released to plenum (%)
	Percent of element	cc (STP)	g-atoms/MT		
<sup>83</sup> Kr	13.7	0.0805	$1.634 \times 10^{-3}$	0.385	0.424
<sup>84</sup> Kr	30.8	0.1810	$3.673 \times 10^{-3}$	1.100	0.334
<sup>85</sup> Kr	7.67	0.0451	$9.147 \times 10^{-3}$	0.217	0.422
<sup>86</sup> Kr	47.9	0.2815	$5.713 \times 10^{-3}$	1.754	0.326
Total krypton		0.5876	$1.193 \times 10^{-2}$	3.456	0.345
<sup>128</sup> Kr				0.024	
<sup>130</sup> Xe				0.058	
<sup>131</sup> Xe	8.10	0.3555	$7.214 \times 10^{-3}$	2.598	0.278
<sup>132</sup> Xe	21.0	0.9216	$1.870 \times 10^{-2}$	7.710	0.243
<sup>134</sup> Xe	28.9	1.268	$2.574 \times 10^{-2}$	9.653	0.267
<sup>136</sup> Xe	42.0	1.843	$3.741 \times 10^{-2}$	15.196	0.246
Total xenon		4.3884	$8.907 \times 10^{-2}$	35.239	0.253

<sup>a</sup> Measured after 549 days of decay (Aug. 22, 1975).

<sup>b</sup> Calculated by ORIGEN computer program on Nov. 9, 1976 for a burnup of 28,580 MWd/MT and 549 days of decay.

fractional release of krypton as compared with xenon. Moreover, the low release values suggest that release occurred only by the recoil-knockout mechanism. The low fuel temperature, as shown in Fig. 3,<sup>14</sup> probably prevented the release of fission gas by diffusion or any other mechanism.

### 3. EXPERIMENTAL APPARATUS AND EQUIPMENT

A schematic diagram of the experimental apparatus that was used in this series is shown in Fig. 4. In each test, a high burnup fuel segment was placed on a quartz holder and inserted into a quartz liner that was prepositioned inside of a quartz furnace tube. The fuel rod segment being tested was heated to the desired temperature level by an electrical resistance heater or a low-frequency induction heater. The simulated defect was provided by drilling a single 0.159-cm (1/16-in.)-diam hole through the Zircaloy cladding of a test segment at the midsection (prior to testing), or by prepressurizing the specimen with helium ( $\sim 302$  psig or 2.08 MPa) and heating it to 900°C to cause rupture.

The released material that did not deposit on the furnace-tube components was carried by a flowing gas mixture of steam-helium or steam-argon (air was used in two tests) through a gold-foil-lined thermal gradient tube where volatile species that are condensible above 150°C deposited. A filter pack containing three HEPA filter papers (Reeve-Angel pure borosilicate Fiberglas) was used to collect the particulate material. Elemental iodine and organic iodides were trapped by impregnated charcoal and silver-exchanged zeolite adsorbers.

Each of the first four charcoal compartments (1a, 1b, 1c, and 2a) contained a volume of charcoal that would fit into an 0.8-cm<sup>3</sup> "rabbit" used in activation analysis. The other cartridges contained greater amounts. Cartridges 1, 2, and 3 contained 12-16 mesh, type G-618 charcoal impregnated with triethylene diamine, whereas cartridge 4 contained 12-16 mesh--98% silver-exchanged 13X zeolite. The steam was condensed and collected in an ice-bath condenser. This was followed by a dry-ice-cooled freeze trap (-78°C) to remove the remaining traces of moisture. Farther downstream, fission-produced gases were adsorbed in two charcoal

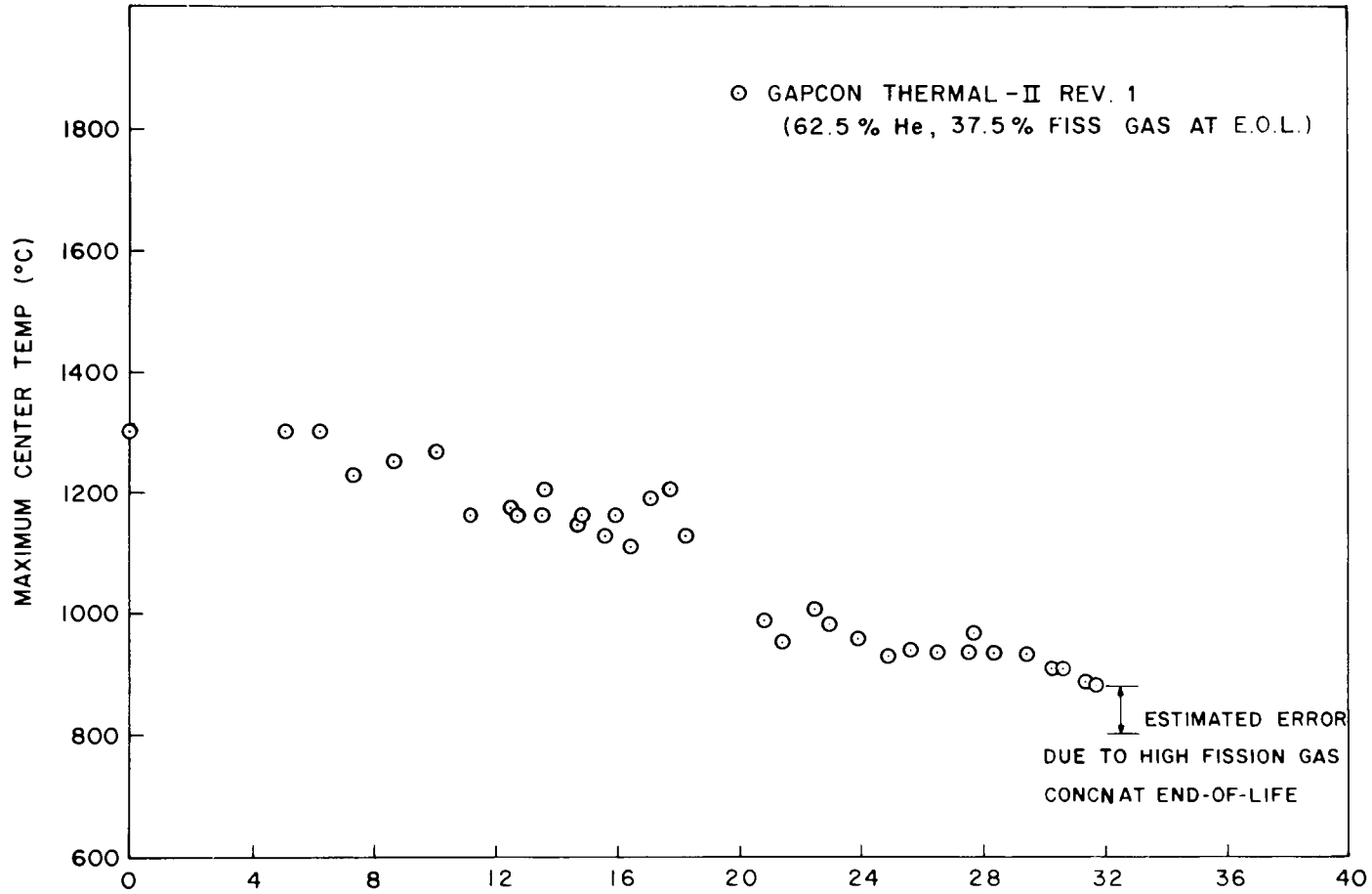


Fig. 3. H. B. Robinson bundle B0-5 temperatures vs burnup at peak axial power location.

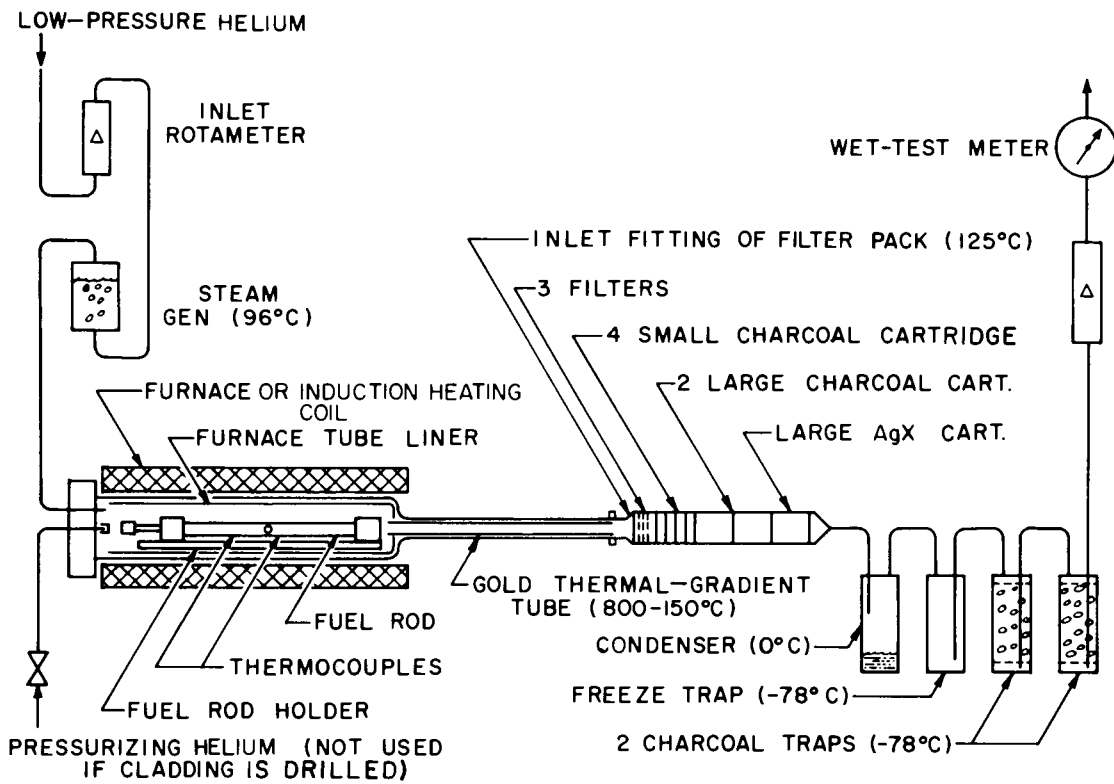


Fig. 4. Experimental apparatus used in the High Burnup Fuel Test Series.

traps, also at dry-ice temperature. A wet-test meter was used to measure the effluent gas which, in addition to argon or helium, contained hydrogen that was produced by the reaction of steam with the Zircaloy cladding. A shielded NaI (Tl activated) crystal was used to monitor the  $^{134}\text{Cs}$  and  $^{137}\text{Cs}$  deposition in the thermal gradient tube and filter pack. The  $^{85}\text{Kr}$  was similarly monitored as it was adsorbed in the charcoal traps.

In tests in which the fuel rod segments were ruptured, the segments were heated with the induction heater shown in Fig. 5. Temperature measurements were made with a carefully calibrated, automatic-scanning optical pyrometer, also shown in Fig. 5. It was positioned in the cell on a trolley located outside the apparatus containment box. Absolute temperature measurements with the pyrometer were complicated by emissivity uncertainties caused by Zircaloy oxidation and by adsorption in the quartz furnace tube, quartz liner, and the Vycor window of the apparatus containment box; induction heating effects caused slight uncertainties in the temperatures indicated by reference thermocouples. The effects were measured in combination and separately, where possible, and appropriate corrections were made. The absolute temperatures determined by the in-cell pyrometer and by an out-of-cell disappearing filament pyrometer are believed to have been accurate to within  $\pm 25^\circ\text{C}$  over the temperature range of the tests.

A roughing filter (shown beneath the fuel rod in Fig. 5) covered with a coarse screen was operated with a downward air flow velocity of approximately 25 cm/sec while fuel-handling operations were in progress. A HEPA filter, rated at 125 scfm, backed up the roughing filter. Whenever a fuel rod was heated, the containment box lid was closed and the air flow was reduced to provide a slight vacuum on the box. Approximately 4 hr was required to clean up the hot cell and remove the collection system components following each experiment. Cleanup was to "green-tag" levels (very low smear and probe count rate) to permit easy access to the hot cell and apparatus and to prevent cross contamination between experiments.

4043-77-IM

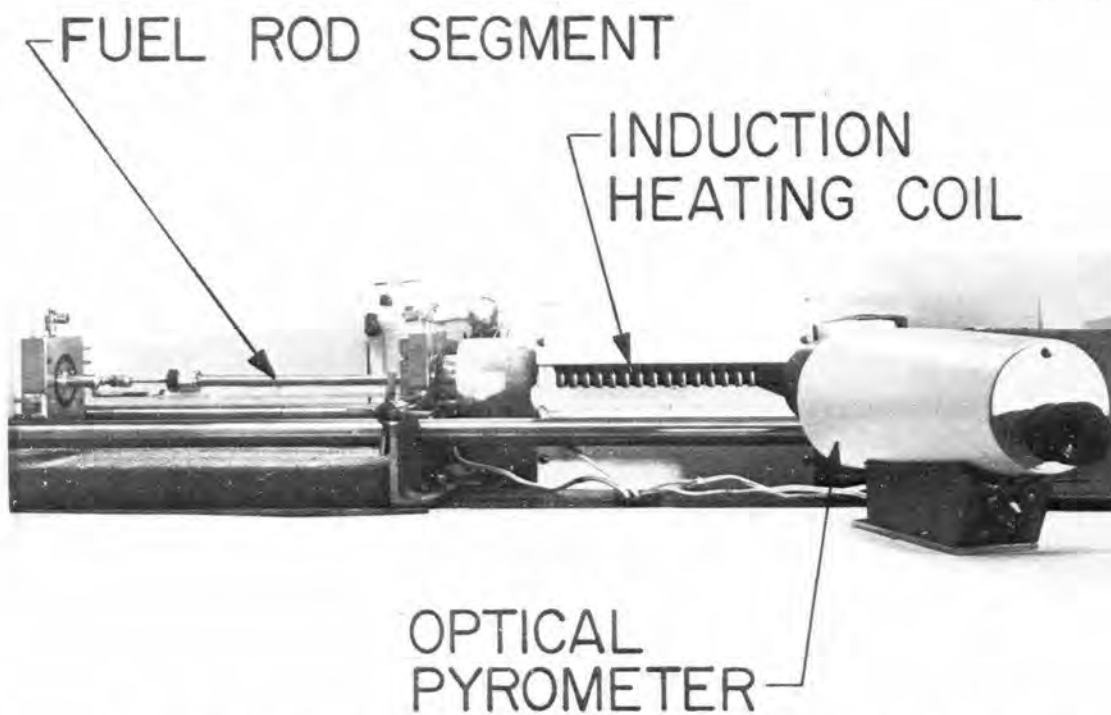


Fig. 5. Photograph of induction heater assembly and automatic optical pyrometer.

#### 4. RESULTS OF HIGH BURNUP FUEL TESTS

##### 4.1 High Burnup Fuel Test 1 (700°C)

The High Burnup Fuel Test Series was initiated with a 700°C test. Fuel rod segment A-7 was heated in a resistance-heated furnace for 5 hr, and a flowing 84% steam--16% argon carrier gas atmosphere was provided. Before testing, a 0.159-cm (1/16-in.)-diam hole was drilled in the cladding at midlength to cause a simulated defect. Proof of penetration was determined by visual inspection and by application of a small amount of argon pressure to the capsule after drilling.

The various components and subcomponents of the apparatus train were counted with a multichannel analyzer using a NaI (Tl) crystal. Table 6 shows the subsequent distribution of  $^{134}\text{Cs}$  that was obtained in the experimental apparatus. From these data, it was determined that 0.0000262% (0.123  $\mu\text{g}$ ) of the total cesium was released from the irradiated capsule. About 99.9% of the cesium that was released was found in the furnace tube. Concentration profiles of  $^{134}\text{Cs}$  along the furnace tube liner and fuel rod holder indicated that most of the cesium deposition occurred in the vicinity of the defect opening in the fuel rod segment, as illustrated schematically in Fig. 6. The deposition behavior suggests that the released cesium species were very reactive with the quartz surfaces of the furnace tube liner and fuel rod holder, forming less volatile silicates. Approximately 0.08% of the released cesium deposited in the gold thermal-gradient tube. An axial concentration profile of  $^{134}\text{Cs}$  is also shown in Fig. 6. Most of the deposition was found in a broad peak between 350 and 600°C.

Table 7 gives a summary of the  $^{129}\text{I}$  distribution in the apparatus components. The quantitative values were determined by activation analysis. About 0.00214% (0.925  $\mu\text{g}$ ) of the total iodine inventory was released. Unlike cesium, most of the iodine (98%) transported downstream to the gold thermal-gradient tube, filter papers, and charcoal. Approximately 7.5 times more iodine mass was released than cesium. Some antimony was also released,  $2.0 \times 10^{-5}\%$  ( $5.4 \times 10^{-4}$   $\mu\text{g}$ ) of the total inventory.

Table 6. Distribution of  $^{134}\text{Cs}$  in High Burnup Fuel Test 1<sup>a</sup>

Location	Temperature (°C)	Amount of $^{134}\text{Cs}$ found in each location			
		$\mu\text{g}^b$	Percent of total <sup>c</sup>	Percent of released	Total cesium ( $\mu\text{g}$ )
Fuel	700	(8908) <sup>d</sup>			( $4.689 \times 10^5$ ) <sup>d</sup>
Furnace tube	700				
Quartz liner		$1.42 \times 10^{-3}$	$1.59 \times 10^{-5}$	60.78	$7.47 \times 10^{-2}$
Quartz fuel-rod holder		$9.14 \times 10^{-4}$	$1.03 \times 10^{-5}$	39.12	$4.81 \times 10^{-2}$
Thermal gradient tube	775-225	$1.81 \times 10^{-6}$	$2.03 \times 10^{-8}$	0.08	$9.53 \times 10^{-5}$
Filter pack components	120				
Stainless-steel inlet fitting		0.0	0.0	0.0	0.0
Other housing components		0.0	0.0	0.0	0.0
First filter paper		$1.0 \times 10^{-7}$	$1.12 \times 10^{-9}$	0.004	$5.26 \times 10^{-6}$
Second filter paper		0.0	0.0	0.0	0.0
Third filter paper		0.0	0.0	0.0	0.0
Charcoal No. 1a		$<3.34 \times 10^{-7}$	$3.75 \times 10^{-9}$	0.014	$1.76 \times 10^{-5}$
Charcoal No. 1b		0.0	0.0	0.0	0.0
Charcoal No. 1c		0.0	0.0	0.0	0.0
Charcoal No. 2a		0.0	0.0	0.0	0.0
Charcoal No. 2b		0.0	0.0	0.0	0.0
Charcoal No. 3		0.0	0.0	0.0	0.0
AgX		0.0	0.0	0.0	0.0
Condenser	0	0.0	0.0	0.0	0.0
Freeze trap	-78	0.0	0.0	0.0	0.0
Cold charcoal traps (two)	-78	0.0	0.0	0.0	0.0
Total		$2.33 \times 10^{-3}$	$2.62 \times 10^{-5}$	100.00	$1.23 \times 10^{-1}$

<sup>a</sup>Steam flow rate,  $319 \text{ cm}^3/\text{min}$  (STP); argon flow rate,  $60 \text{ cm}^3/\text{min}$  (STP); system pressure, 760 torr. Decay time, 911 days (to Nov. 2, 1976).

<sup>b</sup>Amounts less than  $1.0 \times 10^{-7} \mu\text{g}$  are given as 0.0.

<sup>c</sup>Percentage of radioactive nuclide in the fuel rod. The amount of nuclide remaining in the fuel rod was obtained by difference.

<sup>d</sup>Calculated for burnup of 31,360 MWd per MT of original uranium, 183.3 g of uranium originally in 12-in. segment, and 911 days of decay.



Table 7. Distribution of  $^{129}\text{I}$  in High Burnup Fuel Test 1<sup>a</sup>

Location	Temperature (°C)	Amount of $^{129}\text{I}$ found in each location			Total iodine ( $\mu\text{g}$ )
		$\mu\text{g}$ <sup>b</sup>	Percent of total <sup>c</sup>	Percent of released	
Fuel rod	700	$(3.40 \times 10^4)^{\text{d}}$			$(4.314 \times 10^4)^{\text{d}}$
Furnace tube	700				
Quartz liner		$0.0072 \pm 0.0045$ $0.0031$	$2.12 \times 10^{-5}$	0.99	0.0091
Quartz fuel-rod holder		$\leq 0.008$	$2.35 \times 10^{-5}$	1.10	0.01
Thermal gradient tube	775-225	$0.1128 \pm 0.0768$ $0.0758$	$3.32 \times 10^{-4}$	15.48	0.1432
Filter pack components	120				
Stainless-steel inlet fitting		$0.0025 \pm 0.0029$ $0.0025$	$7.35 \times 10^{-6}$	0.34	0.0032
First filter paper		$0.153 \pm 0.015$	$4.50 \times 10^{-4}$	21.00	0.1942
Second and third filter papers		$0.16 \pm 0.01$	$4.71 \times 10^{-4}$	21.96	0.2031
Charcoal No. 1a		$0.285 \pm 0.03$	$8.38 \times 10^{-4}$	39.12	0.3617
Charcoal No. 1b		0.0	0.0	0.0	0.0
Charcoal No. 1c		0.0	0.0	0.0	0.0
Charcoal No. 2a		0.0	0.0	0.0	0.0
Charcoal No. 2b <sup>e</sup>		0.0	0.0	0.0	0.0
Charcoal No. 3 <sup>e</sup>		0.0	0.0	0.0	0.0
AgX <sup>e</sup>		0.0	0.0	0.0	0.0
Condenser <sup>e</sup>	0	0.0	0.0	0.0	0.0
Freeze trap <sup>e</sup>	-78	0.0	0.0	0.0	0.0
Cold charcoal traps (two) <sup>e</sup>	-78	0.0	0.0	0.0	0.0
Total		$0.7285 \pm 0.14$	$2.143 \times 10^{-3}$	100.00	0.9245

<sup>a</sup>Steam flow rate,  $319 \text{ cm}^3/\text{min}$  (STP); argon flow rate,  $60 \text{ cm}^3/\text{min}$  (STP); system pressure, 760 torr. Decay time, 911 days (to Nov. 2, 1976).

<sup>b</sup>Amounts less than  $1.0 \times 10^{-2} \mu\text{g}$  are given as 0.0.

<sup>c</sup>Percentage of radioactive nuclide in fuel rod.

<sup>d</sup>Calculated for burnup of 31,360 MWd per MT of original uranium, 183.3 g of uranium originally in 12-in. segment, and 911 days of decay.

<sup>e</sup>Not analyzed for  $^{129}\text{I}$  content in any of the High Burnup Series Tests; amount assumed to be 0.0.

Approximately  $3.6 \times 10^{-8}\%$  ( $1.5 \times 10^{-4}$   $\mu\text{g}$ ) of the total ruthenium inventory was released; approximately 81% of this material was found in the first charcoal adsorber. No ruthenium was found upstream from the filter pack, which indicates that the released ruthenium species was very volatile. The ruthenium was quantitatively determined by gamma counting the photon peak of  $^{106}\text{Rh}$  (513 keV), daughter of  $^{106}\text{Ru}$ .

#### 4.2 High Burnup Fuel Test 2 (900°C)

The irradiated fuel-rod segment used in this test was maintained at 900°C for 2 hr in a flowing 87% steam--13% argon atmosphere. As in the first test, the defect was provided by drilling a 0.159-cm (1/16-in.)-diam hole through the cladding. Relevant information about the segment (A-4) and its parent fuel rod (D-12) is discussed in Sect. 2. A tightly fitted 9-1/2-in.-long gold liner was positioned in the outlet end of the quartz furnace-tube liner so that a larger fraction of the released cesium could be transported to the thermal gradient tube. A larger-capacity freeze trap and two larger charcoal traps were also employed to ensure complete trapping of  $^{85}\text{Kr}$ .

The posttest distribution of  $^{134}\text{Cs}$  in the experimental apparatus, summarized in Table 8, indicated only a small release of cesium during the testing period: 0.000616% (2.818  $\mu\text{g}$ ) of the total cesium was released. Most of the cesium was found on the components of the furnace tube, especially on the quartz fuel-rod holder (87.7%). Only 0.03% of the released cesium was transported to the thermal gradient tube and beyond. Figure 7 shows the axial deposition of  $^{134}\text{Cs}$  along the furnace tube liner (quartz and gold) and thermal gradient tube. As in the previous test (Sect. 4.1), the quartz demonstrated its reactivity with the released cesium vapor species; most of the cesium was found on the quartz fuel-rod holder near the defect opening. About 12% was deposited on the gold liner in the furnace tube. The  $^{134}\text{Cs}$  peak in the thermal gradient tube was located in a 300 to 500°C temperature range.

A summary of the  $^{129}\text{I}$  distribution in the experimental apparatus is provided in Table 9. Approximately 0.0042% (1.754  $\mu\text{g}$ ) of the total iodine

Table 8. Distribution of  $^{134}\text{Cs}$  in High Burnup Fuel Test 2<sup>a</sup>

Location	Temperature (°C)	Amount $^{134}\text{Cs}$ found in each location			Total cesium ( $\mu\text{g}$ )
		$\mu\text{g}^{\text{b}}$	Percent of total <sup>c</sup>	Percent of released	
Fuel rod	900	(8685) <sup>d</sup>			(4.572 x 10 <sup>5</sup> ) <sup>d</sup>
Furnace tube	900				
Quartz liner		3.06 x 10 <sup>-4</sup>	3.52 x 10 <sup>-6</sup>	0.57	0.016
Gold liner <sup>e</sup>		6.29 x 10 <sup>-3</sup>	7.24 x 10 <sup>-5</sup>	11.75	0.331
Quartz fuel-rod holder		4.69 x 10 <sup>-2</sup>	5.40 x 10 <sup>-4</sup>	87.65	2.469
Thermal gradient tube	900-225	1.26 x 10 <sup>-5</sup>	1.45 x 10 <sup>-7</sup>	0.024	6.63 x 10 <sup>-4</sup>
Filter pack components	130				
Stainless-steel inlet fitting		2.12 x 10 <sup>-7</sup>	2.44 x 10 <sup>-9</sup>	3.96 x 10 <sup>-4</sup>	1.12 x 10 <sup>-5</sup>
Other housing components		0.0	0.0	0.0	0.0
First filter paper		1.02 x 10 <sup>-6</sup>	1.174 x 10 <sup>-8</sup>	1.91 x 10 <sup>-3</sup>	5.37 x 10 <sup>-5</sup>
Second filter paper		0.0	0.0	0.0	0.0
Third filter paper		0.0	0.0	0.0	0.0
Charcoal No. 1a		<2.39 x 10 <sup>-7</sup>	2.75 x 10 <sup>-9</sup>	4.46 x 10 <sup>-4</sup>	1.26 x 10 <sup>-5</sup>
Charcoal No. 1b		0.0	0.0	0.0	0.0
Charcoal No. 1c		0.0	0.0	0.0	0.0
Charcoal No. 2a		0.0	0.0	0.0	0.0
Charcoal No. 2b		0.0	0.0	0.0	0.0
Charcoal No. 3		0.0	0.0	0.0	0.0
AgX		0.0	0.0	0.0	0.0
Condenser	0	0.0	0.0	0.0	0.0
Freeze trap	-78	0.0	0.0	0.0	0.0
Cold charcoal traps (two)	-78	0.0	0.0	0.0	0.0
Total		5.354 x 10 <sup>-2</sup>	6.16 x 10 <sup>-4</sup>	100.00	2.818

<sup>a</sup> Steam flow rate, 378 cm<sup>3</sup>/min (STP); argon flow rate, 57 cm<sup>3</sup>/min (STP); system pressure, 760 torr. Decay time, 911 days (to Nov. 2, 1976).

<sup>b</sup> Amounts less than 1.0 x 10<sup>-7</sup>  $\mu\text{g}$  are given as 0.0.

<sup>c</sup> Percentage of radioactive nuclide in fuel rod.

<sup>d</sup> Calculated for burnup of 30,580 MWd per MT of original uranium, 183.3 g of uranium originally in 12-in. segment, and 911 days of decay.

<sup>e</sup> A 9-1/2-in.-long gold liner was positioned within the 17-1/4-in.-long furnace-tube quartz liner at the outlet end.

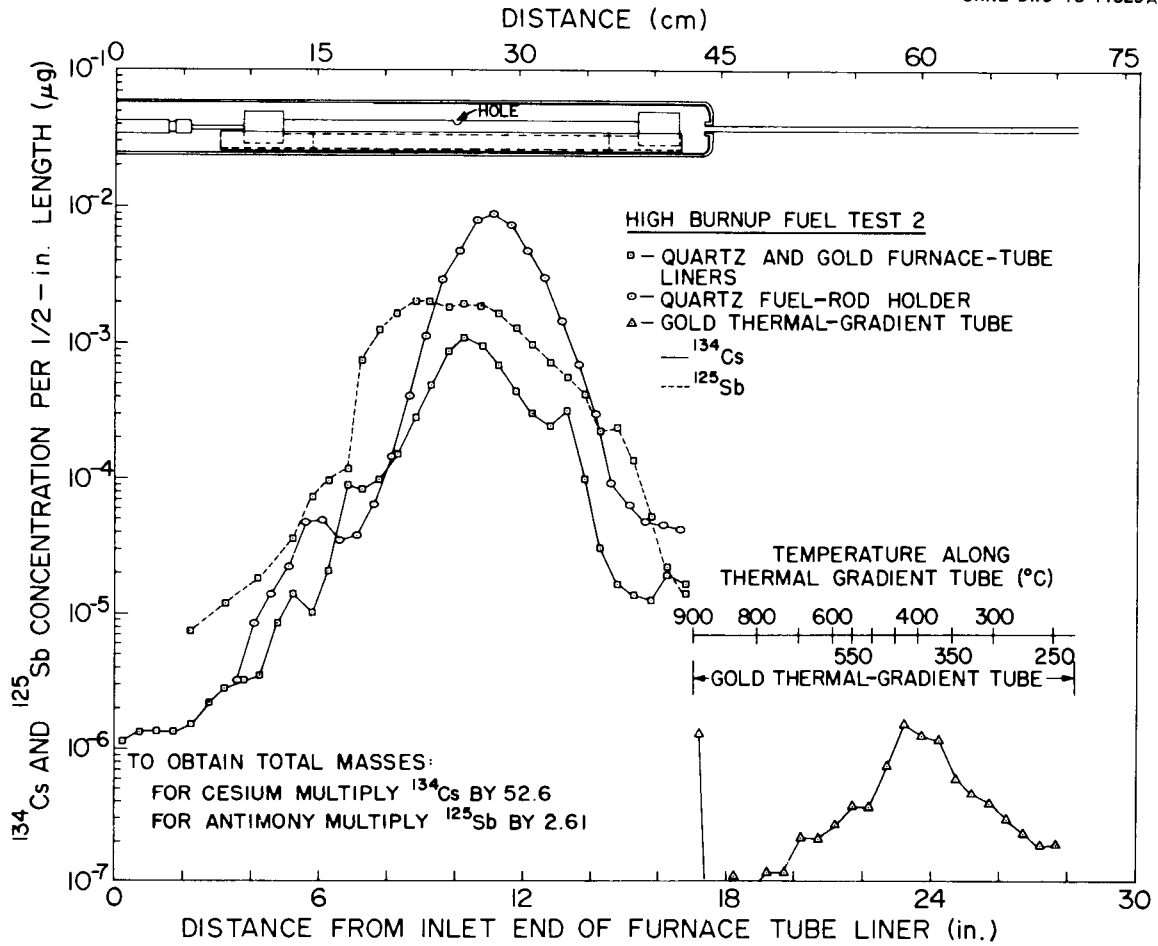


Fig. 7. Distribution of <sup>134</sup>Cs and <sup>125</sup>Sb in furnace tube and <sup>134</sup>Cs in the thermal gradient tube of test HBU-2.

Table 9. Distribution of  $^{129}\text{I}$  in High Burnup Fuel Test 2<sup>a</sup>

Location	Temperature (°C)	Amount of $^{129}\text{I}$ found in each location			Total iodine ( $\mu\text{g}$ )
		$\mu\text{g}$ <sup>b</sup>	Percent of total <sup>c</sup>	Percent of released	
Fuel rod	900	( $3.316 \times 10^4$ ) <sup>d</sup>			( $4.209 \times 10^4$ ) <sup>d</sup>
Furnace tube	900				
Quartz liner		$0.0352 \pm 0.0060$	$1.06 \times 10^{-4}$	2.55	
Gold liner		$0.0300 \pm 0.0048$	$9.05 \times 10^{-5}$	2.17	0.038
Quartz fuel-rod holder		$0.0132 \pm \begin{matrix} 0.0081 \\ 0.0058 \end{matrix}$	$3.98 \times 10^{-5}$	0.96	0.017
Thermal gradient tube	900-225	$0.1145 \pm \begin{matrix} 0.0550 \\ 0.0546 \end{matrix}$	$3.45 \times 10^{-4}$	8.29	0.145
Filter pack components	130				
Stainless-steel inlet fitting		$0.04 \pm 0.004$	$1.21 \times 10^{-4}$	2.89	0.051
First filter paper		$0.319 \pm 0.002$	$9.62 \times 10^{-4}$	23.08	0.405
Second and third filter papers		$0.30 \pm 0.02$	$9.05 \times 10^{-4}$	21.71	0.381
Charcoal No. 1a		$0.5300 \pm 0.05$	$1.60 \times 10^{-3}$	38.35	0.673
Charcoal No. 1b		0.0	0.0	0.0	0.0
Charcoal No. 1c		0.0	0.0	0.0	0.0
Charcoal No. 2a		0.0	0.0	0.0	0.0
Charcoal No. 2b		0.0	0.0	0.0	0.0
Charcoal No. 3		0.0	0.0	0.0	0.0
AgX		0.0	0.0	0.0	0.0
Condenser	0	0.0	0.0	0.0	0.0
Freeze trap	-78	0.0	0.0	0.0	0.0
Cold charcoal traps (two)	-78	0.0	0.0	0.0	0.0
Total		1.382	$4.17 \times 10^{-3}$	100.00	1.755

<sup>a</sup> Steam flow rate,  $378 \text{ cm}^3/\text{min}$  (STP); argon flow rate,  $57 \text{ cm}^3/\text{min}$  (STP); system pressure, 760 torr. Decay time, 911 days (to Nov. 2, 1976).

<sup>b</sup> Amounts less than  $1.0 \times 10^{-2} \mu\text{g}$  are given as 0.0.

<sup>c</sup> Percentage of radioactive nuclide in fuel rod.

<sup>d</sup> Calculated for burnup of 30,580 MWd per MT of original uranium, 183.3 g of uranium originally in 12-in. segment, and 911 days of decay.

<sup>e</sup> A 9-1/2-in.-long gold liner was positioned within the 17-1/4-in.-long furnace-tube quartz liner at the outlet end.

in the rod segment was released, which is a factor of 2 more than was released in the 700°C tests. As in test HBU-1, most of the released iodine (about 94%) transported beyond the furnace tube and was collected as elemental iodine.

Measurable ruthenium, as shown in Table 10, was also released in this test but, unlike test HBU-1, ruthenium was found only in the first charcoal section. Only about  $7 \times 10^{-9}\%$  ( $3 \times 10^{-5} \mu\text{g}$ ) of the total ruthenium was released.

Approximately  $2 \times 10^{-3}\%$  ( $0.053 \mu\text{g}$ ) of the total antimony in the fuel rod segment was released. It was found on the surfaces of the furnace tube liner, which suggests an attraction of the antimony for the gold. The distribution along the furnace tube liner is shown in Fig. 7.

During this test, approximately 15 mCi of  $^{85}\text{Kr}$  was released from the fuel rod segment. This quantity of  $^{85}\text{Kr}$ , an amount equal to 1.1% of segment inventory, is approximately three times that released to the gap and plenum during the operation in the H. B. Robinson reactor. The release began when the temperature of the segment reached about 500°C and ceased approximately 20 min after the test temperature (900°C) was attained.

#### 4.3 High Burnup Fuel Test 4 (500°C)

This experiment of the High Burnup Fuel Test Series was conducted at 500°C for 20 hr with a flowing 88% steam--12% argon atmosphere, using fuel rod segment A-5 from rod D-12. As in the previous tests, a 0.159-cm (1/16-in.)-diam hole was drilled through the cladding at the midpoint of the rod segment to simulate a defect.

A summary of  $^{134}\text{Cs}$  distribution in the experimental apparatus is presented in Table 11. These data show that  $3.6 \times 10^{-6}\%$  ( $0.017 \mu\text{g}$ ) of the total cesium inventory of the rod segment was released. It is evident from the data tabulated that most of the cesium remained in the quartz furnace tube. Only 0.2% of the released cesium was transported downstream; this material was found mainly in the thermal gradient tube and on the first filter paper. Figure 8, which is a schematic illustration of the

Table 10. Distribution of ruthenium in high burnup tests

Test No. <sup>a</sup>	Test temp. (°C)	Test time (min)	Test atmosphere	Thermal gradient tube (μg)	Filter pack inlet fitting (μg)	First filter paper (μg)	Second filter paper (μg)	Third filter paper (μg)	First charcoal (μg)	Rate of release (μg/min)	First charcoal deposition (μg/min)
HBU-5	500	1200	Dry air	0.166	0.085	0.121	$2.26 \times 10^{-4}$	$1.02 \times 10^{-4}$	$160.0 \times 10^{-6}$	0.0016	$6.7 \times 10^{-7}$
HBU-6	700	300	Dry air	0.205	1.12	1.46	$3.52 \times 10^{-4}$	$0.41 \times 10^{-6}$	$81.0 \times 10^{-6}$	0.0093	$2.7 \times 10^{-7}$
HBU-4	500	1200	Steam-Ar	$8.6 \times 10^{-6}$	$1.6 \times 10^{-5}$	$2.8 \times 10^{-5}$	0.0	0.0	$560.0 \times 10^{-6}$	$5.1 \times 10^{-7}$	$4.7 \times 10^{-7}$
HBU-1	700	300	Steam-Ar	0.0 <sup>b</sup>	$0.9 \times 10^{-5}$	$1.9 \times 10^{-5}$	0.0	0.0	$120.0 \times 10^{-6}$	$4.9 \times 10^{-7}$	$4.0 \times 10^{-7}$
HBU-2	900	120	Steam-Ar	0.0	0.0	0.0	0.0	0.0	$33.0 \times 10^{-6}$	$2.7 \times 10^{-7}$	$2.7 \times 10^{-7}$
HBU-11	1200	27	Steam-Ar	0.0	0.0	0.0	0.0	0.0	0.0	0.0	0.0
HBU-7	900	1	Steam-He	- <sup>c</sup>	-	-	0.0	0.0	$8.3 \times 10^{-6}$	-	$83.0 \times 10^{-7}$
HBU-3	900	60	Steam-He	-	-	-	0.0	0.0	$8.8 \times 10^{-6}$	-	$1.5 \times 10^{-7}$
HBU-9	900-1100	8.4	Steam-He	-	-	-	0.0	0.0	$1.1 \times 10^{-6}$	-	$1.3 \times 10^{-7}$
HBU-10	900-1200	10	Steam-He	-	-	-	0.0	0.0	$0.9 \times 10^{-6}$	-	$0.9 \times 10^{-7}$
HBU-12	700-1200 <sup>d</sup>	d	Helium	0.0	0.0	0.0	0.0	0.0	0.0	0.0	0.0

<sup>a</sup>In tests HBU-1, -2, -4, -5, and -6, the fuel rod segments were predrilled to cause the simulated defects. The ruptured segment used in test HBU-7 was also used in test HBU-11. These tests were diffusional release tests. In tests HBU-8, -9, and -10, the segments were pressure-ruptured at 900°C and subsequently heated at the indicated temperatures. In test HBU-12, a special Zircaloy ferrule fitting at the outlet end provided the release opening through which the fission products were purged from the segment with purified helium.

<sup>b</sup>Amounts less than  $10^{-8}$  are given as 0.0.

<sup>c</sup>The dash signifies our inability to measure ruthenium because of the presence of fuel dust.

<sup>d</sup>See Fig. 34 for time-temperature sequence.

Table 11. Distribution of  $^{134}\text{Cs}$  in High Burnup Fuel Test 4<sup>a</sup>

Location	Temperature (°C)	Amount of $^{134}\text{Cs}$ found in each location			Total cesium ( $\mu\text{g}$ )
		$\mu\text{g}^b$	Percent of total <sup>c</sup>	Percent of released	
Fuel rod	500	(8908) <sup>d</sup>			(4.689 x 10 <sup>5</sup> ) <sup>d</sup>
Furnace tube	500				
Quartz liner		2.58 x 10 <sup>-4</sup>	2.90 x 10 <sup>-6</sup>	80.04	1.36 x 10 <sup>-2</sup>
Quartz fuel-rod holder		6.37 x 10 <sup>-5</sup>	7.15 x 10 <sup>-7</sup>	19.76	3.35 x 10 <sup>-3</sup>
Thermal gradient tube	350-200	2.76 x 10 <sup>-7</sup>	3.10 x 10 <sup>-9</sup>	0.086	1.45 x 10 <sup>-5</sup>
Filter pack components	130				
Stainless-steel inlet fitting		3.70 x 10 <sup>-8</sup>	4.15 x 10 <sup>-10</sup>	0.001	1.95 x 10 <sup>-6</sup>
Other housing components		2.37 x 10 <sup>-8</sup>	2.66 x 10 <sup>-10</sup>	0.007	1.25 x 10 <sup>-6</sup>
First filter paper		2.02 x 10 <sup>-7</sup>	2.27 x 10 <sup>-9</sup>	0.063	1.06 x 10 <sup>-5</sup>
Second filter paper		0.0	0.0	0.0	0.0
Third filter paper		0.0	0.0	0.0	0.0
Charcoal No. 1a		<1.17 x 10 <sup>-7</sup>	<1.30 x 10 <sup>-9</sup>	<0.04	<6.16 x 10 <sup>-6</sup>
Charcoal No. 1b		0.0	0.0	0.0	0.0
Charcoal No. 1c		0.0	0.0	0.0	0.0
Charcoal No. 2a		0.0	0.0	0.0	0.0
Charcoal No. 2b		0.0	0.0	0.0	0.0
Charcoal No. 3		0.0	0.0	0.0	0.0
AgX		0.0	0.0	0.0	0.0
Condenser assembly	0				
Condenser housing		0.0	0.0	0.0	0.0
Condensate		0.0	0.0	0.0	0.0
Freeze trap	-78	0.0	0.0	0.0	0.0
Cold charcoal traps (two)	-78	0.0	0.0	0.0	0.0
Total		3.22 x 10 <sup>-4</sup>	3.62 x 10 <sup>-6</sup>	100.00	1.70 x 10 <sup>-2</sup>

<sup>a</sup> Steam flow rate, 422 cm<sup>3</sup>/min (STP); argon flow rate, 58 cm<sup>3</sup>/min (STP); system pressure, 760 torr. Decay time, 911 days (to Nov. 21, 1976).

<sup>b</sup> Amounts less than 1.0 x 10<sup>-8</sup>  $\mu\text{g}$  are given as 0.0.

<sup>c</sup> Percentage of radioactive nuclide in fuel rod.

<sup>d</sup> Calculated for burnup of 31,360 MWd per MT of original uranium, 183.3 g of uranium originally in 12-in. segment, and 911 days of decay.

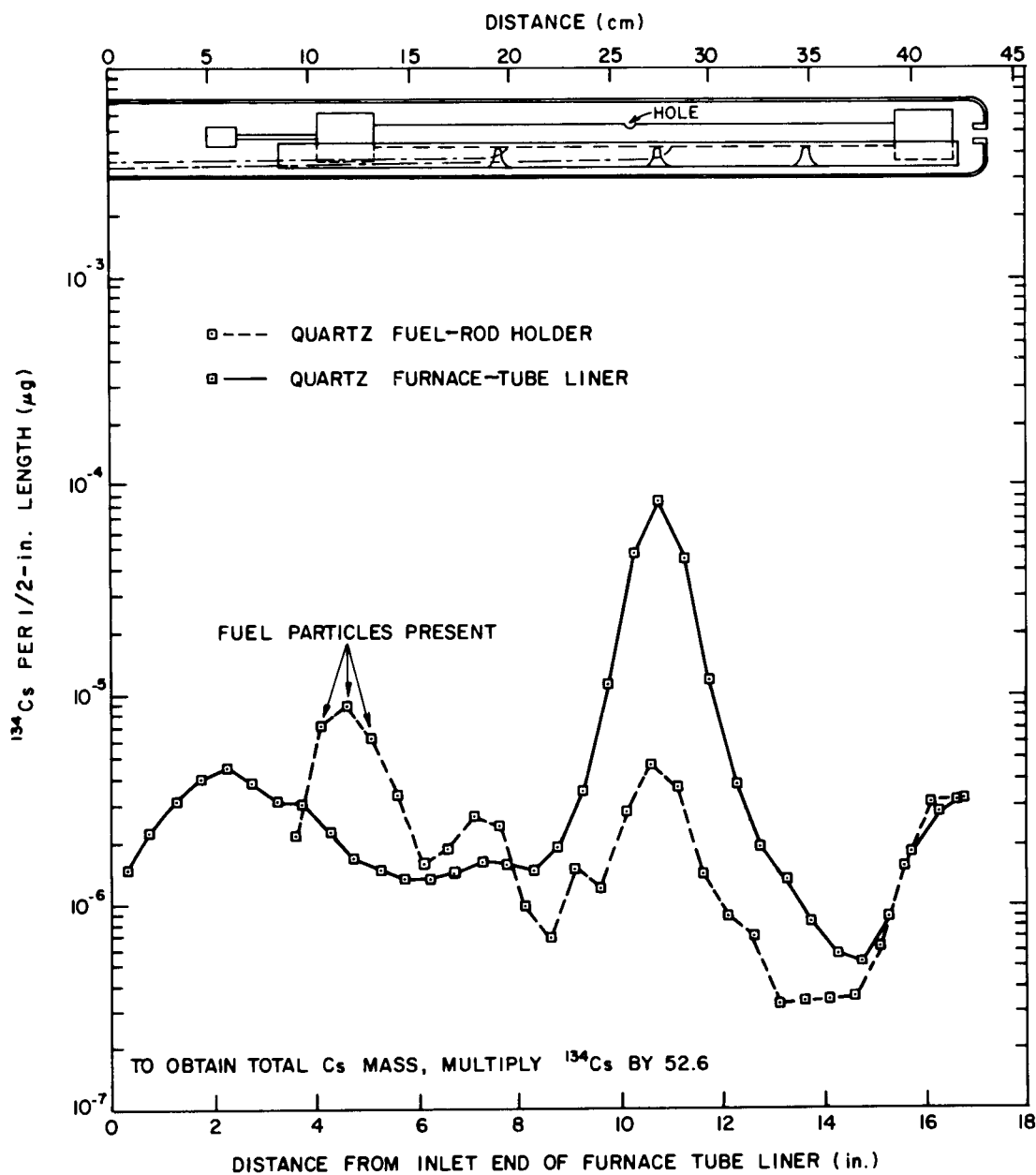


Fig. 8. Axial distributions of cesium on the furnace tube liner and fuel rod holder of test HBU-4.

axial concentration profiles of  $^{134}\text{Cs}$  in the furnace tube, shows that most of the cesium deposited near the defect opening. (This was also the case in the first two tests in steam atmospheres.) About 80% of the released cesium deposited on the quartz liner of the furnace tube and 19.3% deposited on the quartz fuel-rod holder.

Table 12 summarizes the  $^{129}\text{I}$  distribution in the collection apparatus. These data show that  $2.42 \times 10^{-4}\%$  ( $0.105 \mu\text{g}$ ) of the total iodine inventory was released. About six times more iodine than cesium was released, which indicated that the primary species of iodine that escaped from the segment was probably elemental iodine.

As depicted graphically in Fig. 9, approximately 0.63% (8.6 mCi) of the original  $^{85}\text{Kr}$  inventory was released in the first 13 hr at temperature. This rate of  $^{85}\text{Kr}$  release was lower than that observed in the  $900^\circ\text{C}$  test (HBU-2) in which 15 mCi (1.1% of the total  $^{85}\text{Kr}$  in the capsule) was released within a 20-min period at  $900^\circ\text{C}$ .

Approximately  $1.5 \times 10^{-7}\%$  ( $6.1 \times 10^{-4} \mu\text{g}$ ) of the total ruthenium inventory was released; as in tests HBU-1 and -2, it was found on cooler surfaces downstream. Table 10 gives the distribution in the apparatus. The largest portion ( $\sim 91\%$ ) of the released ruthenium was in the first charcoal cartridge.

#### 4.4 High Burnup Fuel Test 5 ( $500^\circ\text{C}$ , Dry Air)

This experiment was performed at  $500^\circ\text{C}$  for 20 hr. Fuel specimen A-5 from fuel rod D-12 was also used in High Burnup Fuel Test 4 which was conducted at  $500^\circ\text{C}$  over a 20-hr period in a flowing steam-argon atmosphere (Sect. 4.3). The specimen was heated with a resistance heater and maintained in a flowing dry-air atmosphere.

The posttest appearance of the fuel rod segment is shown in Fig. 10. The swollen region in the vicinity of the hole was caused by oxidation of the  $\text{UO}_2$  fuel. A small amount of oxidized fuel can be seen protruding from the hole.

Approximately 0.53% (7.3 mCi) of the original  $^{85}\text{Kr}$  inventory was released during the test. The chronology of this release is displayed

Table 12. Distribution of  $^{129}\text{I}$  in High Burnup Fuel Test 4<sup>a</sup>

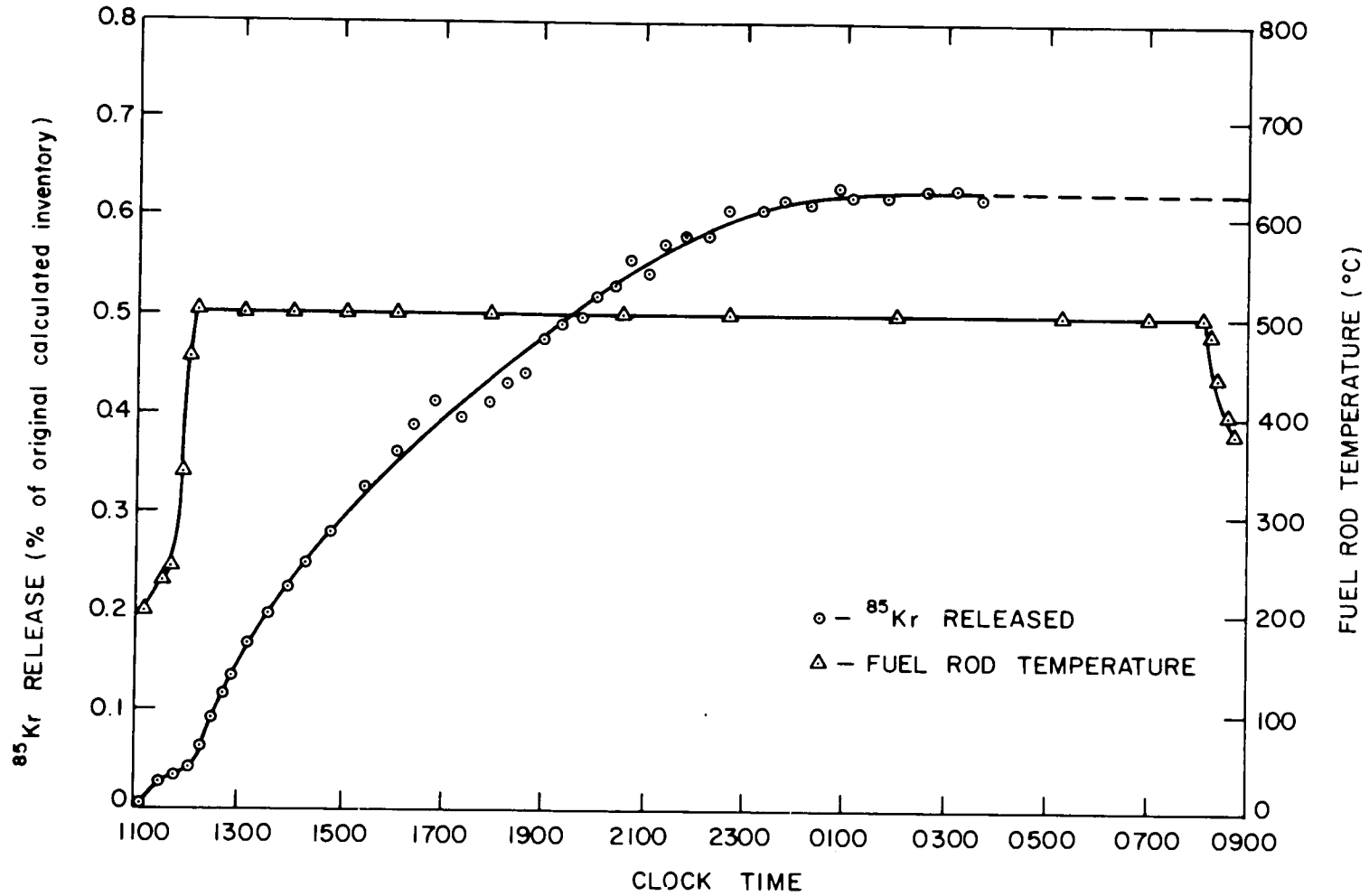
Location	Temperature (°C)	Amount of $^{129}\text{I}$ found each location		Total iodine ( $\mu\text{g}$ )	
		$\mu\text{g}^{\text{b}}$	Percent of total <sup>c</sup>		Percent of released
Fuel rod	500	$(3.40 \times 10^4)^{\text{d}}$		$(4.315 \times 10^4)^{\text{d}}$	
Furnace tube	500				
Quartz liner		$0.0222 \pm 0.006$ $0.005$	$6.53 \times 10^{-5}$	26.94	0.028
Quartz fuel-rod holder		$0.0091 \pm 0.005$ $0.004$	$2.68 \times 10^{-5}$	11.04	0.012
Thermal gradient tube	350-200	$0.0025 \pm 0.004$ $0.003$	$7.35 \times 10^{-6}$	3.03	0.003
Filter pack components	130				
Stainless-steel inlet fitting		$0.0026 \pm 0.003$	$7.65 \times 10^{-6}$	3.16	0.003
First filter paper		$\leq 0.014$	$4.12 \times 10^{-5}$	16.99	0.018
Second and third filter papers		$\leq 0.004$	$1.18 \times 10^{-5}$	4.85	0.005
Charcoal No. 1a		$0.0280 \pm 0.003$	$8.24 \times 10^{-5}$	33.98	0.036
Charcoal No. 1b		0.0	0.0	0.0	0.0
Charcoal No. 1c		0.0	0.0	0.0	0.0
Charcoal No. 2a		0.0	0.0	0.0	0.0
Charcoal No. 2b		0.0	0.0	0.0	0.0
Charcoal No. 3		0.0	0.0	0.0	0.0
AgX		0.0	0.0	0.0	0.0
Condenser	0	0.0	0.0	0.0	0.0
Freeze trap	-78	0.0	0.0	0.0	0.0
Cold charcoal traps (two)	-78	0.0	0.0	0.0	0.0
Total		$0.0824 \pm 0.021$ $0.018$	$2.42 \times 10^{-4}$	100.00	0.105

<sup>a</sup> Steam flow rate,  $422 \text{ cm}^3/\text{min}$  (STP); argon flow rate,  $58 \text{ cm}^3/\text{min}$  (STP); system pressure, 760 torr. Decay time, 911 days (to Nov. 2, 1976).

<sup>b</sup> Amounts less than  $1.0 \times 10^{-2} \mu\text{g}$  are given as 0.0.

<sup>c</sup> Percentage of radioactive nuclide in fuel rod.

<sup>d</sup> Calculated for burnup of 31,360 MWd per MT of original uranium, 183.3 g of uranium originally in 12-in. segment, and 911 days of decay.



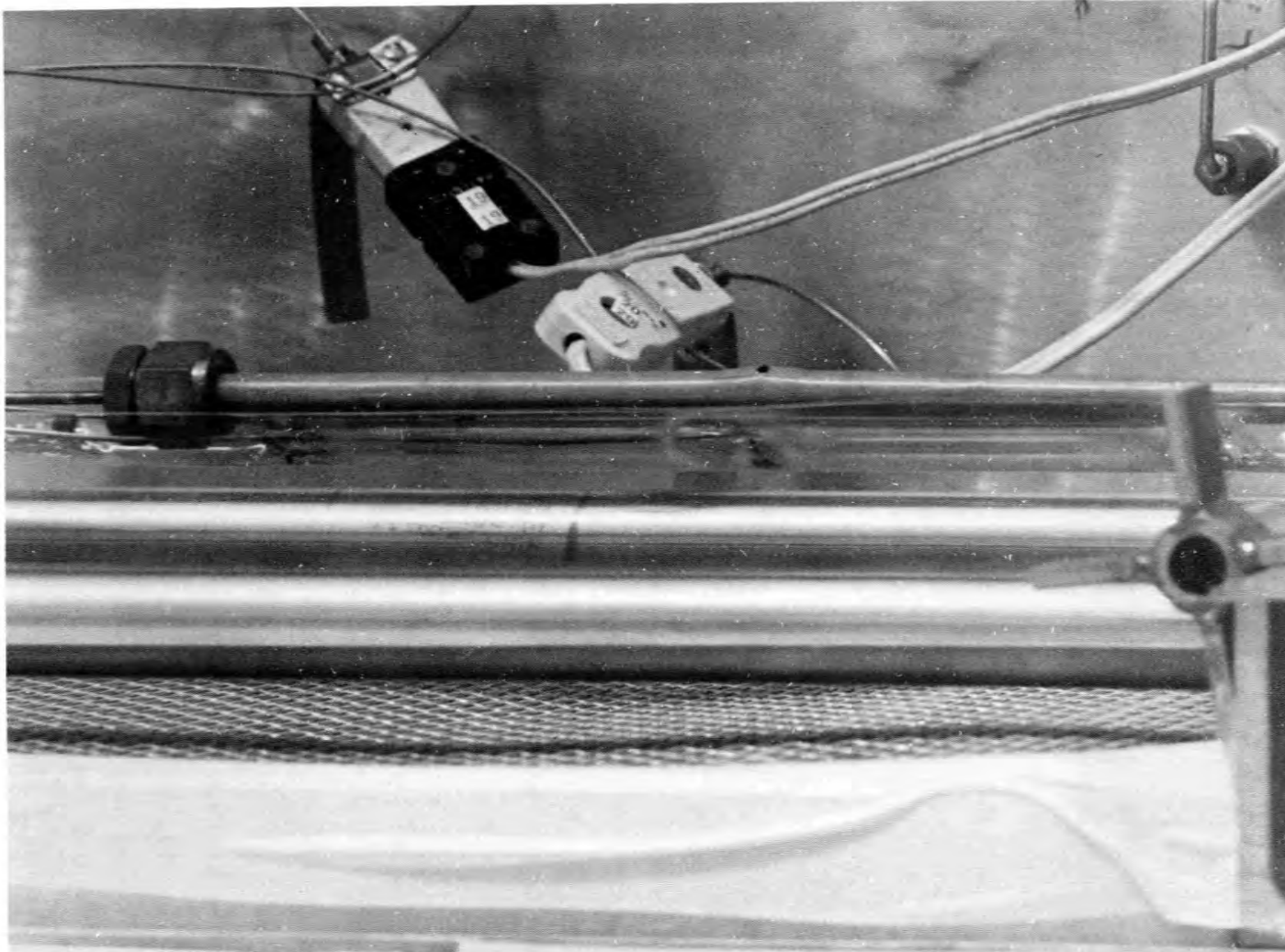


Fig. 10. Fuel rod segment A-5 of rod D-12 after a 20-hr exposure to air at 500°C.

graphically in Fig. 11. This rod segment was used in a previous 20-hr test at 500°C, during which time about 0.63% (8.6 mCi) of the original  $^{85}\text{Kr}$  escaped; thus, the additional release observed in this test is probably due to oxidation of the fuel. As is evident in Fig. 11, cessation of krypton release occurred after 4 hr of testing; this suggests that the defect hole became plugged and prevented further oxidation of the fuel. Apparently, the release of other fission product nuclides was similarly halted.

The posttest distribution of  $^{134}\text{Cs}$  in the collection system is summarized in Table 13. These data indicate that  $5.1 \times 10^{-7}\%$  ( $2.4 \times 10^{-3} \mu\text{g}$ ) of the total cesium inventory was released. If it is assumed that little additional cesium was released after 4 hr, as is likely, then the linear release rate would be  $1.3 \times 10^{-7}\%/hr$  (as compared with a linear release rate of  $1.8 \times 10^{-7}\%/hr$  in High Burnup Fuel Test 4).

Small particles of oxidized fuel were present on the fuel rod holder. Determinations were made of  $^{144}\text{Ce}$  (assumed to remain unseparated from the fuel) which indicated that approximately 5.84 mg of fuel remained on the holder even after loose particles were removed. This amount of fuel originally contained 5.83  $\mu\text{g}$  of  $^{137}\text{Cs}$ , precisely the amount found by the direct counting of  $^{137}\text{Cs}$  on the fuel rod holder. In order to obtain an estimate of the very small amount of cesium deposited on the fuel rod holder from transported vapor, we used the ratio of cesium on the holder to cesium on the quartz liner as measured in test HBU-6 (a dry air test at 700°C in which no fuel dusting occurred). We calculated that 0.00082  $\mu\text{g}$  of cesium deposited on the fuel rod holder from the vapor phase compared with 5.83  $\mu\text{g}$  present within adhering particles of fuel.

The distribution of iodine at the end of the test is given in Table 14. Approximately 0.014% (6.028  $\mu\text{g}$ ) of the iodine inventory was released. Most of the released iodine (96%) transported downstream beyond the furnace tube and was primarily collected as elemental iodine. About 88% was found on the charcoal. The cesium release was insignificant compared with the iodine release. Iodine found in the thermal gradient tube was primarily located at the cool end at temperatures <275°C.

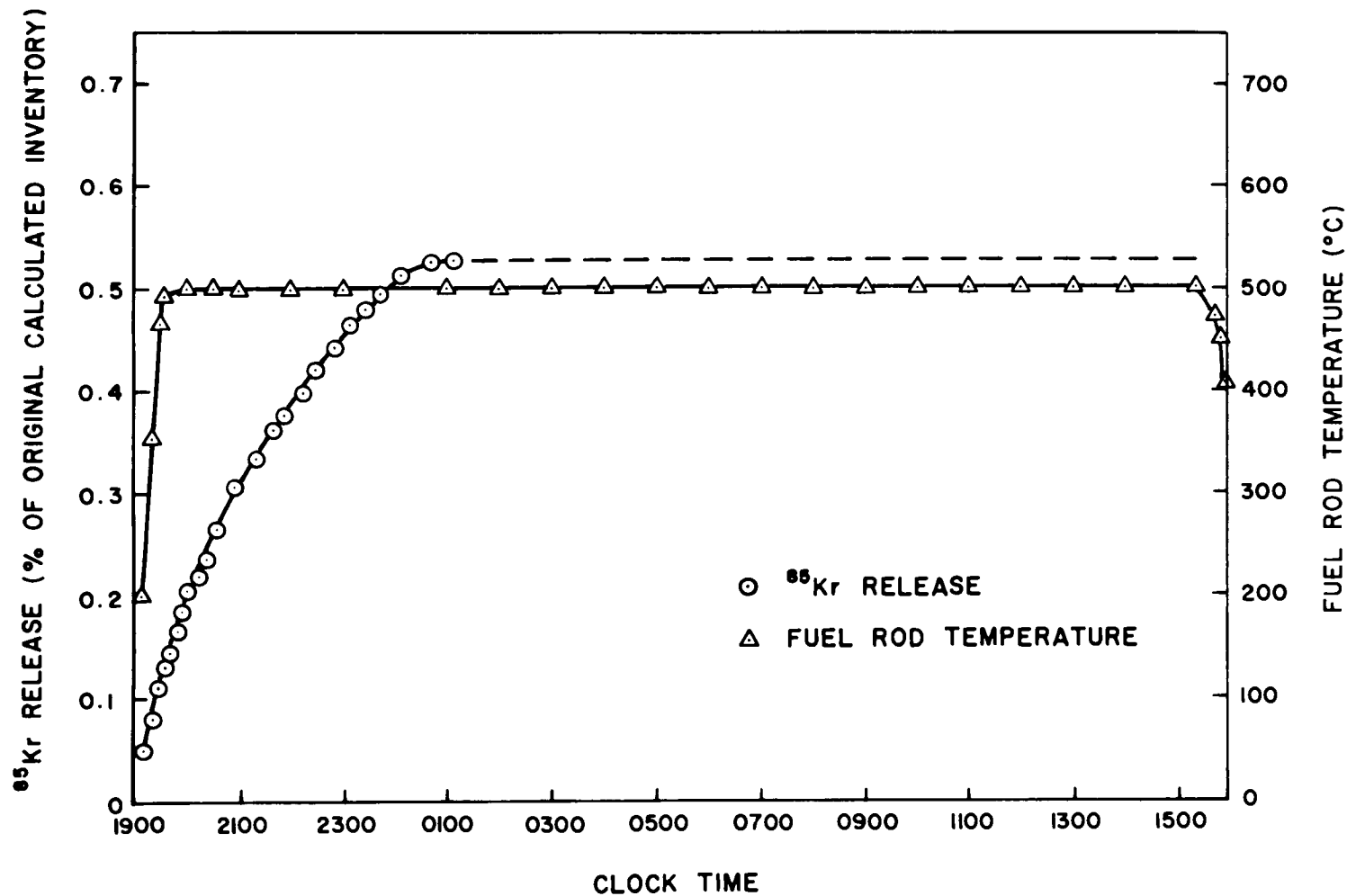


Table 13. Distribution of  $^{134}\text{Cs}$  in High Burnup Fuel Test 5<sup>a</sup>

Location	Temperature (°C)	Amount of $^{134}\text{Cs}$ found in each location			Total cesium ( $\mu\text{g}$ )
		$\mu\text{g}$ <sup>b</sup>	Percent of total <sup>c</sup>	Percent of released	
Fuel rod	500	(8908) <sup>d</sup>			(4.689 x 10 <sup>-5</sup> ) <sup>d</sup>
Furnace tube	500				
Quartz liner		1.93 x 10 <sup>-5</sup>	2.17 x 10 <sup>-7</sup>	42.20	1.02 x 10 <sup>-3</sup>
Quartz fuel-rod holder		1.55 x 10 <sup>-5</sup> <sup>e</sup>	1.74 x 10 <sup>-7</sup>	33.89	8.16 x 10 <sup>-4</sup>
Thermal gradient tube	640-200	6.07 x 10 <sup>-6</sup>	6.80 x 10 <sup>-8</sup>	13.27	3.20 x 10 <sup>-4</sup>
Filter pack components	125				
Stainless-steel inlet fitting		1.4 x 10 <sup>-6</sup> <sup>f</sup>	1.57 x 10 <sup>-8</sup>	3.06	7.37 x 10 <sup>-5</sup>
Other housing components		0.0	0.0	0.0	0.0
First filter paper		3.42 x 10 <sup>-6</sup>	3.84 x 10 <sup>-8</sup>	7.48	1.80 x 10 <sup>-4</sup>
Second filter paper		9.90 x 10 <sup>-9</sup>	1.11 x 10 <sup>-10</sup>	0.02	5.21 x 10 <sup>-7</sup>
Third filter paper		9.25 x 10 <sup>-9</sup>	1.04 x 10 <sup>-10</sup>	0.02	4.87 x 10 <sup>-7</sup>
Charcoal No. 1a		2.45 x 10 <sup>-8</sup>	2.75 x 10 <sup>-10</sup>	0.05	1.29 x 10 <sup>-6</sup>
Charcoal No. 1b		0.0	0.0	0.0	0.0
Charcoal No. 1c		0.0	0.0	0.0	0.0
Charcoal No. 2a		0.0	0.0	0.0	0.0
Charcoal No. 2b		0.0	0.0	0.0	0.0
Charcoal No. 3		0.0	0.0	0.0	0.0
AgX		0.0	0.0	0.0	0.0
Freeze trap	-78	0.0	0.0	0.0	0.0
Cold charcoal traps (two)	-78	0.0	0.0	0.0	0.0
Total		4.57 x 10 <sup>-5</sup>	5.13 x 10 <sup>-7</sup>	100.00	2.41 x 10 <sup>-3</sup>

<sup>a</sup>Dry-air flow rate, 351 cm<sup>3</sup>/min (STP); system pressure, 760 torr. Decay time, 911 days (to Nov. 2, 1976).

<sup>b</sup>Amounts less than 1.0 x 10<sup>-9</sup>  $\mu\text{g}$  are given as 0.0.

<sup>c</sup>Percentage of radioactive nuclide in fuel rod.

<sup>d</sup>Calculated for burnup of 31,360 MWD per MT of original uranium, 183.3 g of uranium originally in 12-in. segment, and 911 days of decay.

<sup>e</sup>Estimated amount of vapor-deposited  $^{134}\text{Cs}$ . Excludes 0.25  $\mu\text{g}$  present with adhering small particles of fuel.

<sup>f</sup>Estimated amount. Cesium-134 could not be detected because of high  $^{106}\text{Ru}$  activity.

Table 14. Distribution of  $^{129}\text{I}$  in High Burnup Fuel Test 5<sup>a</sup>

Location	Temperature (°C)	Amount of $^{129}\text{I}$ found in each location			Total iodine ( $\mu\text{g}$ )
		$\mu$	Percent of total <sup>c</sup>	Percent of released	
Fuel rod	500	(3.40 x 10 <sup>4</sup> ) <sup>d</sup>			(4.315 x 10 <sup>4</sup> ) <sup>d</sup>
Furnace tube	500				
Quartz liner		0.0	1.47 x 10 <sup>-6</sup>	0.01	0.001
Quartz fuel-rod holder		0.1673 ± 0.009	4.92 x 10 <sup>-4</sup>	3.52	0.212
Thermal gradient tube	640-200	0.3475 ± 0.053	1.02 x 10 <sup>-3</sup>	7.32	0.441
Filter pack components	125				
Stainless-steel inlet fitting		0.0062 ± 0.003	1.82 x 10 <sup>-5</sup>	0.13	0.008
First filter paper		≤0.03	8.82 x 10 <sup>-5</sup>	≤0.63	≤0.038
Second and third filter papers		≤0.03	8.82 x 10 <sup>-5</sup>	≤0.63	≤0.038
Charcoal No. 1a		4.1680 ± 0.1	1.23 x 10 <sup>-2</sup>	87.76	5.290
Charcoal No. 1b		0.0	0.0	0.0	0.0
Charcoal No. 1c		0.0	0.0	0.0	0.0
Charcoal No. 2a		0.0	0.0	0.0	0.0
Charcoal No. 2b <sup>e</sup>		0.0	0.0	0.0	0.0
Charcoal No. 3 <sup>e</sup>		0.0	0.0	0.0	0.0
AgX <sup>e</sup>		0.0	0.0	0.0	0.0
Condenser <sup>e</sup>	0	0.0	0.0	0.0	0.0
Freeze trap <sup>e</sup>	-78	0.0	0.0	0.0	0.0
Cold charcoal traps (two) <sup>e</sup>	-78	0.0	0.0	0.0	0.0
Total		4.7495 ± 0.17	1.4 x 10 <sup>-2</sup>	100.00	6.028

<sup>a</sup> Dry-air flow rate, 354 cm<sup>3</sup>/min (STP); system pressure, 760 torr. Decay time, 911 days (to Nov. 2, 1976).

<sup>b</sup> Amounts less than 1.0 x 10<sup>-2</sup>  $\mu\text{g}$  are given as 0.0.

<sup>c</sup> Percentage of radioactive nuclide in fuel rod.

<sup>d</sup> Calculated for burnup of 31,360 MWd per MT of original uranium, 183.3 g of uranium originally in 12-in. segment, and 911 days of decay.

<sup>e</sup> Not analyzed for  $^{129}\text{I}$  content in any of the High Burnup Series Tests; amount assumed to be 0.0.

The most notable result of this experiment was the relatively large release of ruthenium. Only trace amounts were released in the three prior tests, which were conducted in steam. The ruthenium distribution data, which are presented in Table 15, indicate that  $9.04 \times 10^{-5}\%$  (0.373  $\mu\text{g}$ ) of the total ruthenium inventory was released. Also, about 99% of the released ruthenium deposited on the cooler surfaces of the collection apparatus, especially at the outlet end of the gold thermal-gradient tube (300 to 200°C) as illustrated in Fig. 12, in the stainless steel inlet to the filter pack (125°C), and on the first filter paper (125°C).

#### 4.5 High Burnup Fuel Test 6 (700°C, Dry Air)

Test HBU-6 was the second experiment conducted in the High Burnup Fuel Test Series in which a dry air atmosphere was employed. A resistance heater, which surrounded the furnace tube, was used to maintain fuel rod segment A-2 of fuel rod D-12 at 700°C for 5 hr. Unlike the rod segment employed in test HBU-5, no previous testing had been performed on this fuel specimen. Determination of radial gap size via a gas flow technique indicated a pellet-to-clad gap space in the fuel rod segment of about 18  $\mu\text{m}$  (see Appendix A). The distributions of radionuclides  $^{134}\text{Cs}$ ,  $^{106}\text{Ru}$ , and  $^{129}\text{I}$  at the conclusion of the test are summarized in Tables 16-18 respectively.

Figure 13 shows the region of the hole in which some swelling occurred as a result of fuel oxidation. Also, as in test HBU-5, a small quantity of fuel can be seen protruding from the defect hole.

The exterior coloration of the cladding was copper-to-pink, and the surface texture appeared to be smooth and unbroken. This cladding surface phenomenon has been observed in all our tests (irradiated and unirradiated) conducted at 700°C, irrespective of the test atmosphere (steam or air).

The release of  $^{85}\text{Kr}$  during the experiment (see Fig. 14) amounted to approximately 1.24% (15.5 mCi) of the original inventory. Because no other tests were performed with the fuel specimen, this value represents the release of recoil-implanted krypton (releasable at  $\leq 700^\circ\text{C}$ ) from the fuel and cladding surface layers of the gap region, as well as krypton released by fuel oxidation.

Table 15. Distribution of  $^{106}\text{Ru}$  in High Burnup Fuel Test 5<sup>a</sup>

Location	Temperature (°C)	Amount of $^{106}\text{Ru}$ found in each location			Total ruthenium ( $\mu\text{g}$ )
		$\mu\text{g}^{\text{b}}$	Percent of total <sup>c</sup>	Percent of released	
Fuel rod	500	(5928) <sup>d</sup>			(4.168 x 10 <sup>5</sup> ) <sup>d</sup>
Furnace tube	500				
Quartz liner		6.14 x 10 <sup>-5</sup>	1.04 x 10 <sup>-6</sup>	1.15	4.32 x 10 <sup>-3</sup>
Quartz fuel-rod holder		0.0	0.0	0.0	0.0
Thermal gradient tube	640-200	2.36 x 10 <sup>-3</sup>	3.98 x 10 <sup>-5</sup>	44.04	1.66 x 10 <sup>-1</sup>
Filter pack components	125				
Stainless-steel inlet fitting		1.21 x 10 <sup>-3</sup>	2.04 x 10 <sup>-5</sup>	22.58	8.51 x 10 <sup>-2</sup>
Other housing components		1.00 x 10 <sup>-7</sup>	1.68 x 10 <sup>-8</sup>	0.002	7.02 x 10 <sup>-5</sup>
First filter paper		1.72 x 10 <sup>-3</sup>	2.90 x 10 <sup>-5</sup>	32.10	1.21 x 10 <sup>-1</sup>
Second filter paper		3.22 x 10 <sup>-6</sup>	5.43 x 10 <sup>-8</sup>	0.060	2.26 x 10 <sup>-4</sup>
Third filter paper		1.45 x 10 <sup>-6</sup>	2.45 x 10 <sup>-8</sup>	0.027	1.02 x 10 <sup>-4</sup>
Charcoal No. 1a		2.27 x 10 <sup>-6</sup>	3.83 x 10 <sup>-8</sup>	0.042	1.60 x 10 <sup>-4</sup>
Charcoal No. 1b		0.0	0.0	0.0	0.0
Charcoal No. 1c		0.0	0.0	0.0	0.0
Charcoal No. 2a		0.0	0.0	0.0	0.0
Charcoal No. 3		0.0	0.0	0.0	0.0
AgX		0.0	0.0	0.0	0.0
Freeze	-78	0.0	0.0	0.0	0.0
Cold charcoal traps (two)	-78	0.0	0.0	0.0	0.0
Total		5.36 x 10 <sup>-3</sup>	9.04 x 10 <sup>-5</sup>	100.00	3.77 x 10 <sup>-1</sup>

<sup>a</sup>Dry-air flow rate, 354 cm<sup>3</sup>/min (STP); system pressure, 760 torr. Decay time, 911 days (to Nov. 2, 1976).

<sup>b</sup>Amounts less than 1.0 x 10<sup>-7</sup>  $\mu\text{g}$  are given as 0.0.

<sup>c</sup>Percentage of radioactive nuclide in fuel rod.

<sup>d</sup>Calculated for burnup of 31,360 MWd per MT of original uranium, 183.3 g of uranium originally in 12-in. segment, and 911 days of decay.

ORNL DWG. 77-1162A

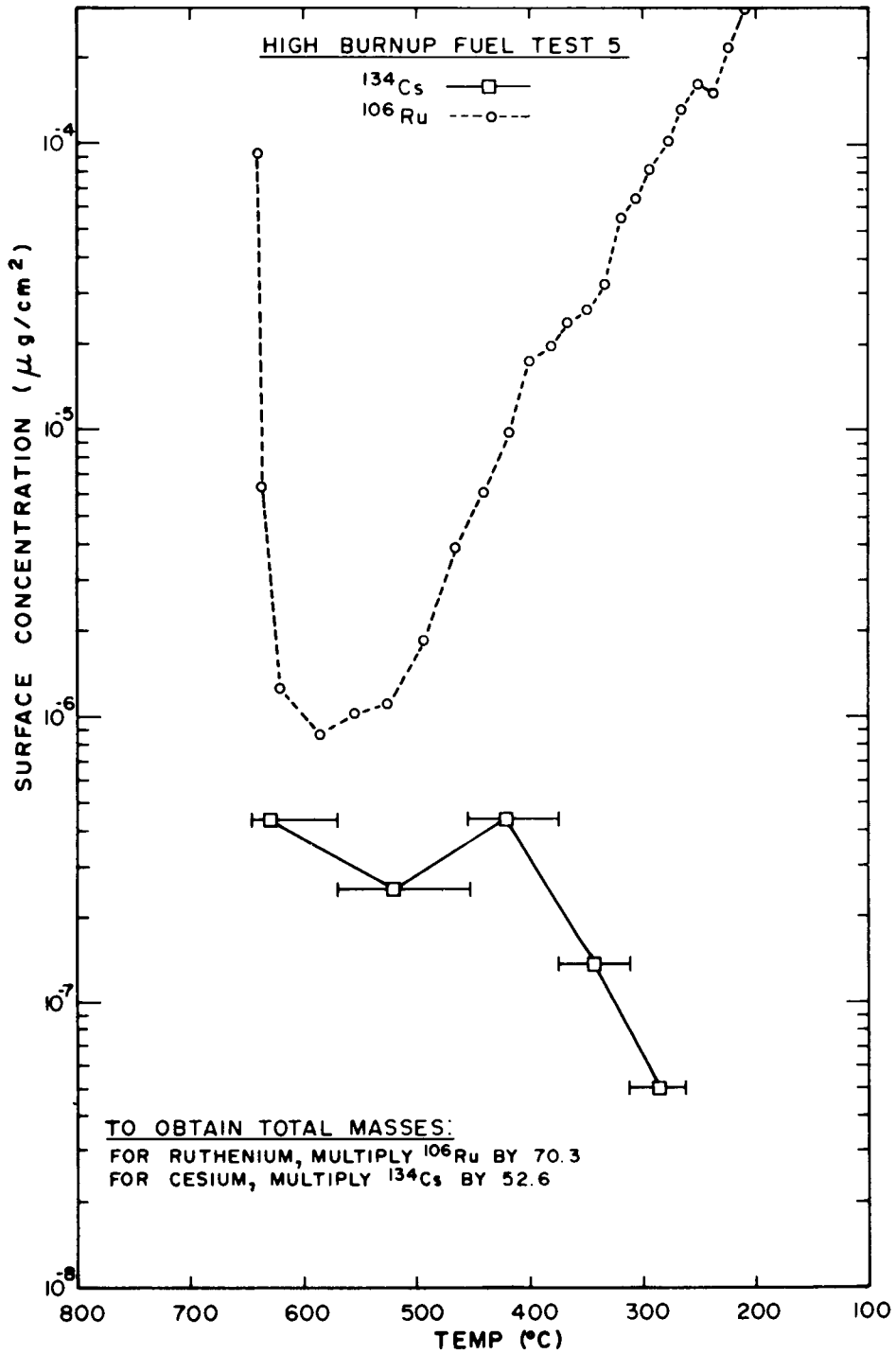


Fig. 12. Distribution of  $^{134}\text{Cs}$  and  $^{106}\text{Ru}$  deposited in the thermal gradient tube during run HBU-5.

Table 16. Distribution of  $^{134}\text{Cs}$  in High Burnup Fuel Test 6<sup>a</sup>

Location	Temperature (°C)	Amount of $^{134}\text{Cs}$ found in each location			Total cesium ( $\mu\text{g}$ )
		$\mu\text{g}$ <sup>b</sup>	Percent of total <sup>c</sup>	Percent of released	
Fuel rod	700	(8192) <sup>d</sup>			(4.312 x 10 <sup>5</sup> ) <sup>d</sup>
Furnace tube	700				
Quartz liner		1.93 x 10 <sup>-2</sup>	2.36 x 10 <sup>-4</sup>	16.48	1.016
Quartz fuel-rod holder		1.55 x 10 <sup>-2</sup>	1.90 x 10 <sup>-4</sup>	13.27	8.18 x 10 <sup>-1</sup>
Thermal gradient tube	700-210	7.97 x 10 <sup>-2</sup>	9.73 x 10 <sup>-4</sup>	68.06	4.195
Filter pack components	125				
Stainless-steel inlet fitting		7.10 x 10 <sup>-4</sup>	8.66 x 10 <sup>-6</sup>	0.61	3.74 x 10 <sup>-2</sup>
Other housing components					
First filter paper		1.85 x 10 <sup>-3</sup>	2.66 x 10 <sup>-5</sup>	1.58	9.74 x 10 <sup>-2</sup>
Second filter paper		0.0	0.0	0.0	0.0
Third filter paper		0.0	0.0	0.0	0.0
Charcoal No. 1a		0.0	0.0	0.0	0.0
Charcoal No. 1b		0.0	0.0	0.0	0.0
Charcoal No. 1c		0.0	0.0	0.0	0.0
Charcoal No. 2a		0.0	0.0	0.0	0.0
Charcoal No. 2b		0.0	0.0	0.0	0.0
AgX		0.0	0.0	0.0	0.0
Freeze trap	-78	0.0	0.0	0.0	0.0
Cold charcoal traps (two)	-78	0.0	0.0	0.0	0.0
Total		0.1171	1.43 x 10 <sup>-3</sup>	100.00	6.164

<sup>a</sup> Dry-air flow rate, 363 cm<sup>3</sup>/min (STP); system pressure, 760 torr. Decay time, 911 days (to Nov. 2, 1976).

<sup>b</sup> Amounts less than 1.0 x 10<sup>-8</sup>  $\mu\text{g}$  are given as 0.0.

<sup>c</sup> Percentage of radioactive nuclide in fuel rod.

<sup>d</sup> Calculated for burnup of 28,850 MWD per MT of original uranium, 183.3 g of uranium originally in 12-in. segment, and 911 days of decay.

Table 17. Distribution of  $^{129}\text{I}$  in High Burnup Fuel Test 6<sup>a</sup>

Location	Temperature (°C)	Amount of $^{129}\text{I}$ found in each location			Total iodine ( $\mu\text{g}$ )
		$\mu\text{g}^b$	Percent of total <sup>c</sup>	Percent of released	
Fuel rod	700	(3.128 x 10 <sup>4</sup> ) <sup>d</sup>			(3.970 x 10 <sup>4</sup> ) <sup>d</sup>
Furnace tube					
Quartz liner		0.0040 ± 0.004 0.002	1.28 x 10 <sup>-5</sup>	0.03	0.005
Quartz fuel-rod holder		0.0173 ± 0.009 0.008	5.53 x 10 <sup>-5</sup>	0.11	0.022
Thermal gradient tube	700-210	0.2181 ± 0.013	6.97 x 10 <sup>-4</sup>	1.45	0.277
Filter pack components	125				
Stainless-steel inlet fitting		0.0113 ± 0.003 0.003	3.61 x 10 <sup>-5</sup>	0.07	0.014
First filter paper		0.094 ± 0.04	3.01 x 10 <sup>-4</sup>	0.63	0.119
Second and third filter papers		≤ 0.094	3.01 x 10 <sup>-4</sup>	0.63	0.119
Charcoal No. 1a		14.5220 ± 0.30	4.64 x 10 <sup>-2</sup>	96.89	18.431
Charcoal No. 1b		0.0280 ± 0.003	8.95 x 10 <sup>-5</sup>	0.19	0.036
Charcoal No. 1c		0.0	0.0	0.0	0.0
Charcoal No. 2a		0.0	0.0	0.0	0.0
Charcoal No. 2b		0.0	0.0	0.0	0.0
Charcoal No. 3		0.0	0.0	0.0	0.0
AgX		0.0	0.0	0.0	0.0
Condenser	0	0.0	0.0	0.0	0.0
Freeze trap	-78	0.0	0.0	0.0	0.0
Cold charcoal traps (two)	-78	0.0	0.0	0.0	0.0
Total		14.9887 ± 0.34 0.33	4.79 x 10 <sup>-2</sup>	100.00	19.023

<sup>a</sup>Dry-air flow rate, 363 cm<sup>3</sup>/min (STP); system pressure, 760 torr. Decay time, 911 days (to Nov. 2, 1976).

<sup>b</sup>Amounts less than 1.0 x 10<sup>-2</sup>  $\mu\text{g}$  are given as 0.0.

<sup>c</sup>Percentage of radioactive nuclide in fuel rod.

<sup>d</sup>Calculated for burnup of 28,850 MWd per MT of original uranium, 183.3 g of uranium originally in 12-in. segment, and 911 days of decay.

Table 18. Distribution of  $^{106}\text{Ru}$  in High Burnup Fuel Test 6<sup>a</sup>

Location	Temperature (°C)	Amount of $^{106}\text{Ru}$ found in each location			Total ruthenium ( $\mu\text{g}$ )
		$\mu\text{g}$ <sup>b</sup>	Percent of total <sup>c</sup>	Percent of released	
Fuel rod	700	(5452) <sup>d</sup>			(3.83 x 10 <sup>5</sup> ) <sup>d</sup>
Furnace tube	700				
Quartz liner		0.0	0.0	0.0	0.0
Quartz fuel-rod holder		0.0	0.0	0.0	0.0
Gold thermal gradient tube	700-210	2.91 x 10 <sup>-3</sup>	5.34 x 10 <sup>-5</sup>	7.35	2.05 x 10 <sup>-1</sup>
Filter pack components	125				
Stainless-steel inlet fitting		1.59 x 10 <sup>-2</sup>	2.92 x 10 <sup>-4</sup>	40.13	1.116
Other housing components		0.0	0.0	0.0	0.0
First filter paper		2.08 x 10 <sup>-2</sup>	3.82 x 10 <sup>-4</sup>	52.50	1.462
Second filter paper		5.01 x 10 <sup>-6</sup>	9.19 x 10 <sup>-8</sup>	0.013	3.52 x 10 <sup>-4</sup>
Third filter paper		5.82 x 10 <sup>-7</sup>	1.07 x 10 <sup>-8</sup>	0.002	4.09 x 10 <sup>-5</sup>
Charcoal No. 1a		1.15 x 10 <sup>-6</sup>	2.11 x 10 <sup>-8</sup>	0.003	8.07 x 10 <sup>-5</sup>
Charcoal No. 1b		0.0	0.0	0.0	0.0
Charcoal No. 1c		0.0	0.0	0.0	0.0
Charcoal No. 2a		0.0	0.0	0.0	0.0
Charcoal No. 2b		0.0	0.0	0.0	0.0
Charcoal No. 3		0.0	0.0	0.0	0.0
AgX		0.0	0.0	0.0	0.0
Freeze trap	-78	0.0	0.0	0.0	0.0
Cold charcoal traps (two)	-78	0.0	0.0	0.0	0.0
Total		3.96 x 10 <sup>-2</sup>	7.27 x 10 <sup>-4</sup>	100.00	2.785

<sup>a</sup> Dry-air flow rate, 363 cm<sup>3</sup>/min (STP); system pressure, 760 torr. Decay time, 911 days (to Nov. 2, 1976).

<sup>b</sup> Amounts less than 1.0 x 10<sup>-7</sup>  $\mu\text{g}$  are given as 0.0.

<sup>c</sup> Percentage of radioactive nuclide in fuel rod.

<sup>d</sup> Calculated for burnup of 28,850 MWd per MT of original uranium, 183.3 g of uranium originally in 12-in. segment, and 911 days of decay.

ORNL-PHOTO 2153-77

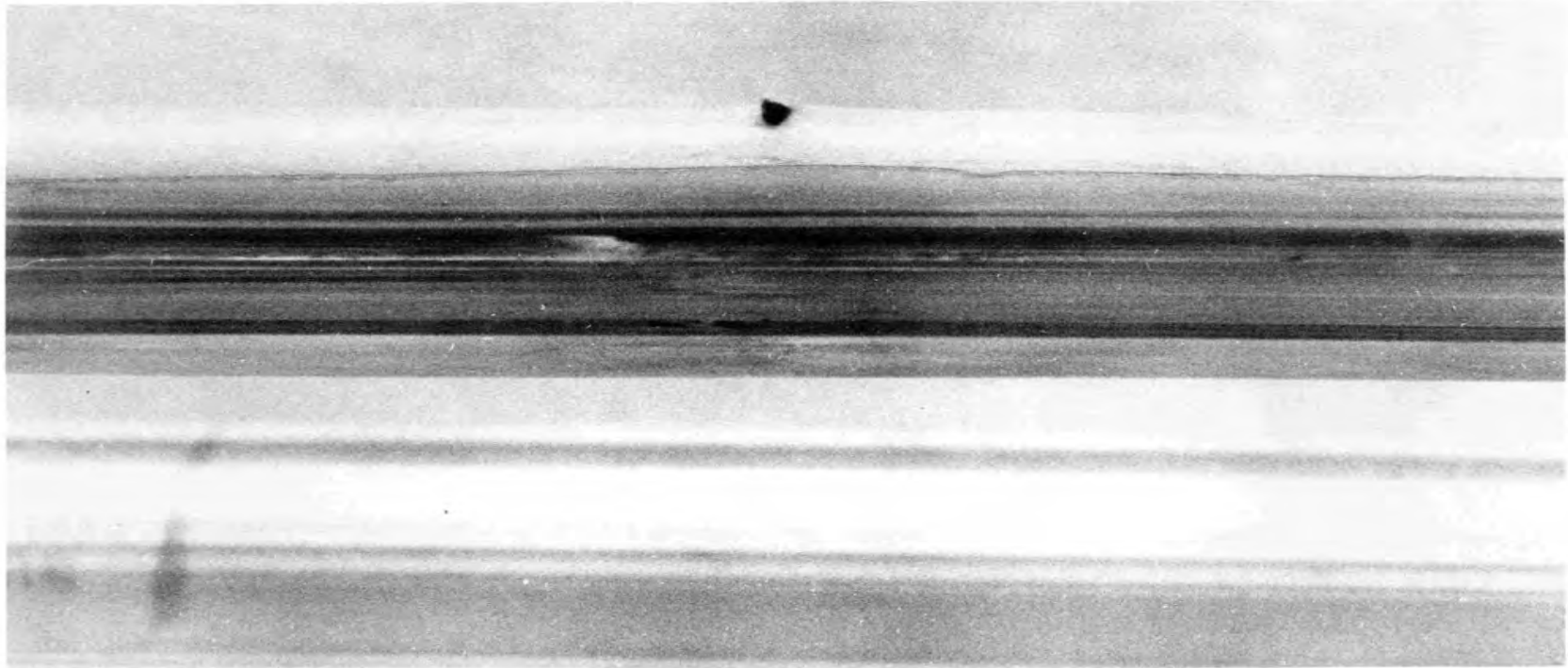


Fig. 13. Fuel rod segment A-2 of rod D-12 after a 5-hr exposure to air at 700°C.

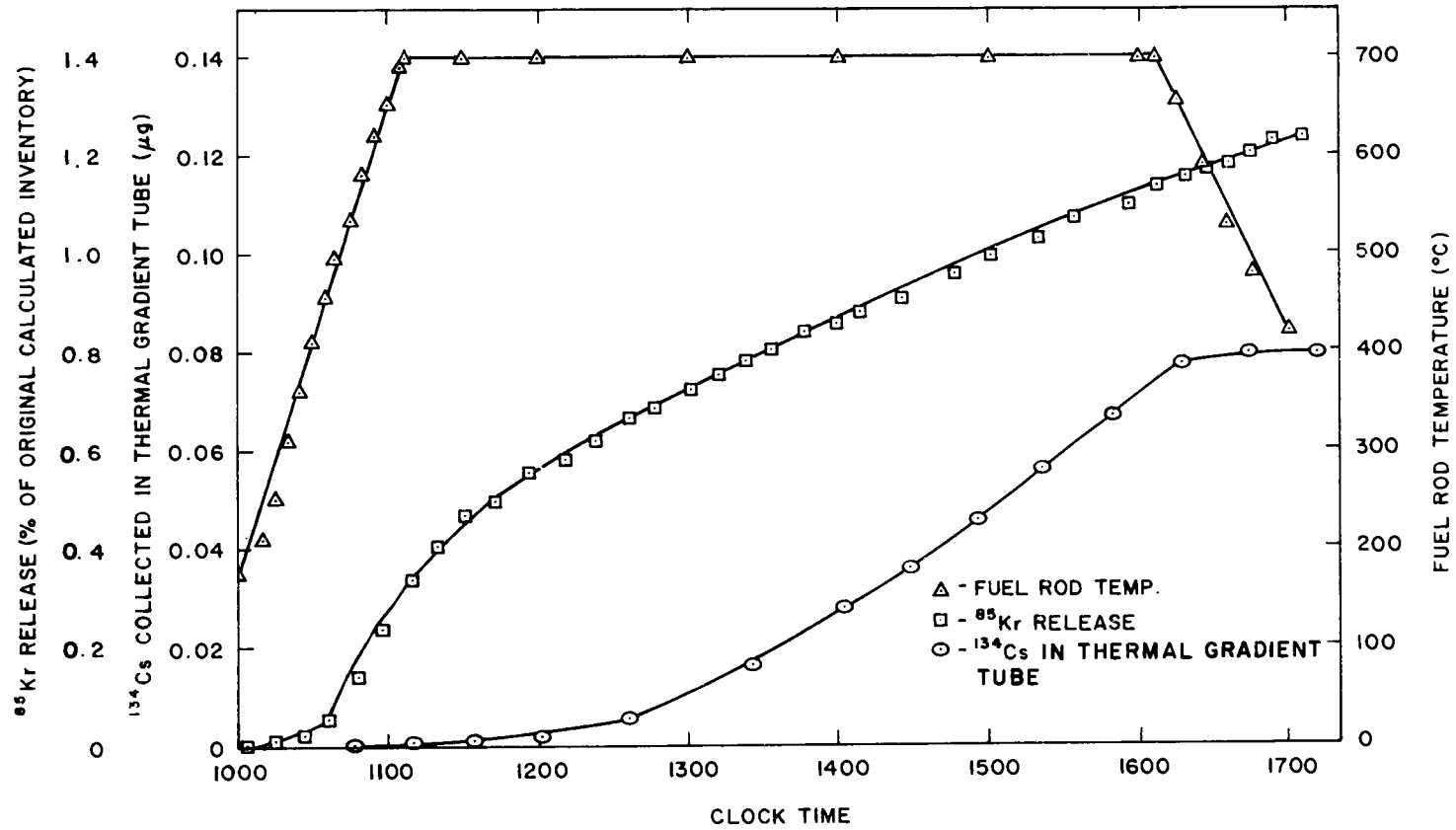


Fig. 14. Temperature and release of  $^{85}\text{Kr}$  and  $^{134}\text{Cs}$  during test HBU-6.

Approximately  $1.43 \times 10^{-3}\%$  (6.16  $\mu\text{g}$ ) of the total cesium inventory of the rod segment was released. Contrary to the results obtained for rods tested in steam where less than 0.2% of the released cesium was transported beyond the quartz furnace tube, about 70% of the released cesium did so in this test. Most of it deposited in the gold thermal-gradient tube. Concentration profiles of  $^{134}\text{Cs}$  and  $^{106}\text{Ru}$  along the thermal gradient tube are presented in Fig. 15. The cesium peak occurs at about  $400^\circ\text{C}$ . Continuous monitoring of the thermal gradient tube and filter pack, as is depicted graphically in Fig. 14, indicates that little cesium deposited there in the first hour after the test temperature ( $700^\circ\text{C}$ ) was reached. Subsequently, a desorption rate of about  $0.02 \mu\text{g}$  of  $^{134}\text{Cs}$  per hr (or  $1.08 \mu\text{g}$  of cesium per hr) resulted. The released cesium appears to have reacted initially with the quartz liner in a manner which passivates it, thus allowing additional released cesium to be transported downstream. The  $^{134}\text{Cs}$  distribution displayed in Fig. 15 indicates that the cesium was more or less evenly deposited on the furnace tube liner downstream of the defect hole.

Table 16, which is a summary of the iodine deposition, shows that 0.048% (19.02  $\mu\text{g}$ ) of the iodine inventory in the segment was released. All but 0.14% of the released iodine was found downstream, primarily as elemental iodine; about 97% was found on charcoal section 1a. Three times more iodine was released than cesium.

As in test HBU-5, there was considerable ruthenium release; approximately  $7.27 \times 10^{-4}\%$  (2.78  $\mu\text{g}$ ) of the total ruthenium inventory was released. Similarly, the distribution data presented in Table 10 indicate that the ruthenium released is in a very volatile form. In effect, all of the released ruthenium was transported downstream to the cool end ( $300$  to  $125^\circ\text{C}$ ) of the collection train before being deposited. About 7% deposited at the end of the gold thermal-gradient tube, yielding a profile displayed in Fig. 15; the remainder deposited on the stainless-steel inlet fitting and the first filter paper, both at about  $125^\circ\text{C}$ .

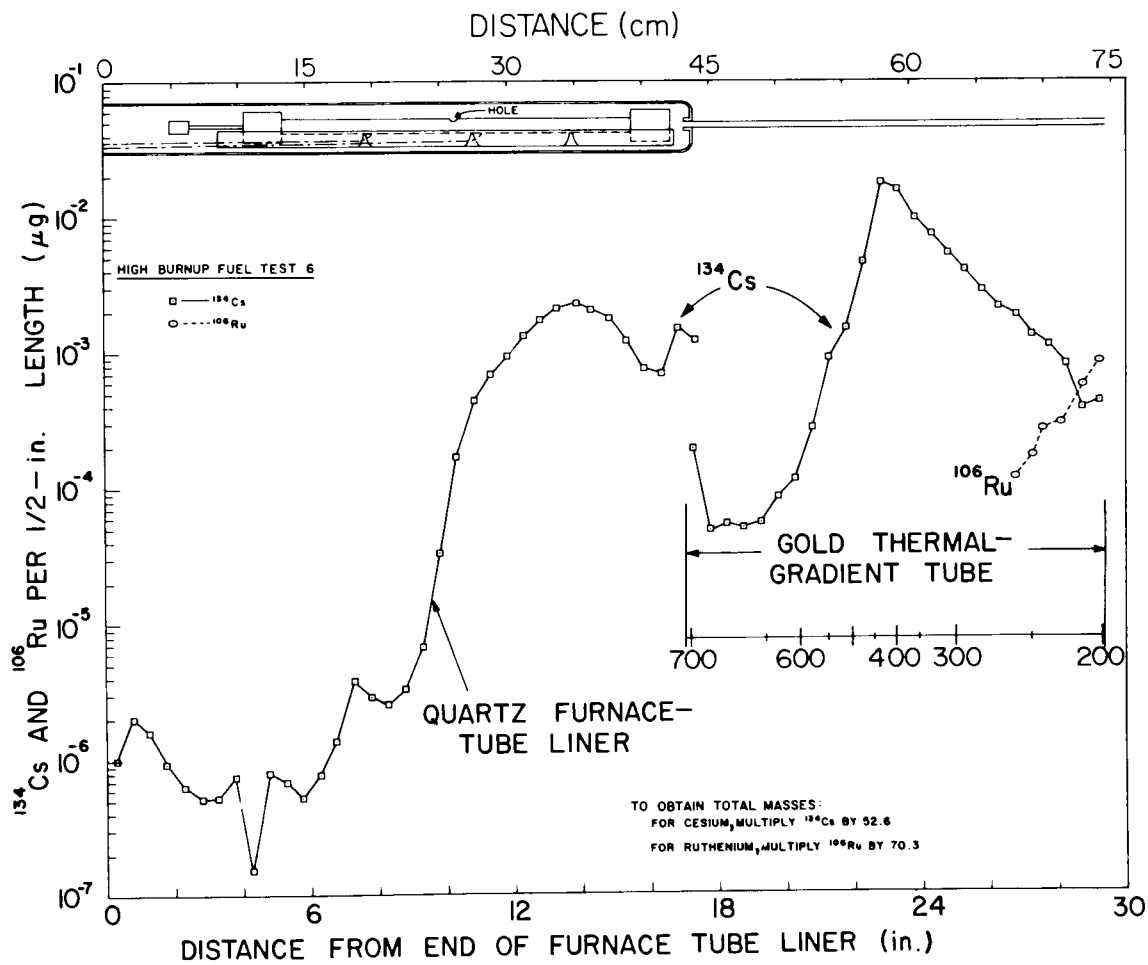


Fig. 15. Distribution of  $^{134}\text{Cs}$  and  $^{106}\text{Ru}$  in the furnace tube liner and thermal gradient tube in test HBU-6.

#### 4.6 High Burnup Fuel Test 7 (900°C)

This experiment was conducted at 900°C for 1 min in a flowing steam and helium atmosphere. Its principal objective was to measure quantitatively the fission products released at the time of rupture. In prior tests with predrilled rod segments, the releases were only diffusional in nature.

In the prerupture stage of the test, approximately 302 psig (2.08 MPa) of helium pressure was added to the rod segment (B-6 of fuel rod H-15) while it was at about 500°C. Because of a slight leak at one of the end fittings, a pressure adjustment was made while the segment was at 760°C. Subsequently, the temperature of the rod was raised at a rate of 2.7°C/sec to 908°C, where rupture occurred; at this point, the pressure was 275 psig (1.89 MPa). A photograph of the ruptured rod is shown in Fig. 16.

Table 19 gives the distribution of vapor-deposited  $^{134}\text{Cs}$  as found in the experimental apparatus after the test. These data indicate that 0.0286% (130.6  $\mu\text{g}$ ) of the total cesium inventory was released. The amount of cesium released in 2 hr by diffusion from a predrilled hole in test HBU-2 (also at 900°C steam) was only 0.00061% (2.82  $\mu\text{g}$ ), a factor of 47 less than was released in the vapor form in this test. Examination of the data in Table 19 reveals that 13% of the released cesium was transported beyond the furnace tube and deposited in the thermal gradient tube and on the first paper of the filter pack. In the predrilled experiments, which were also conducted in steam, only a fraction of a percent of the cesium was transported downstream. Part of this difference may be the result of the higher steam flow rate used with the burst experiments.

Fuel dust was ejected from the rod segment during rupture. Based on the analysis of  $^{154}\text{Eu}$  (assuming no loss of europium from the  $\text{UO}_2$  particles), it is estimated that 0.0160% (33.2 mg) of the fuel was released. As can be seen from the data presented in Table 20, which is a summary of the distribution of fuel particles in the experimental apparatus, the largest amount of this dust (98%) was found in the furnace tube.

ORNL-PHOTO 3774-77



Fig. 16. Posttest view of the rod segment used in test HBU-7, as taken through the cell window.

Table 19. Distribution of  $^{134}\text{Cs}$  in High Burnup Fuel Test 7<sup>a</sup>

Location	Temperature (°C)	Amount of $^{134}\text{Cs}$ found in each location			Total cesium ( $\mu\text{g}$ )
		$\mu\text{g}^{\text{b}}$	Percent of total <sup>c</sup>	Percent of released	
Fuel rod (original)	900	(8685) <sup>d</sup>			( $4.572 \times 10^5$ ) <sup>d</sup>
Furnace tube	200-700				
Quartz liner		1.932	$2.22 \times 10^{-2}$	77.87	101.6
Quartz fuel-rod holder		$2.25 \times 10^{-1}$	$2.59 \times 10^{-3}$	9.07	11.84
Thermal gradient tube	690-240	$1.66 \times 10^{-1}$	$1.91 \times 10^{-3}$	6.69	8.7
Filter pack components	130				
Stainless-steel inlet fitting		$8.90 \times 10^{-3}$	$1.01 \times 10^{-4}$	0.36	0.4
Other housing components		0.0	0.0	0.0	0.0
First filter paper		$1.49 \times 10^{-1}$	$1.72 \times 10^{-3}$	6.01	7.84
Second filter paper		$9.69 \times 10^{-5}$	$1.12 \times 10^{-6}$	0.004	0.005
Third filter paper		0.0	0.0	0.0	0.0
Charcoal No. 1a		0.0	0.0	0.0	0.0
Charcoal No. 1b		0.0	0.0	0.0	0.0
Charcoal No. 1c		0.0	0.0	0.0	0.0
Charcoal No. 2a		0.0	0.0	0.0	0.0
Charcoal No. 2b		0.0	0.0	0.0	0.0
Charcoal No. 3		0.0	0.0	0.0	0.0
AgX		0.0	0.0	0.0	0.0
Condenser	0	0.0	0.0	0.0	0.0
Freeze trap	-78	0.0	0.0	0.0	0.0
Cold charcoal traps (two)	-78	0.0	0.0	0.0	0.0
Total released		2.481	0.0286	100.0	130.58

<sup>a</sup>Steam flow rate,  $1840 \text{ cm}^3/\text{min}$  (STP); helium flow rate,  $280 \text{ cm}^3/\text{min}$  (STP); system pressure, 760 torr. Decay time, 911 days (to Nov. 2, 1976).

<sup>b</sup>Amounts less than  $1.0 \times 10^{-8} \mu\text{g}$  are given as 0.0.

<sup>c</sup>Percentage of radioactive nuclide in fuel rod.

<sup>d</sup>Calculated for burnup of 30,580 MWd per MT of original uranium, 183.3 g of uranium originally in 12-in. segment, and 911 days of decay.

Table 20. Distribution of  $\text{UO}_2$  fuel particles released at the time of rupture in High Burnup Fuel Test 7

Location	$\text{UO}_2$ fuel particles <sup>a</sup>		$^{134}\text{Cs}$ present in fuel particles <sup>b</sup> ( $\mu\text{g}$ )
	mg	Percent of released	
Furnace tube			
Quartz liner	29.88 <sup>c</sup>	89.97	1.248
Fuel rod holder	2.61	7.86	0.109
Thermal gradient tube			
Filter pack			
Stainless-steel inlet fitting	0.17	0.51	0.007
First filter paper	0.55	1.66	0.023
Total	33.21	100.0	1.387 <sup>d</sup>

<sup>a</sup>Estimated on the basis of  $^{154}\text{Eu}$  analysis. It was assumed that there was no loss of europium from the  $\text{UO}_2$  particles.

<sup>b</sup>Calculation based on  $^{134}\text{Cs}/^{154}\text{Eu}$  ratio in loose fuel particles.

<sup>c</sup>Loose particles, 7.46 mg; adhering particles, 22.43 mg.

<sup>d</sup>Equivalent to 73.0  $\mu\text{g}$  of total cesium.

Profiles of  $^{134}\text{Cs}$  deposition along the quartz furnace-tube liner, the fuel rod holder, and the gold liner of the quartz thermal-gradient tube are shown in Fig. 17 (loose particles of fuel were dumped from the furnace tube liner before scanning). About 32.6% of the  $^{134}\text{Cs}$  in the liner and on the holder was present in adhering fuel particles. The largest amount of the released cesium, both as vapor and cesium in fuel particles, was found at the rupture location. A cesium peak occurred in the thermal gradient tube at about 400°C.

It was determined in posttest analysis that 0.0265% (11.13  $\mu\text{g}$ ) of the iodine inventory was released from the segment. Iodine distribution in the apparatus is tabulated in Table 21. These data suggest that iodine was released primarily as  $\text{CsI}$ ; only about 3.6% of the iodine deposited as elemental iodine. A comparison of the cesium data in Table 19 with iodine data in Table 21 shows that approximately 12 times more cesium (mass) was

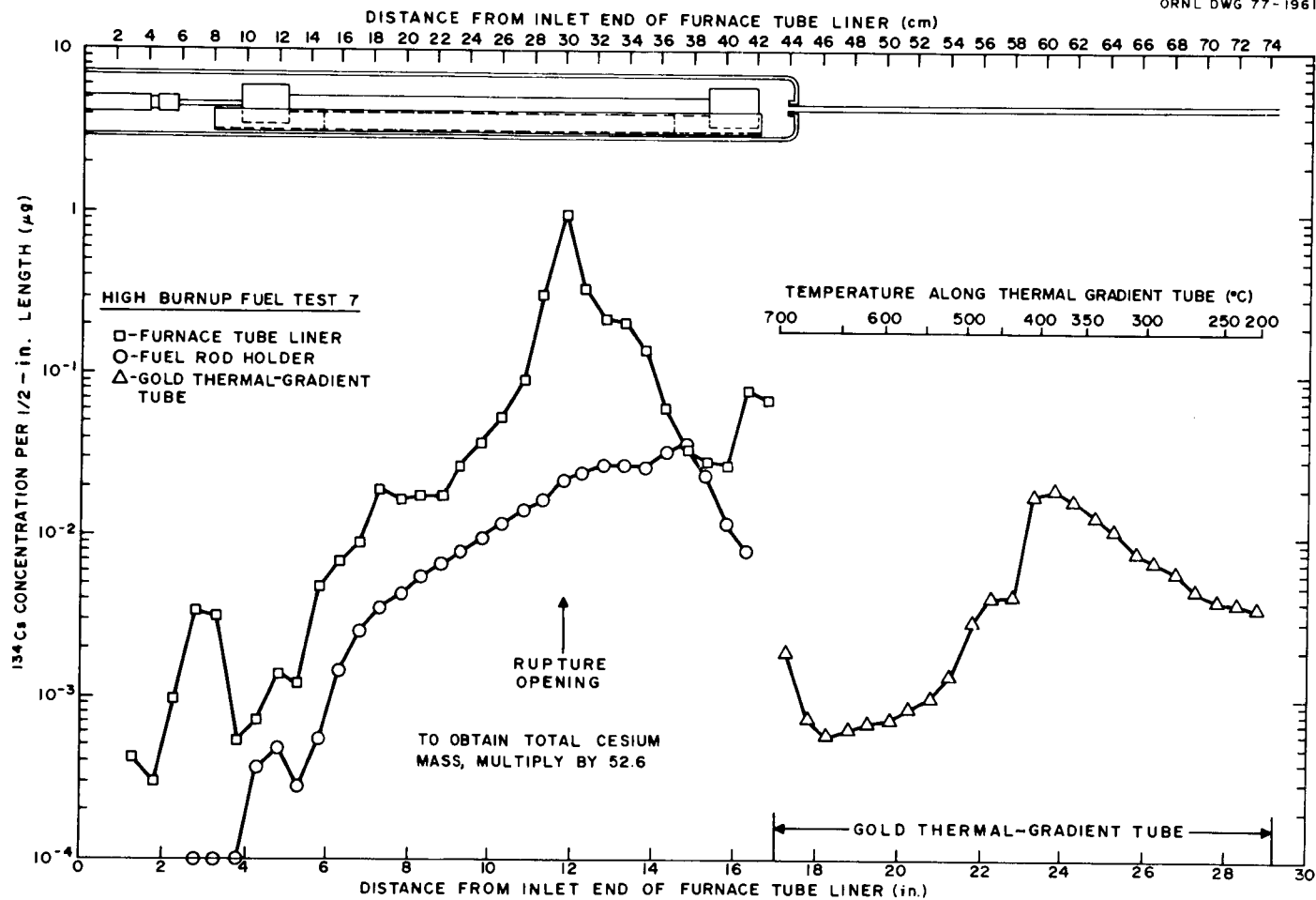


Fig. 17. Distribution of  $^{134}\text{Cs}$  in furnace tube and thermal gradient tube of test HBU-7.

Table 21. Distribution of  $^{129}\text{I}$  in High Burnup Fuel Test 7<sup>a</sup>

Location	Temperature (°C)	Amount of $^{129}\text{I}$ found in each location			Total iodine ( $\mu\text{g}$ )
		$\mu\text{g}^{\text{b}}$	Percent of total <sup>c</sup>	Percent of released	
Fuel rod	900	$(3.316 \times 10^4)^{\text{d}}$			$(4.208 \times 10^4)^{\text{d}}$
Furnace tube	200-700				
Quartz liner		$1.71 \pm 0.5$	$5.17 \times 10^{-3}$	19.49	2.17
Quartz fuel-rod holder		$1.40 \pm 0.6$	$4.22 \times 10^{-3}$	15.96	1.78
Thermal gradient tube	690-240	$3.09 \pm 0.03$	$9.32 \times 10^{-3}$	35.23	3.92
Filter pack components	130				
Stainless-steel inlet fitting		$0.265 \pm 0.03$	$7.99 \times 10^{-4}$	3.02	0.34
First filter paper		$1.99 \pm 0.01$	$6.00 \times 10^{-3}$	22.69	2.52
Second and third filter papers		$0.032 \pm 0.006$	$9.65 \times 10^{-5}$	0.36	0.04
Charcoal No. 1a		$0.285 \pm 0.03$	$8.60 \times 10^{-4}$	3.25	0.36
Charcoal No. 1b		0.0	0.0	0.0	0.0
Charcoal No. 1c		0.0	0.0	0.0	0.0
Charcoal No. 2a		0.0	0.0	0.0	0.0
Charcoal No. 2b <sup>e</sup>		0.0	0.0	0.0	0.0
Charcoal No. 3 <sup>e</sup>		0.0	0.0	0.0	0.0
AgX <sup>3</sup>		0.0	0.0	0.0	0.0
Condenser <sup>e</sup>	0	0.0	0.0	0.0	0.0
Freeze trap <sup>e</sup>	-78	0.0	0.0	0.0	0.0
Cold charcoal traps (two) <sup>e</sup>	-78	0.0	0.0	0.0	0.0
Total		$8.772 \pm 1.2$	$2.65 \times 10^{-2}$	100.00	11.13

<sup>a</sup>Steam flow rate, 1840 cm<sup>3</sup>/min (STP); helium flow rate, 280 cm<sup>3</sup>/min (STP); system pressure, 760 torr. Decay time, 911 days (to Nov. 2, 1976).

<sup>b</sup>Amounts less than  $1.0 \times 10^{-2}$   $\mu\text{g}$  are given as 0.0.

<sup>c</sup>Percentage of radioactive nuclide in fuel rod.

<sup>d</sup>Calculated for burnup of 30,580 MWd per MT of original uranium originally in 12-in. segment, and 911 days of decay.

<sup>e</sup>Not analyzed for  $^{129}\text{I}$  content in any of the High Burnup Series Tests; amount assumed to be 0.0.

released than iodine. The iodine that was found in the thermal gradient tube was deposited in the same temperature region as was the cesium (Fig. 17).

About 0.97% (12.9 mCi) of the total  $^{85}\text{Kr}$  inventory was released during the course of the experiment. This  $^{85}\text{Kr}$  release was almost equal to that obtained in HBU-2, a 2-hr test at  $900^\circ\text{C}$ . In HBU-2, 15 mCi (1.1% of the total  $^{85}\text{Kr}$  in the capsule) was released. However, cessation of release was noted after 20 min. The release rate of  $^{85}\text{Kr}$  is depicted graphically in Fig. 18. Because of the slight leak at one of the end fittings of the rod segment, krypton started collecting in the cold charcoal traps during the heatup period before rupture. Also, approximately 36% of the released krypton was collected slowly over a 37-min period after the rod had been cooled to  $400^\circ\text{C}$ .

The results obtained for cesium by continuous monitoring of the thermal gradient tube and filter pack, also shown in Fig. 18, indicates that most of the cesium deposited there shortly after the rupture occurred.

Table 10 shows that  $8.3 \times 10^{-6}$   $\mu\text{g}$  of ruthenium that was released as a vapor was collected in the first charcoal cartridge. The presence of ejected fuel dust on many of the upstream surfaces prevented the measurement of ruthenium on these surfaces; the activity of the condensed ruthenium vapor was insignificant compared with the activity of the dust.

#### 4.7 High Burnup Fuel Test 8 ( $900^\circ\text{C}$ )

Test HBU-8 was also conducted at  $900^\circ\text{C}$  in a steam-helium atmosphere, but the fuel rod segment (B-2 of fuel rod H-15) was maintained at the test temperature for 1 hr rather than 1 min as in HBU-7.

Approximately 307 psig (2.12 MPa) of helium was applied internally to the rod segment while it was at  $745^\circ\text{C}$  during the prerupture heat treatment. Subsequently, the temperature was raised steadily at the rate of about  $2.4^\circ\text{C}/\text{sec}$  until rupture occurred at  $895^\circ\text{C}$ . The recorder chart for the fuel rod pressure indicated that swelling (drop in pressure) began at about  $833^\circ\text{C}$ . Immediately before rupture, the internal pressure of the rod was 269 psig (1.85 MPa). Figure 19 shows the posttest appearance of the

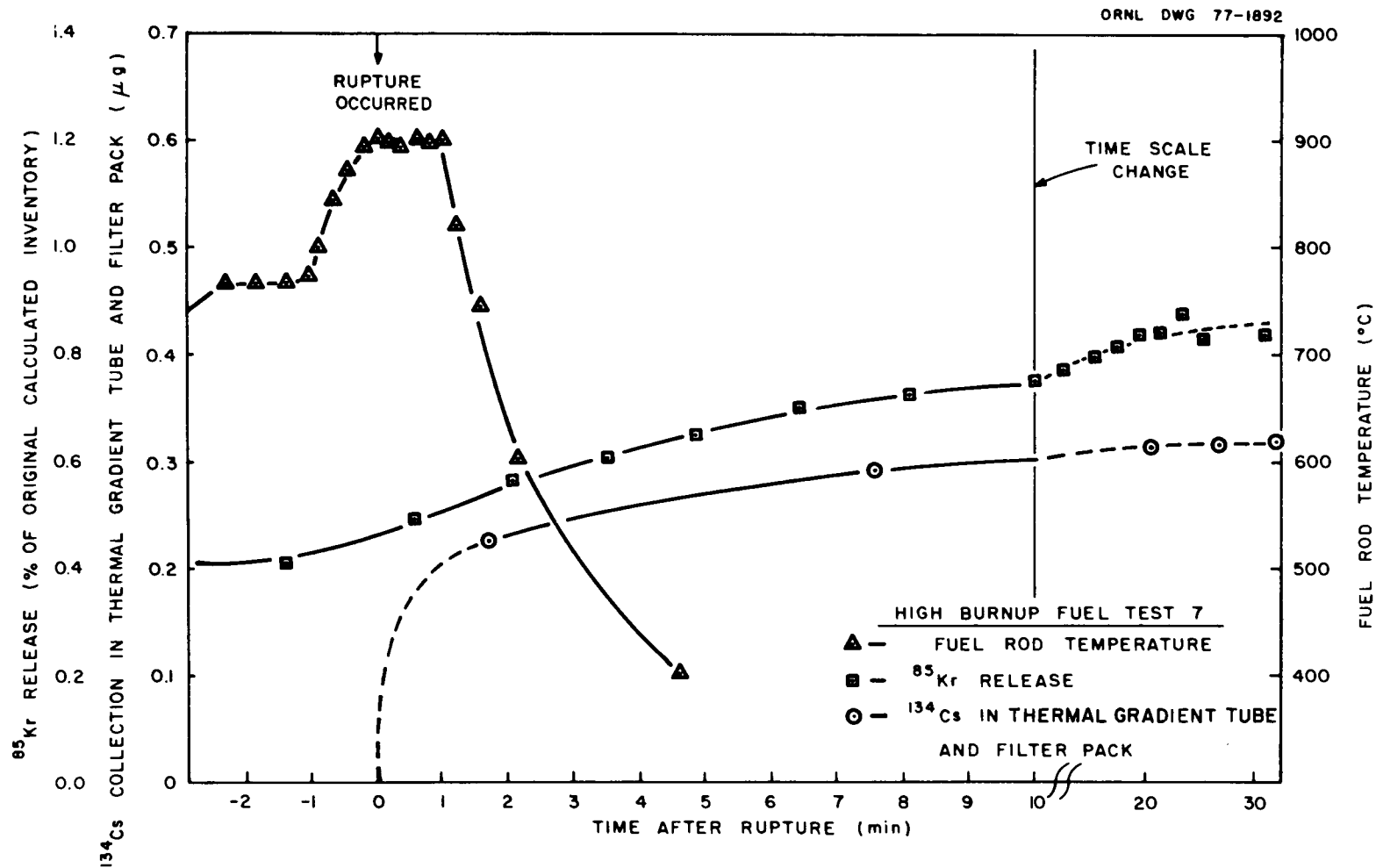


Fig. 18. Collection of <sup>134</sup>Cs in the thermal gradient tube and filter pack and of <sup>85</sup>Kr in the cold charcoal traps during test HBU-7.

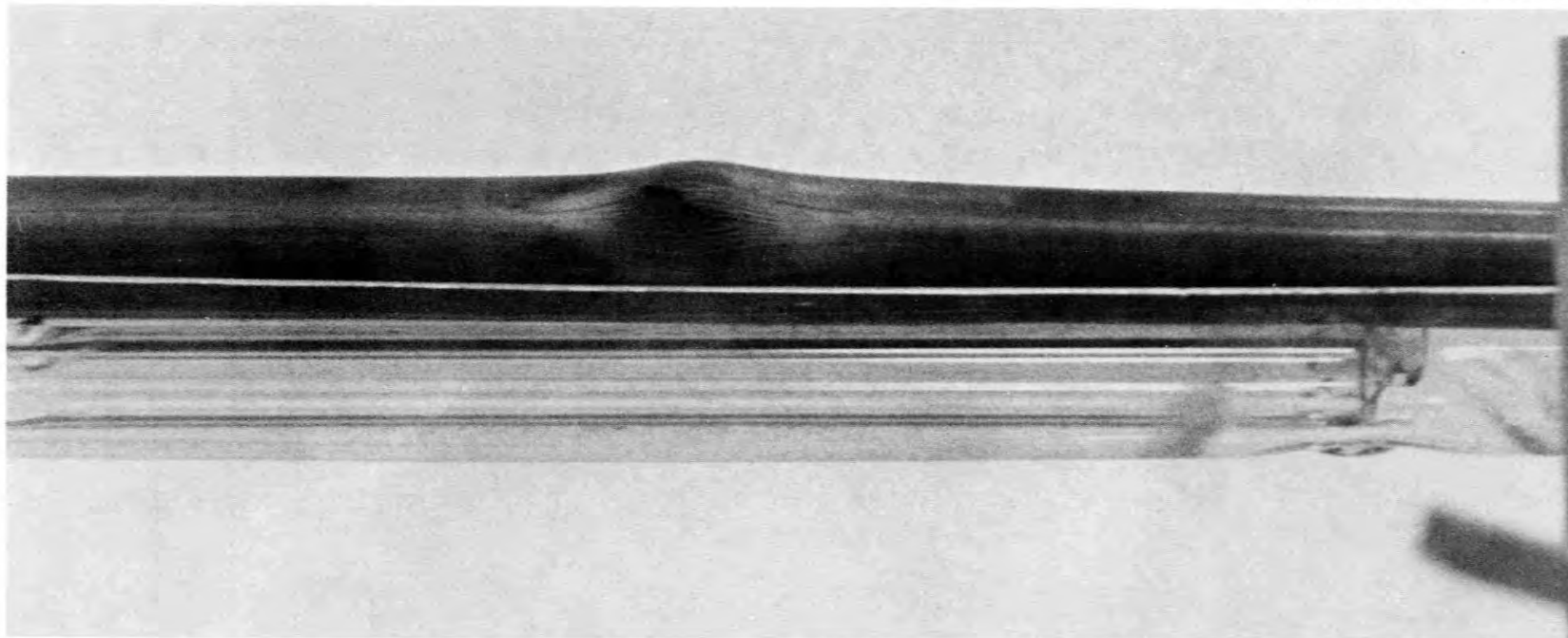


Fig. 19. Photograph of High Burnup Fuel Test 8 fuel rod rotated toward viewer from test position.

segment. The swollen area was visibly larger than the one obtained in test HBU-7.

Axial temperature profiles of the segment at 20 and 52 min after rupture are displayed graphically in Fig. 20. (The profile prior to rupture was determined with a mockup rod.) With rupture, there was a loss of induction coupling at the opening, as shown by the dip in temperature. A gradual but continuous temperature decrease at the rupture location resulted from oxidation of the thinned Zircaloy and/or slow enlargement of the opening.

The distribution of released  $^{134}\text{Cs}$  (deposited as vapor) at the conclusion of the experiment is summarized in Table 22. These data show that  $8.66 \times 10^{-3}\%$  (39.6  $\mu\text{g}$ ) of the total cesium inventory was released. Compared with test HBU-7, a factor of 3.3 less cesium was released; this provides further evidence that the amount of material released with rupture is dominant, at least at  $900^\circ\text{C}$ . The relatively large amount of cesium transported and the broad deposition peak in the thermal gradient tube probably resulted from the use of an increased steam flow rate beginning with test HBU-7.

The distribution of  $\text{UO}_2$  fuel particles released at the time of rupture is shown in Table 23; approximately 85 mg of the  $\text{UO}_2$  ( $4.08 \times 10^{-2}\%$  of the fuel in the segment) was ejected. Less than 1% of this dust was transported beyond the furnace tube; most of it was found in the vicinity of the rupture location.

The distribution of  $^{134}\text{Cs}$  along the furnace tube liner, fuel rod holder, and gold thermal-gradient tube is presented graphically in Fig. 21. Prior to counting and scanning the furnace tube liner, the loose fuel particles were tapped into a bottle. Note that about 42% of the  $^{134}\text{Cs}$  in the liner (after removing loose fuel particles), about 90% on the holder, and about 0.4% in the thermal gradient tube remained as fuel-particle cesium. A dark material adhered to the liner opposite the rupture opening. The thermal-gradient-tube profile showed a peak at about  $340^\circ\text{C}$ .

As shown by the data in Table 24, about 0.032% (13.5  $\mu\text{g}$ ) of the iodine inventory was released. Comparing the iodine (mass) distribution with that

ORNL DWG 77-1992

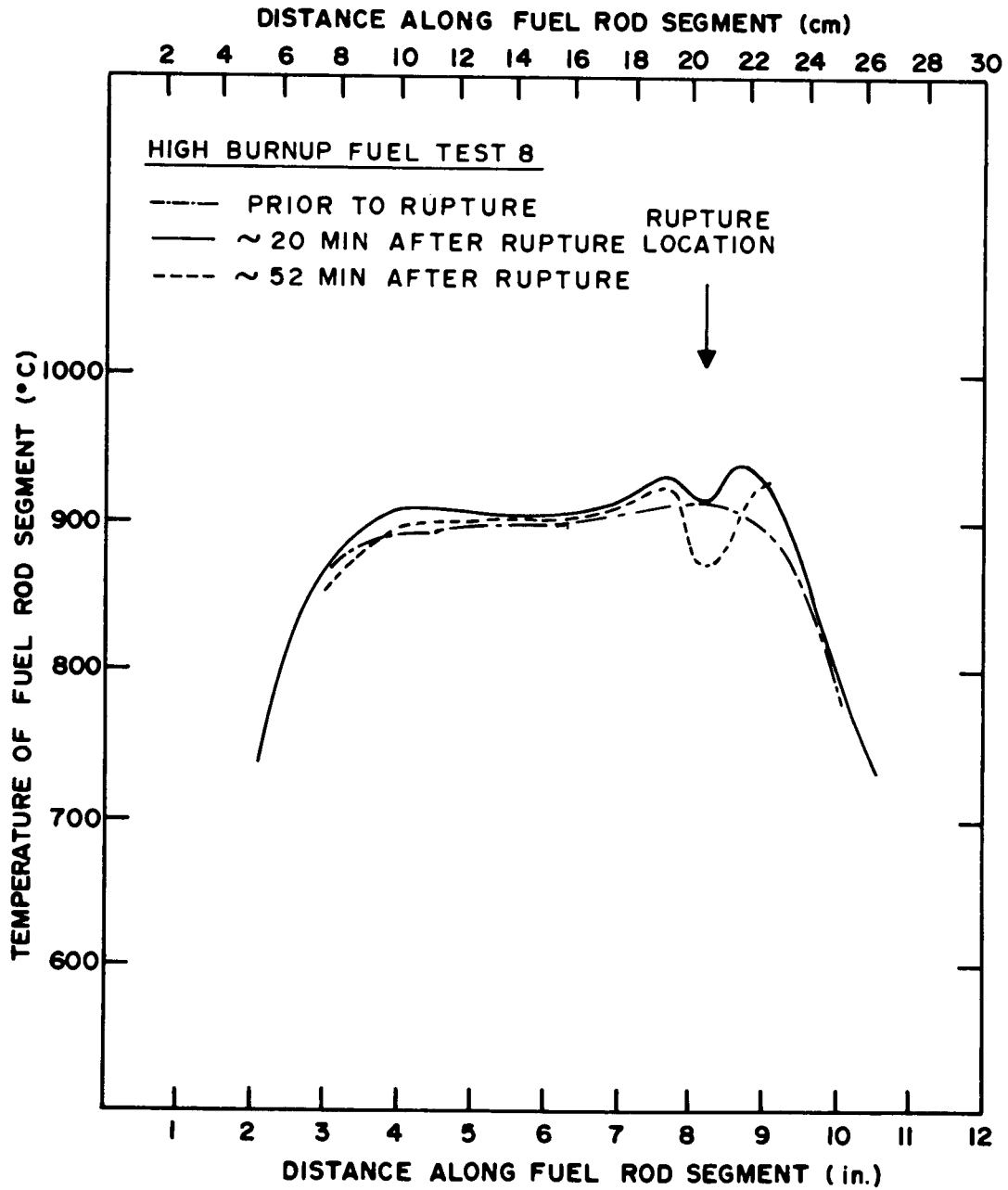


Fig. 20. Axial temperature profile of test HBU-8 fuel rod segment during test.

Table 22. Distribution of  $^{134}\text{Cs}$  in High Burnup Fuel Test 8<sup>a</sup>

Location	Temperature (°C)	Amount of $^{134}\text{Cs}$ found in each location			Total cesium ( $\mu\text{g}$ )
		$\mu\text{g}^{\text{b}}$	Percent of total <sup>c</sup>	Percent of released	
Fuel rod (original)	900	(8685) <sup>d</sup>			(4,572 x 10 <sup>5</sup> ) <sup>d</sup>
Furnace tube	~200-700				
Quartz liner		0.5542	6.38 x 10 <sup>-3</sup>	73.65	29.17
Quartz fuel-rod holder		0.0805	9.27 x 10 <sup>-4</sup>	10.70	4.24
Thermal gradient tube	690-225	7.07 x 10 <sup>-2</sup>	8.14 x 10 <sup>-4</sup>	9.40	3.72
Filter pack components	130				
Stainless-steel inlet fitting		5.53 x 10 <sup>-3</sup>	6.37 x 10 <sup>-5</sup>	0.73	0.29
Other housing components		0.0	0.0	0.0	0.0
First filter paper		4.15 x 10 <sup>-2</sup>	4.78 x 10 <sup>-4</sup>	5.52	2.18
Second filter paper		3.35 x 10 <sup>-7</sup>	3.86 x 10 <sup>-9</sup>	4.45 x 10 <sup>-5</sup>	1.76 x 10 <sup>-5</sup>
Third filter paper		2.47 x 10 <sup>-7</sup>	3.16 x 10 <sup>-9</sup>	3.64 x 10 <sup>-5</sup>	1.44 x 10 <sup>-5</sup>
Charcoal No. 1a		0.0	0.0	0.0	0.0
Charcoal No. 1b		0.0	0.0	0.0	0.0
Charcoal No. 1c		0.0	0.0	0.0	0.0
Charcoal No. 2a		0.0	0.0	0.0	0.0
Charcoal No. 2b		0.0	0.0	0.0	0.0
Charcoal No. 3		0.0	0.0	0.0	0.0
AgX		0.0	0.0	0.0	0.0
Condenser	0	0.0	0.0	0.0	0.0
Freeze trap	-78	0.0	0.0	0.0	0.0
Cold charcoal traps (two)	-78	0.0	0.0	0.0	0.0
Total released		0.7524	8.66 x 10 <sup>-3</sup>	100.0	39.60

<sup>a</sup> Steam flow rate: 926 cm<sup>3</sup>/min (STP) based on condensate volume, ~1700 cm<sup>3</sup>/min (STP) based on steam generator temperature; helium flow rate, 309 cm<sup>3</sup>/min (STP); system pressure, 760 torr. Decay time, 911 days (to Nov. 2, 1976).

<sup>b</sup> Amounts less than 1.0 x 10<sup>-8</sup>  $\mu\text{g}$  are given as 0.0.

<sup>c</sup> Percentage of radioactive nuclide in fuel rod.

<sup>d</sup> Calculated for burnup of 30,580 MWd per MT of original uranium, 183.3 g of uranium originally in 12-in. segment, and 911 days of decay.

Table 23. Distribution of  $\text{UO}_2$  fuel particles released at the time of rupture in High Burnup Fuel Test 8

Location	$\text{UO}_2$ fuel particles <sup>a</sup>		$^{134}\text{Cs}$ present in fuel particles <sup>b</sup> ( $\mu\text{g}$ )
	mg	Percent of release	
Furnace tube			
Quartz liner	64.38 <sup>c</sup>	75.96	2.689
Fuel rod holder	19.68	23.22	0.822
Thermal gradient tube	0.0072	0.008	0.0003
Filter pack			
Stainless-steel inlet fitting	0.0934	0.11	0.0039
First filter paper	0.589	0.70	0.0246
Total	84.75	100.0	3.540 <sup>d</sup>

<sup>a</sup>Estimated on the basis of  $^{154}\text{Eu}$  analysis. It was assumed that there was no loss of europium from the  $\text{UO}_2$  particles.

<sup>b</sup>Calculation based on  $^{134}\text{Cs}/^{154}\text{Eu}$  ratio in loose fuel particles.

<sup>c</sup>Loose particles, 54.5 mg; adhering particles, 9.79 mg.

<sup>d</sup>Equivalent to 186  $\mu\text{g}$  of total cesium.

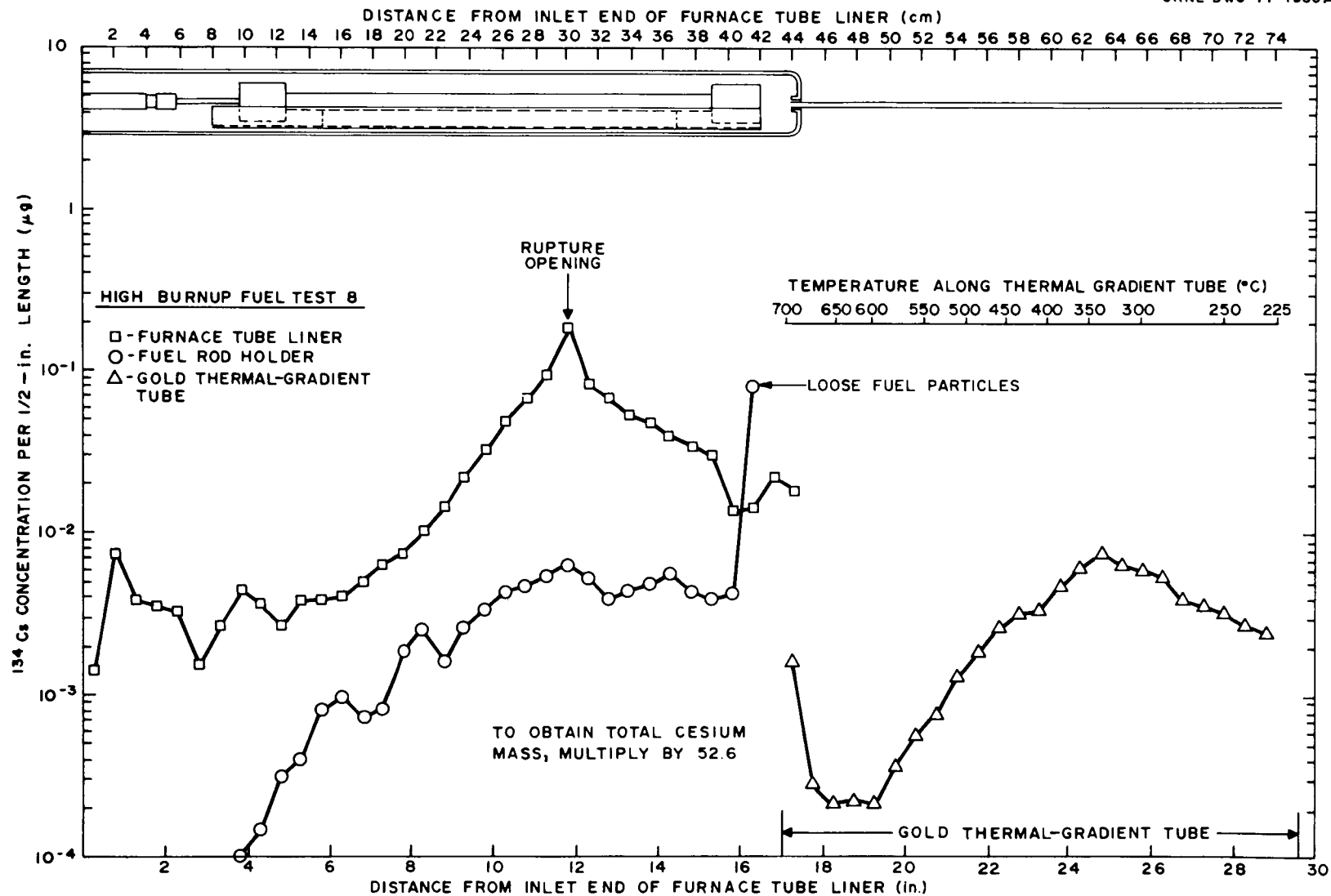


Fig. 21. Distribution of <sup>134</sup>Cs in furnace tube and thermal gradient tube of test HBU-8.

Table 24. Distribution of  $^{129}\text{I}$  in High Burnup Fuel Test No. 8<sup>a</sup>

Location	Temperature (°C)	Amount of $^{129}\text{I}$ found in each location			Total iodine ( $\mu\text{g}$ )
		( $\mu\text{g}$ ) <sup>b</sup>	Percent of total <sup>c</sup>	Percent of released	
Fuel rod	900	(3.316 x 10 <sup>4</sup> ) <sup>d</sup>			(4.208 x 10 <sup>4</sup> ) <sup>d</sup>
Furnace tube	~200-700				
Quartz liner		0.11 ± 0.03	3.32 x 10 <sup>-4</sup>	1.03	0.14
Quartz fuel-rod holder		0.084 ± 0.006	2.53 x 10 <sup>-4</sup>	0.79	0.11
Thermal gradient tube	690-225	0.199 ± 0.03	6.00 x 10 <sup>-4</sup>	1.87	0.25
Filter pack components	130				
Stainless-steel inlet fitting		2.51	7.57 x 10 <sup>-3</sup>	23.54	3.18
First filter paper		1.49 ± 0.2	4.49 x 10 <sup>-3</sup>	13.97	1.89
Second and third filter papers		1.12 ± 0.04	3.38 x 10 <sup>-3</sup>	10.50	1.42
Charcoal No. 1a		5.151 ± 0.1	1.55 x 10 <sup>-2</sup>	48.30	6.54
Charcoal No. 1b		0.0	0.0	0.0	0.0
Charcoal No. 1c		0.0	0.0	0.0	0.0
Charcoal No. 2a		0.0	0.0	0.0	0.0
Charcoal No. 2b <sup>e</sup>		0.0	0.0	0.0	0.0
Charcoal No. 3 <sup>e</sup>		0.0	0.0	0.0	0.0
AgX <sup>e</sup>		0.0	0.0	0.0	0.0
Condenser <sup>e</sup>	0	0.0	0.0	0.0	0.0
Freeze trap <sup>e</sup>	-78	0.0	0.0	0.0	0.0
Cold charcoal traps (two) <sup>e</sup>	-78	0.0	0.0	0.0	0.0
Total		10.664 ± 4.1	3.22 x 10 <sup>-2</sup>	100.00	13.53

<sup>a</sup> Steam flow rate, 926 cm<sup>3</sup>/min (STP) based on condensate volume, ~1700 cm<sup>3</sup>/min (STP) based on steam generator temperature; helium flow rate, 309 cm<sup>3</sup>/min (STP); system pressure, 760 torr. Decay time, 911 days (to Nov. 2, 1976).

<sup>b</sup> Amounts less than 1.0 x 10<sup>-2</sup>  $\mu\text{g}$  are given as 0.0.

<sup>c</sup> Percentage of radioactive nuclide in fuel rod.

<sup>d</sup> Calculated for burnup of 30,580 MWd per MT of original uranium originally in 12-in. segment, and 911 days of decay.

<sup>e</sup> Not analyzed for  $^{129}\text{I}$  content in any of the High Burnup Series Tests; amount assumed to be 0.0.

of cesium in Table 22, and assuming that iodine was released primarily as CsI or elemental iodine, it is determined that about 78% of the iodine was collected as elemental iodine. (It was assumed that any excess iodine other than that needed to form CsI with any cesium present on a component of the apparatus was elemental iodine.) The iodine deposition in the thermal gradient tube was primarily found in the temperature range 275 to 225°C.

The data shown in Fig. 22 indicate that about 80% (0.115  $\mu\text{g}$ ) of the  $^{134}\text{Cs}$  that was transported to the thermal gradient tube and filter pack deposited there within 15 min after rupture. Figure 22 also presents data for  $^{85}\text{Kr}$  which were collected in the cold charcoal traps. As is shown, 1.26% (16.8 mCi) of the original  $^{85}\text{Kr}$  inventory in the segment was released, which is comparable to releases observed in the previous two tests conducted at 900°C.

Again, as was the case in the other steam atmosphere tests, a trace of ruthenium was released. About  $8.8 \times 10^{-6}$   $\mu\text{g}$  of ruthenium was determined to be in the first charcoal cartridge; a similar amount was found there in test HBU-7.

#### 4.8 High Burnup Fuel Test 9 (900 to 1100°C)

Fuel rod segment B-5 of fuel rod H-15 was pressurized with approximately 302 psig (2.08 MPa) of helium while the rod segment was at 755°C. The segment was then heated at a rate of 2.5°C/sec to 910°C, where rupture occurred. At rupture, the pressure of the rod had dropped to 264 psig (1.82 MPa). Immediately following rupture, the fuel rod temperature was raised at a rate of 1.8°C/sec to 1100°C and held for 8.4 min before cooling. Figure 23 is a photograph of the ruptured rod segment.

The axial-temperature profile of the rod segment about 7 min after rupture is shown in Fig. 24. The dashed-line profiles at 900 and 1100°C were obtained with a simulated rod. All the measurements were taken with a mobile, automatic optical pyrometer. The temperature at the rupture opening at this time had dropped to about 1015°C, whereas the hot spots on each side of the opening were at 1185 and 1140°C. During the 10-min test period, the cool region expanded as a result of oxidation of the

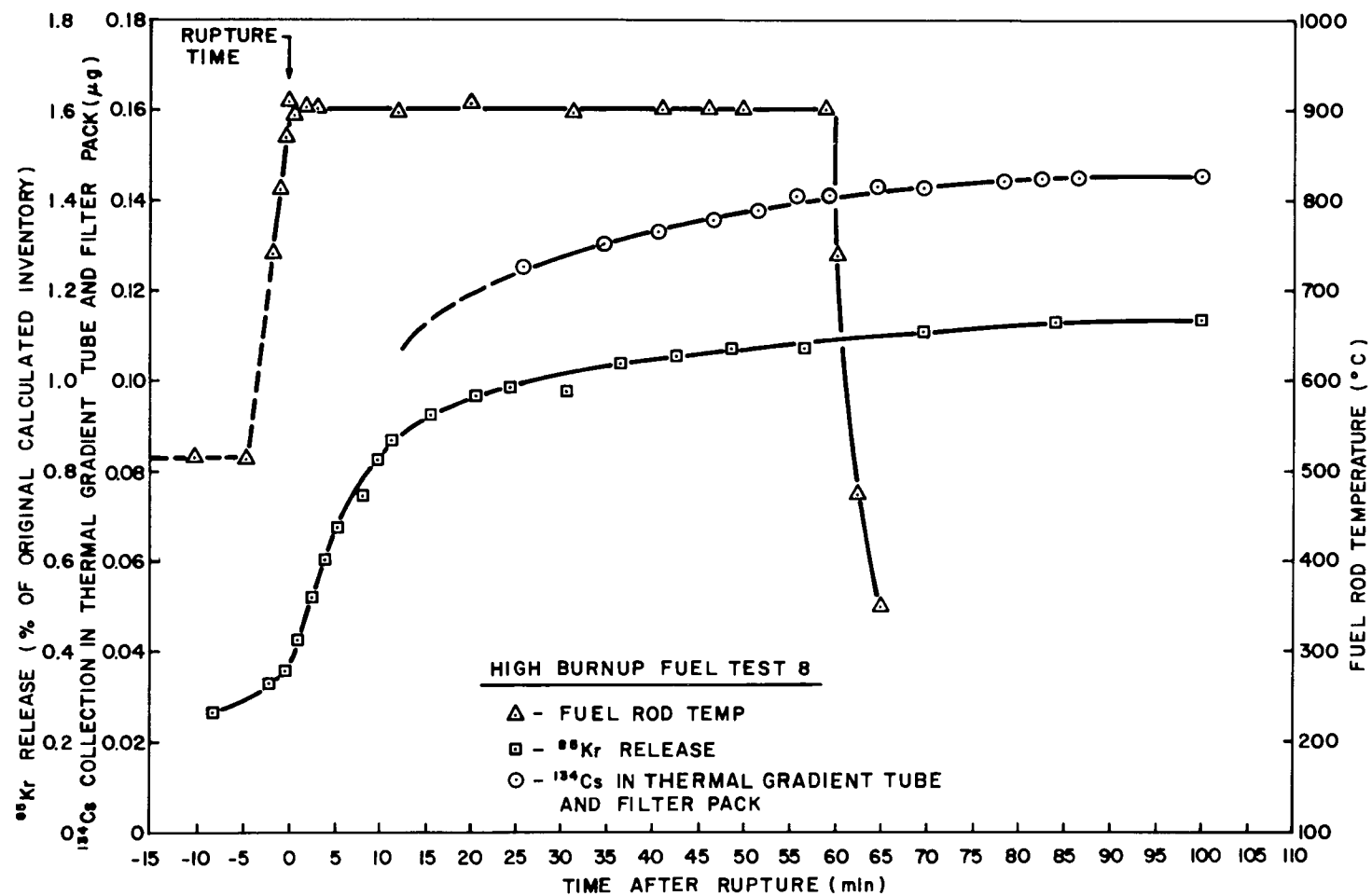


Fig. 22. Collection of <sup>134</sup>Cs in the thermal gradient tube and filter pack and of <sup>85</sup>Kr in the cold charcoal traps during test HBU-8.

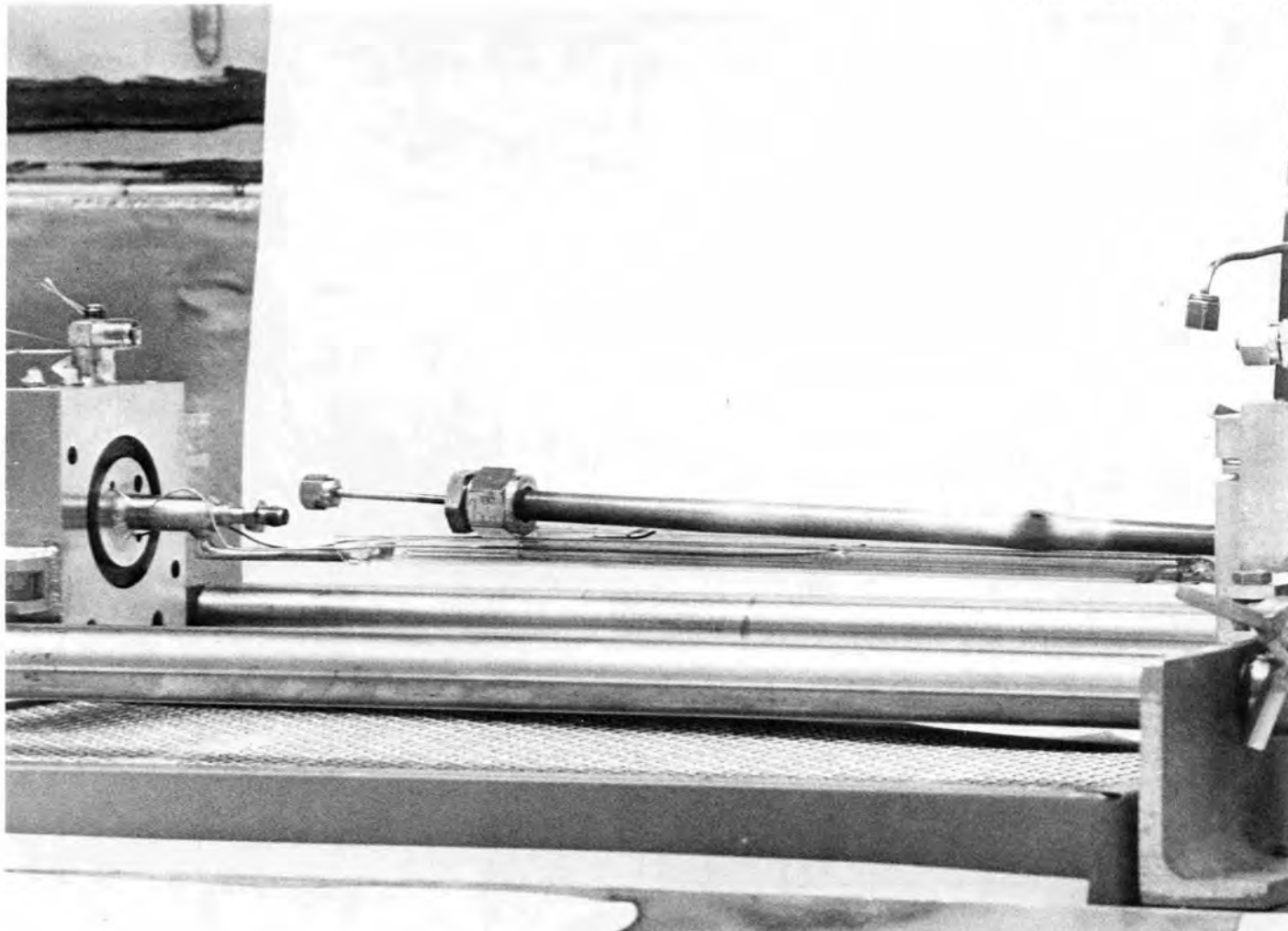


Fig. 23. Appearance of ruptured fuel rod segment of High Burnup Fuel Test 9, with rupture opening rotated toward viewer.

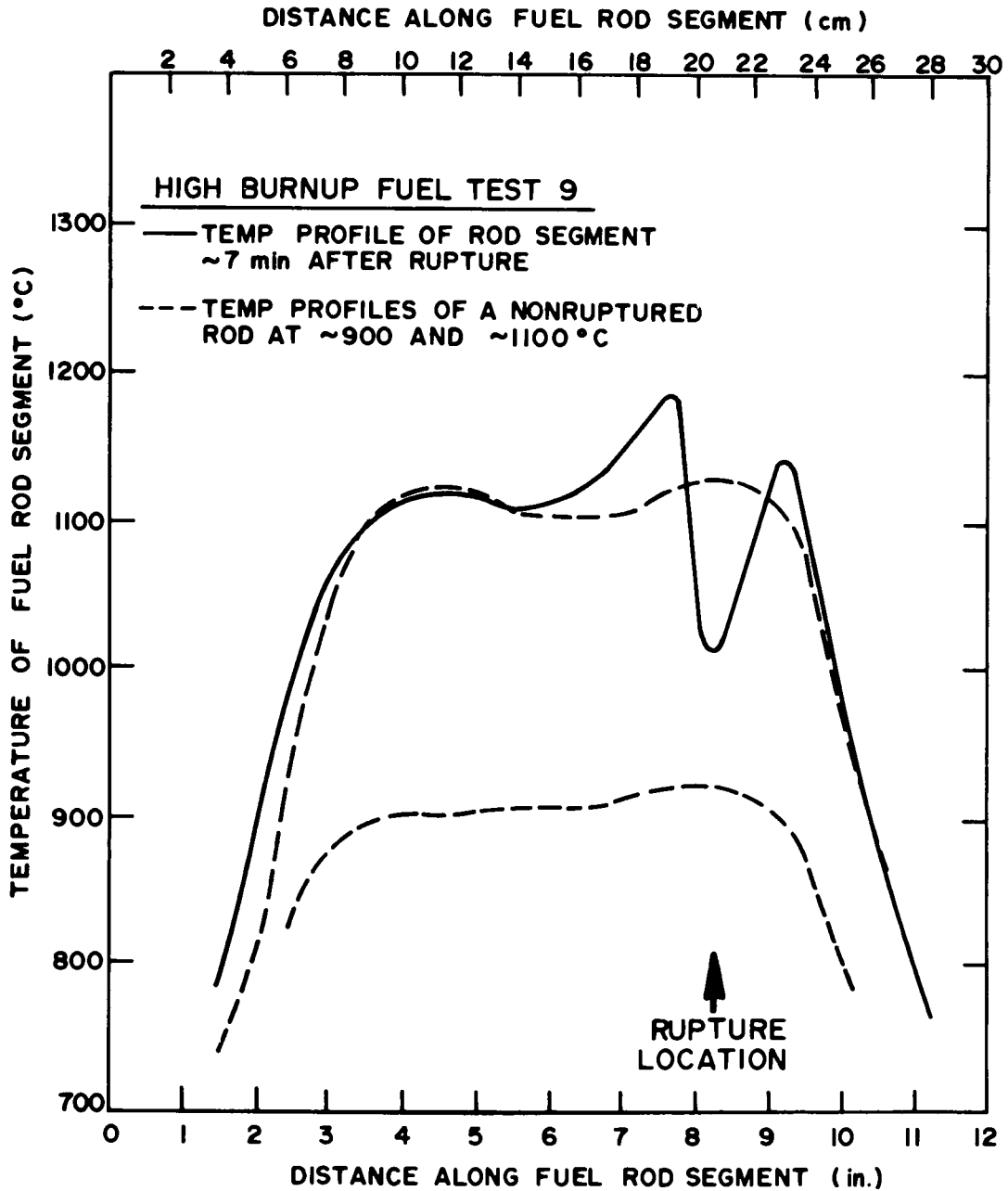


Fig. 24. Axial temperature profile of test HBU-9 fuel rod segment during test.

thinned cladding around the rupture opening and possibly by axial enlargement of the rupture opening. (Induction heating of  $ZrO_2$  and split tubing is relatively inefficient.)

In this test, it is estimated that 0.018% (37.4 mg) of the  $UO_2$  fuel was released in the burst; about 99% of it was found on the quartz furnace-tube liner and holder in the region of the rupture opening. Table 25 summarizes the distribution in the apparatus.

The data listed in Table 26 indicate that 0.0240% (112.3  $\mu\text{g}$ ) of the total cesium in the rod segment was released as vapor. About 96.5% of it was found in the furnace tube on the quartz surfaces near the rupture opening. The  $^{134}\text{Cs}$  concentration distribution along the furnace tube liner (after removing loose fuel particles), fuel rod holder, and thermal gradient tube is shown in Fig. 25. The principal deposition was in the vicinity of the rupture. The cesium peak in the thermal gradient tube was at the  $350^\circ\text{C}$  location. The  $^{134}\text{Cs}$  concentration included both cesium vapor and cesium in adhering fuel particles that were present. Analysis showed that  $\sim 11.7\%$  of the  $^{134}\text{Cs}$  in the liner, 34.7% on the fuel rod holder, and 5.4% in the thermal gradient tube could be classified as the latter type.

The collection of  $^{134}\text{Cs}$  in the thermal gradient tube and filter pack occurred as shown in Fig. 26. About 27% (0.025  $\mu\text{g}$ ) of the collected cesium was deposited shortly after rupture. Continuous monitoring showed that deposition of cesium ceased when the induction heater was turned off.

Figure 26 also presents graphically the collection of  $^{85}\text{Kr}$  in the cold charcoal traps. Data analysis revealed that 1.47% (20.1 mCi) of the total  $^{85}\text{Kr}$  inventory was released.

A summary for the posttest distribution of iodine is given in Table 27. A total of 16.9  $\mu\text{g}$  of iodine was found which represents 0.039% of the calculated segment inventory. As in test HBU-8 (see Table 24), most of the released iodine ( $\sim 84\%$ ) was collected as elemental iodine; little cesium was found on the same surfaces as the iodine.

Table 10 shows that a trace of ruthenium ( $1.1 \times 10^{-6}$   $\mu\text{g}$ ) was also collected on the charcoal in this test.

Table 25. Distribution of  $\text{UO}_2$  fuel particles released at the time of rupture in High Burnup Fuel Test 9

Location	$\text{UO}_2$ fuel particles <sup>a</sup>		$^{134}\text{Cs}$ present in fuel particles <sup>b</sup> ( $\mu\text{g}$ )
	mg	Percent of released	
Furnace tube			
Quartz liner	34.44 <sup>c</sup>	92.20	1.475
Fuel rod holder	2.521	6.75	0.108
Thermal gradient tube	0.056	0.15	0.0024
Filter pack			
Stainless-steel inlet fitting	0.079	0.21	0.0034
First filter paper	0.257	0.69	0.011
Total	37.35	100.0	1.600 <sup>d</sup>

<sup>a</sup>Estimated on the basis of  $^{154}\text{Eu}$  analysis. It was assumed that there was no loss of europium from the  $\text{UO}_2$  particles.

<sup>b</sup>Calculation based on  $^{134}\text{Cs}/^{154}\text{Eu}$  ratio in loose fuel particles.

<sup>c</sup>Loose particles, 29.03 mg; adhering particles, 5.41 mg.

<sup>d</sup>Equivalent to 84.1  $\mu\text{g}$  of total cesium.

Table 26. Distribution of  $^{134}\text{Cs}$  in High Burnup Fuel Test 9<sup>a</sup>

Location	Temperature (°C)	Amount of $^{134}\text{Cs}$ found in each location			Total cesium ( $\mu\text{g}$ )
		$\mu\text{g}^{\text{b}}$	Percent of total <sup>c</sup>	Percent of released	
Fuel rod (original)	900-1100	$8.908 \times 10^3$			$4.689 \times 10^5^{\text{d}}$
Furnace	~200-800				
Quartz liner		1.855	$2.08 \times 10^{-2}$	86.94	97.64
Quartz fuel-rod holder		$2.032 \times 10^{-1}$	$2.28 \times 10^{-3}$	9.52	10.70
Thermal gradient tube	690-210	$4.239 \times 10^{-2}$	$4.76 \times 10^{-4}$	1.99	2.23
Filter pack components	135				
Stainless-steel inlet fitting		$3.26 \times 10^{-3}$	$3.66 \times 10^{-5}$	0.15	0.17
Other housing components		0.0	0.0	0.0	0.0
First filter paper		$2.98 \times 10^{-2}$	$3.35 \times 10^{-4}$	1.40	1.57
Second filter paper		0.0	0.0	0.0	0.0
Third filter paper		0.0	0.0	0.0	0.0
Charcoal No. 1a		0.0	0.0	0.0	0.0
Charcoal No. 1b		0.0	0.0	0.0	0.0
Charcoal No. 1c		0.0	0.0	0.0	0.0
Charcoal No. 2a		0.0	0.0	0.0	0.0
Charcoal No. 2b		0.0	0.0	0.0	0.0
Charcoal No. 3		0.0	0.0	0.0	0.0
AgX		0.0	0.0	0.0	0.0
Condenser	0	0.0	0.0	0.0	0.0
Freeze trap	-78	0.0	0.0	0.0	0.0
Cold charcoal traps (two)	-78	0.0	0.0	0.0	0.0
Total released		2.134	0.0240	100.0	112.31

<sup>a</sup>Steam flow rate,  $1563 \text{ cm}^3/\text{min}$ ; helium flow rate,  $299 \text{ cm}^3/\text{min}$  (STP); system pressure, 760 torr. Decay time, 911 days (to Nov. 2, 1976).

<sup>b</sup>Amounts less than  $1.0 \times 10^{-8} \mu\text{g}$  are given as 0.0.

<sup>c</sup>Percentage of radioactive nuclide in fuel rod.

<sup>d</sup>Calculated for burnup of 31,360 MWd per MT of original uranium, 183.3 g of uranium originally in 12-in. segment, and 911 days of decay.

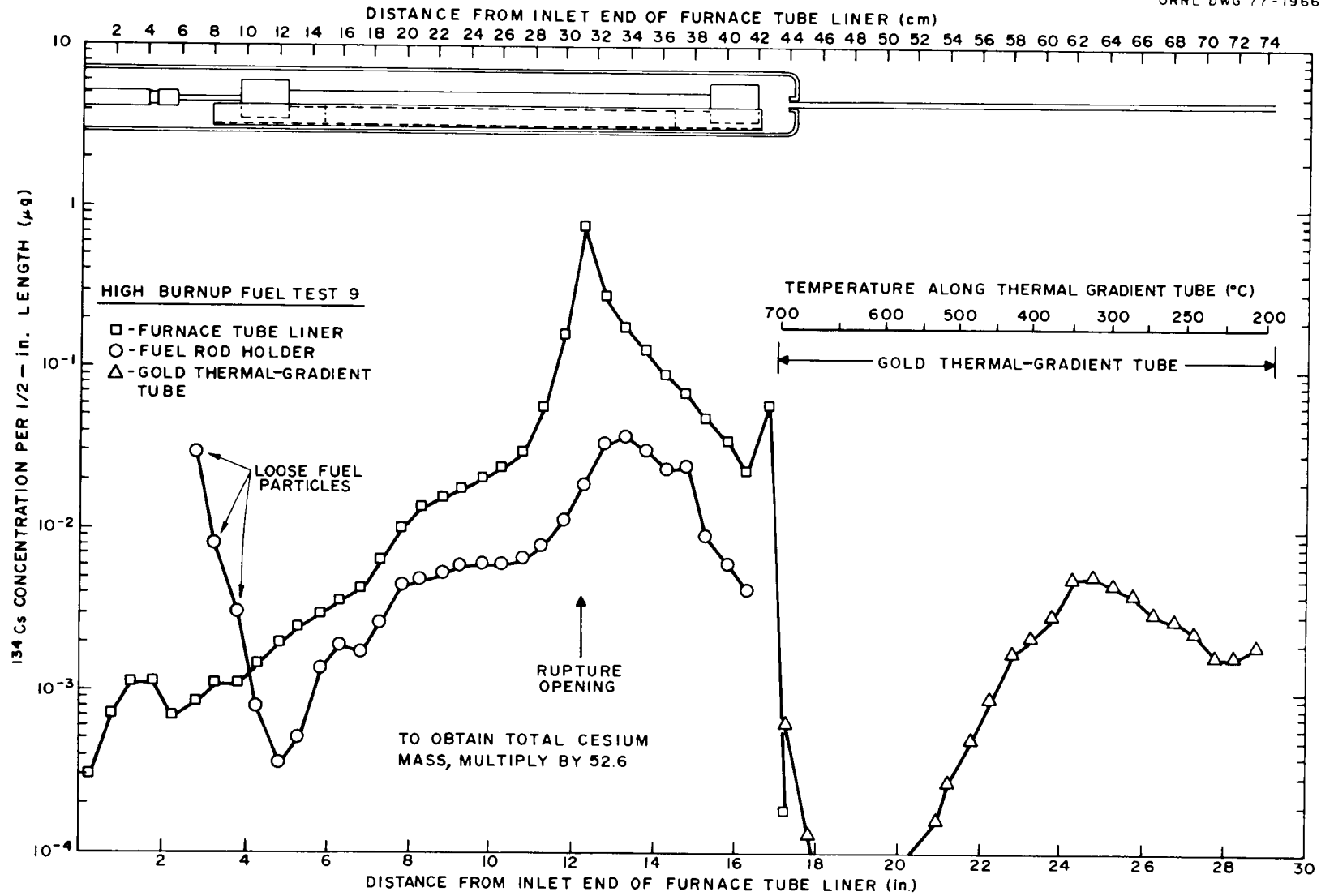


Fig. 25. Distribution of  $^{134}\text{Cs}$  in furnace tube and thermal gradient tube of test HBU-9.

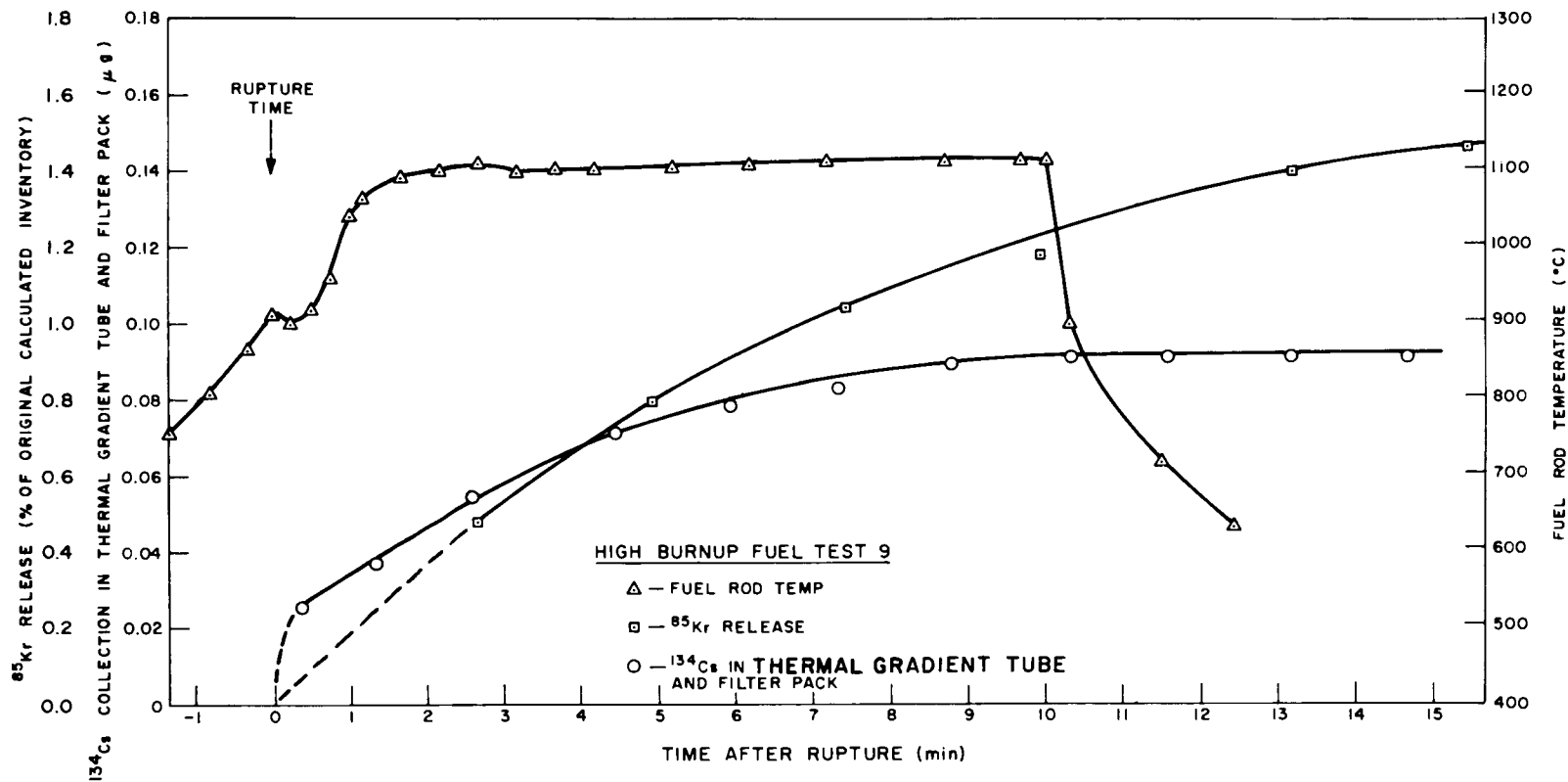


Fig. 26. Collection of <sup>134</sup>Cs in the thermal gradient tube and filter pack and of <sup>85</sup>Kr in the cold charcoal traps during test HBU-9.

Table 27. Distribution of  $^{129}\text{I}$  in High Burnup Fuel Test 9<sup>a</sup>

Location	Temperature (°C)	Amount of $^{129}\text{I}$ found in each location			Total iodine ( $\mu\text{g}$ )
		$\mu\text{g}$ <sup>b</sup>	Percent of total <sup>c</sup>	Percent of released	
Fuel rod	900-1100	$(3.40 \times 10^4)^d$			$(4.315 \times 10^4)^d$
Furnace tube	~200-800				
Quartz liner		$0.039 \pm 0.003$	$1.15 \times 10^{-4}$	0.29	0.05
Quartz fuel-rod holder		$0.063 \pm 0.006$	$1.85 \times 10^{-4}$	0.47	0.08
Thermal gradient tube	690-210	$0.69 \pm 0.06$	$2.03 \times 10^{-3}$	5.17	0.87
Filter pack components	135				
Stainless-steel inlet fitting		$2.10 \pm 0.05$	$6.18 \times 10^{-3}$	15.75	2.66
First filter paper		$1.33 \pm 0.04$	$3.91 \times 10^{-3}$	9.98	1.69
Second and third filter papers		$1.10 \pm 0.04$	$3.24 \times 10^{-3}$	8.25	1.40
Charcoal No. 1a		$8.013 \pm 0.2$	$2.36 \times 10^{-2}$	60.09	10.17
Charcoal No. 1b		0.0	0.0	0.0	0.0
Charcoal No. 1c		0.0	0.0	0.0	0.0
Charcoal No. 2a		0.0	0.0	0.0	0.0
Charcoal No. 2b		0.0	0.0	0.0	0.0
Charcoal No. 3		0.0	0.0	0.0	0.0
AgX		0.0	0.0	0.0	0.0
Condenser	0	0.0	0.0	0.0	0.0
Freeze trap	-78	0.0	0.0	0.0	0.0
Cold charcoal traps (two)	-78	0.0	0.0	0.0	0.0
Total		$13.335 \pm 0.4$	$3.92 \times 10^{-2}$	100.00	16.92

<sup>a</sup>Steam flow rate,  $1563 \text{ cm}^3/\text{min}$  (STP); helium flow rate,  $299 \text{ cm}^3/\text{min}$  (STP); system pressure, 760 torr. Decay time, 911 days (to Nov. 2, 1976).

<sup>b</sup>Amounts less than  $1.0 \times 10^{-2} \mu\text{g}$  are given as 0.0.

<sup>c</sup>Percentage of radioactive nuclide in fuel rod.

<sup>d</sup>Calculated for burnup of 31,360 MWd per MT of original uranium originally in 12-in. segment, and 911 days of decay.

#### 4.9 High Burnup Fuel Test 10 (900 to 1200°C)

This test, which utilized segment A-6 of fuel rod D-12, was conducted over a 10-min period at 1200°C in a flowing steam-helium atmosphere following rupture at approximately 900°C. In the prerupture stage of the test, 308 psig (2.12 MPa) of helium pressure was added to the segment at about 745°C. Subsequently, the temperature of the segment was raised at a rate of 5.1°C/sec to 898°C where rupture occurred; at this point, the pressure was 291 psig (2.01 MPa). A photograph of the ruptured rod is shown in Fig. 27.

A scan of the fuel rod segment was made with a mobile, automatic optical pyrometer about 5 min after rupture. This scan yielded the axial temperature profile shown in Fig. 28. As in previous rupture tests, a depression in the temperature occurred at the rupture location because of a loss of inductive coupling. After rupture, there was a gradual but steady decrease in temperature at the rupture fissure; this was probably caused by axial expansion of this opening and by oxidation of the thinned cladding.

A summary of the distribution of released  $^{134}\text{Cs}$  (deposited as vapor) in the experimental apparatus at the conclusion of the test is given in Table 28. These data show that 0.0611% (280  $\mu\text{g}$ ) of the total cesium inventory was released. This is a factor of about 2.5 more cesium (mass) released than in test HBU-9, which was conducted at 1100°C. Approximately 88.3% was transported downstream to the thermal gradient tube and to the first filter paper of the filter pack.

As in previous experiments, in which the fuel rod segments were ruptured with helium pressure, fuel dust was ejected. On the basis of  $^{154}\text{Eu}$  analysis (assuming no loss of europium from the fuel particles), it is estimated that 0.022% (46.0 mg) of the fuel was ejected from the rod segment. The manner in which the dust was dispersed throughout the apparatus is summarized in Table 29. About 2% of the ejected fuel was found on the first filter paper of the filter pack. The remainder was found in the quartz furnace-tube liner near the rupture location.

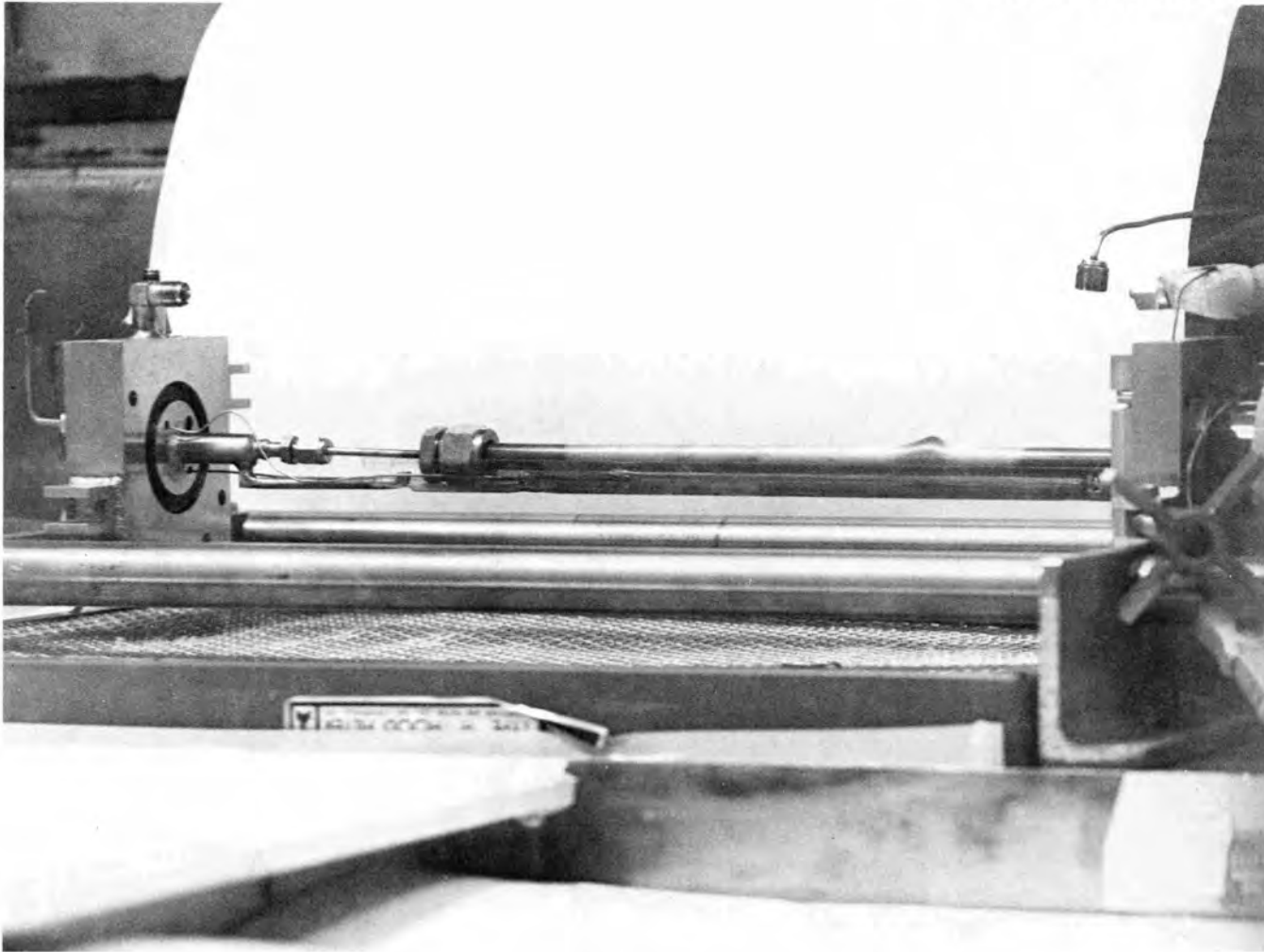


Fig. 27. Posttest view of the rod segment used in test HBU-10, as seen through the cell window.

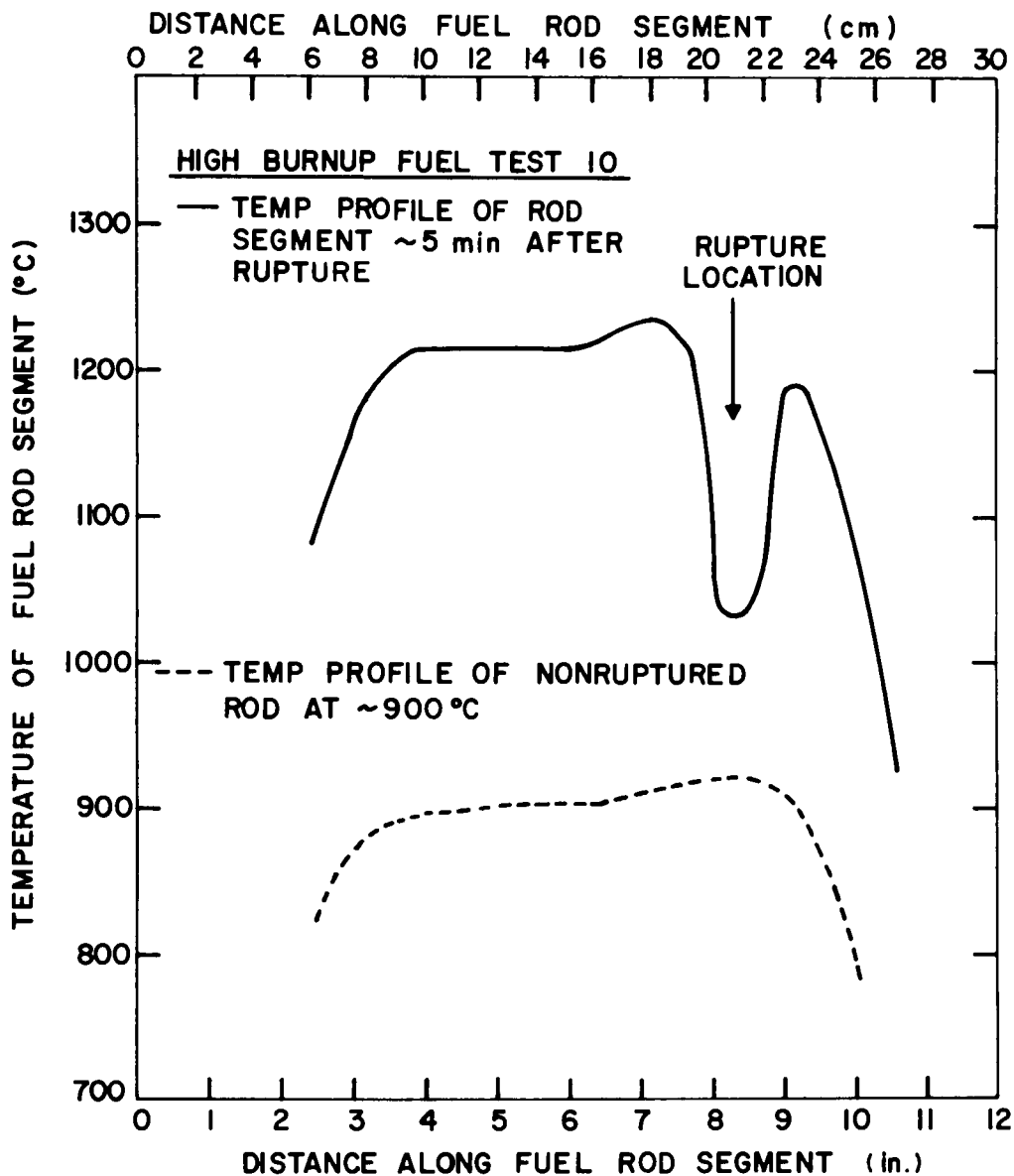


Fig. 28. Axial temperature profile of test HBU-10 fuel rod segment during test.

Table 28. Distribution of  $^{134}\text{Cs}$  in High Burnup Fuel Test 10<sup>a</sup>

Location	Temperature (°C)	Amount of $^{134}\text{Cs}$ found in each location			Total cesium ( $\mu\text{g}$ )
		$\mu\text{g}$ <sup>b</sup>	Percent <sup>c</sup> of total	Percent of released	
Fuel rod	900-1200	(8685) <sup>d</sup>			$4.572 \times 10^5$ <sup>d</sup>
Furnace tube	~200-900				
Quartz liner		4.460	$5.14 \times 10^{-2}$	84.01	234,766
Quartz fuel-rod holder		0.228	$2.63 \times 10^{-3}$	4.29	12,001
Thermal gradient tube	700-225	0.326	$3.75 \times 10^{-3}$	6.14	17,160
Filter pack components	130				
Stainless-steel inlet fitting		0.019	$2.19 \times 10^{-4}$	0.36	1,000
Other housing components		$7.46 \times 10^{-6}$	$3.44 \times 10^{-7}$	$1.41 \times 10^{-4}$	$3.927 \times 10^{-4}$
First and second filter papers		0.276	$3.18 \times 10^{-3}$	5.20	14,528
Third filter paper		0.0	0.0	0.0	0.0
Charcoal No. 1a		$1.93 \times 10^{-7}$	$2.22 \times 10^{-9}$	$3.64 \times 10^{-6}$	$1.016 \times 10^{-5}$
Charcoal No. 1b		0.0	0.0	0.0	0.0
Charcoal No. 1c		0.0	0.0	0.0	0.0
Charcoal No. 2a		0.0	0.0	0.0	0.0
Charcoal No. 2b		0.0	0.0	0.0	0.0
Charcoal No. 3		0.0	0.0	0.0	0.0
AgX		0.0	0.0	0.0	0.0
Condenser	0	0.0	0.0	0.0	0.0
Freeze trap	-78	0.0	0.0	0.0	0.0
Cold charcoal traps (two)	-78	0.0	0.0	0.0	0.0
Total released		5.309	$6.11 \times 10^{-2}$	100.0	279,455

<sup>a</sup>Steam flow rate, 1246 cm<sup>3</sup>/min (STP); helium flow rate, 368 cm<sup>3</sup>/min (STP); system pressure, 760 torr. Decay time, 911 days (to Nov. 2, 1976).

<sup>b</sup>Amounts less than  $1.0 \times 10^{-8}$   $\mu\text{g}$  are given as 0.0.

<sup>c</sup>Percent of radioactive nuclide in fuel rod.

<sup>d</sup>Calculated for burnup of 30,580 MWd/per MT of original uranium originally in 12-in. segment, and 911 days of decay.

Table 29. Distribution of  $\text{UO}_2$  fuel particles released at the time of rupture in High Burnup Fuel Test 10

Location	$\text{UO}_2$ fuel particles <sup>a</sup>		$^{134}\text{Cs}$ present in fuel particles <sup>b</sup> ( $\mu\text{g}$ )
	mg	% of released	
Furnace tube			
Quartz liner	41.04 <sup>c</sup>	89.17	1.714
Fuel rod holder	3.64	7.91	0.152
Thermal gradient	0.22	0.47	0.09
Filter pack			
Stainless-steel inlet fitting	0.12	0.26	0.005
First filter paper	1.01	2.19	0.042
Total	46.03	100.0	1.922 <sup>d</sup>

<sup>a</sup>Estimated on the basis of  $^{154}\text{Eu}$  analysis. It was assumed that there was no loss of europium from the  $\text{UO}_2$  particles.

<sup>b</sup>Calculation based on  $^{134}\text{Cs}/^{154}\text{Eu}$  ratio in loose fuel particles.

<sup>c</sup>Loose particles, 23.52 mg; adhering fuel particles, 18.25 mg.

<sup>d</sup>Equivalent to 101  $\mu\text{g}$  of the total cesium.

The distribution of  $^{134}\text{Cs}$  (in both vapor-deposited and fuel dust-associated forms) along the furnace tube liner, fuel rod holder, and thermal gradient tube is presented graphically in Fig. 29. (Loose fuel particles were removed from the furnace tube liner prior to gamma scanning.) Analytical estimates indicate that about 16.4% of the  $^{134}\text{Cs}$  in the liner, 66.7% on the fuel rod holder, and 2.8% in the thermal gradient tube were associated with fuel dust. Most of the cesium in the furnace tube deposited on the quartz surface of the furnace tube liner in the region of the rupture. (As noted in previous tests, the released cesium reacted readily with the quartz components.) Approximately 6% of the cesium deposited in the thermal gradient tube.

The rate of deposition of  $^{134}\text{Cs}$  in the thermal gradient tube and filter pack is shown in Fig. 30. Approximately 8% of this cesium was

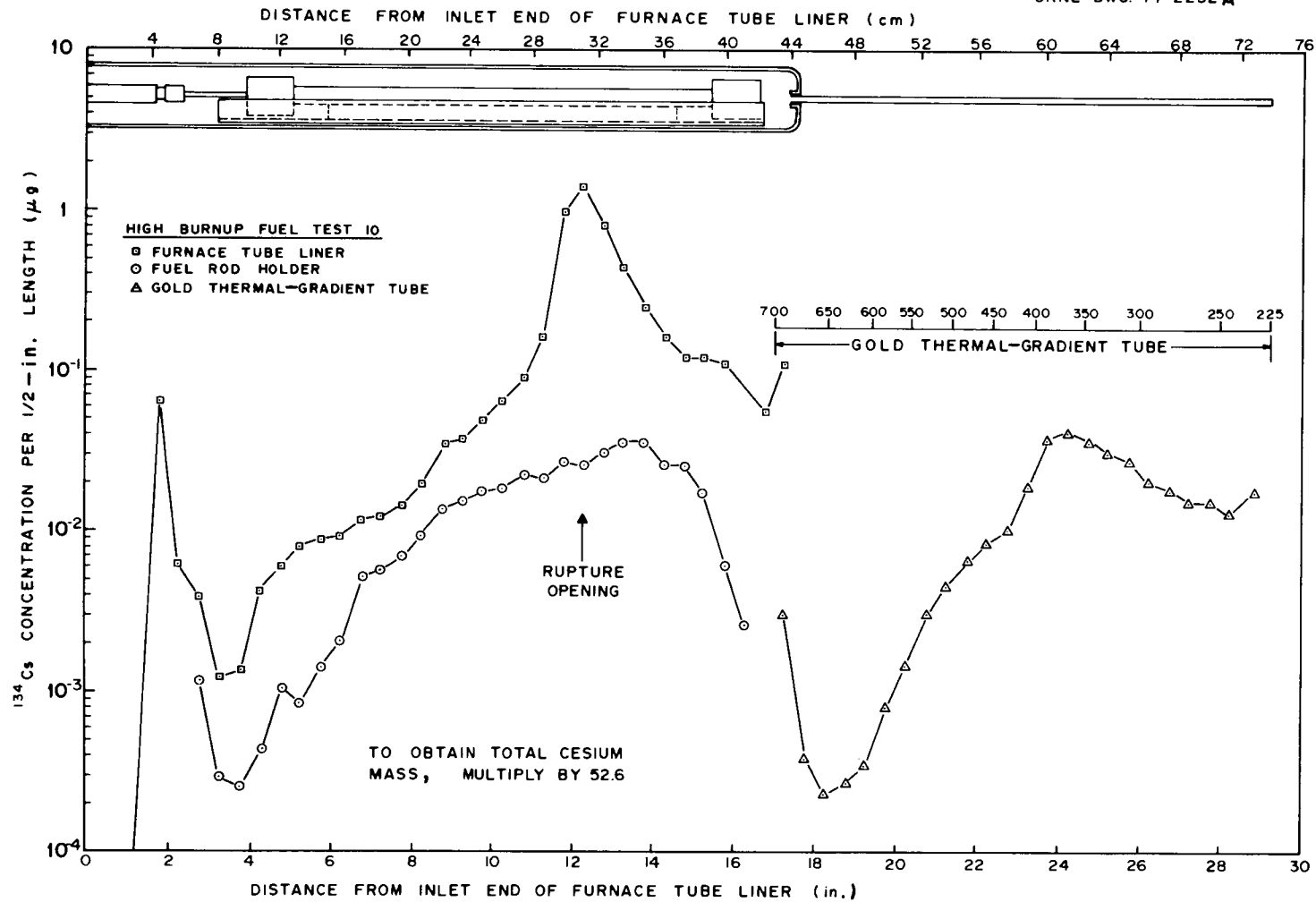


Fig. 29. Distribution of <sup>134</sup>Cs in furnace tube and thermal gradient tube of test HBU-10.

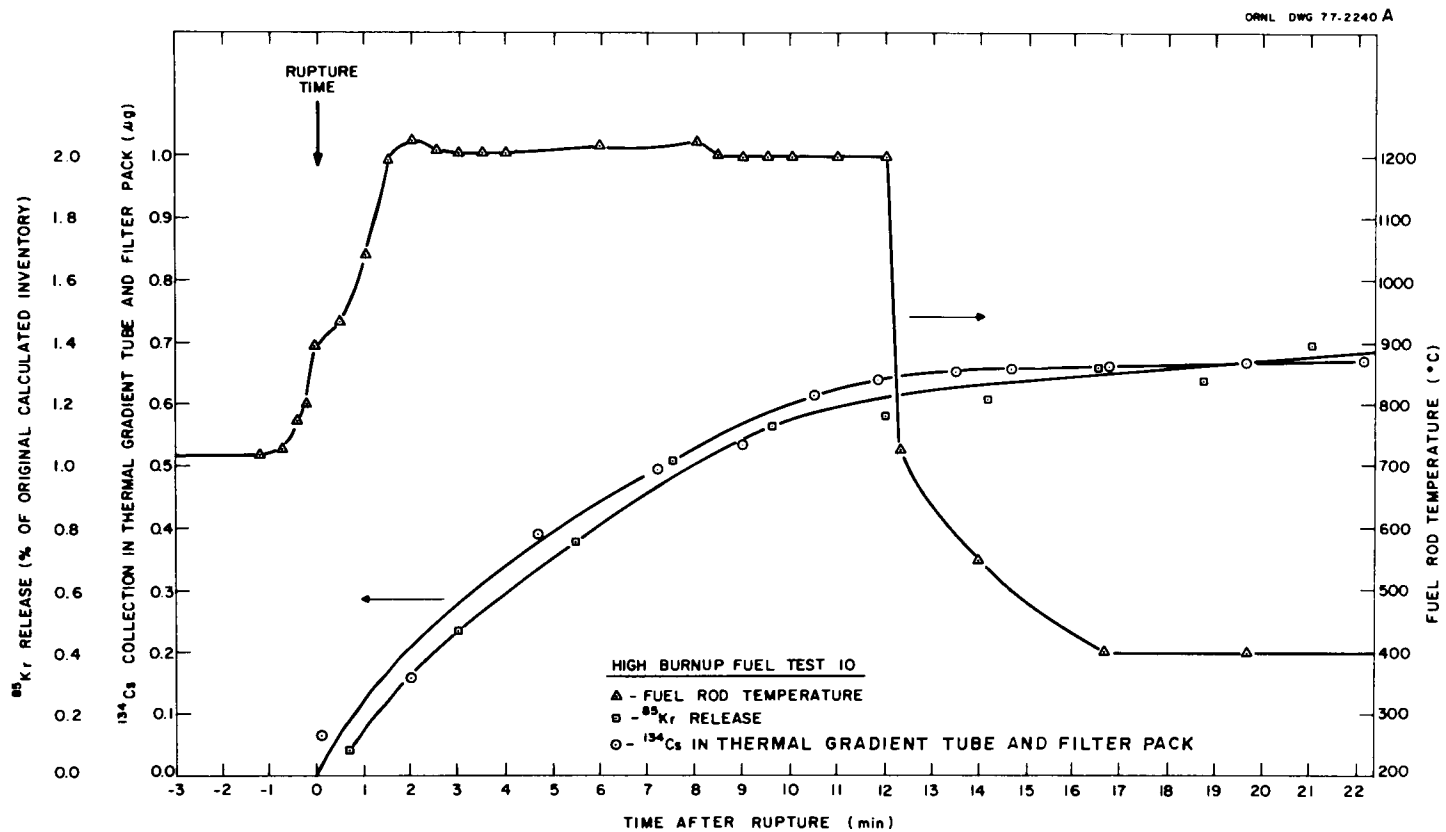


Fig. 30. Collection of  $^{134}\text{Cs}$  in the thermal gradient tube and filter pack and of  $^{85}\text{Kr}$  in the cold charcoal traps during High Burnup Fuel Test 10.

associated with fuel particles that were found on the first filter paper in the filter pack.

The rate of collection of  $^{85}\text{Kr}$  in the cold charcoal traps is also displayed in Fig. 30. It was determined that 1.69% (22.4 mCi) of the total  $^{85}\text{Kr}$  in the rod segment was released.

The posttest distribution of iodine is summarized in Table 30. About 0.033% (13.9  $\mu\text{g}$ ) of the iodine inventory was released. As in tests HBU-8 and -9, most ( $\sim 97\%$ ) of the iodine was found downstream beyond the furnace tube, and about half of it was collected as elemental iodine. The iodine that deposited in the thermal gradient tube was found primarily at the cesium peak location (Fig. 29) at 300 to 400°C. This suggests that CsI was the deposited species.

In this test as well as the other steam tests discussed previously, trace amount ( $9.2 \times 10^{-7}$   $\mu\text{g}$ ) of ruthenium was collected on the charcoal. The amount apparently decreases with the test temperature (Table 10).

#### 4.10 High Burnup Fuel Test 11 (1200°C)

This test was conducted to better define the diffusional escape of fission products from fuel rods with expanded and ruptured cladding and to test the assumption of the additivity of the burst and diffusional release components in the release models. Previous tests measured either diffusional release from a hole drilled in unexpanded cladding or the combined release resulting from rupture followed by diffusion from the expanded, ruptured cladding. These release data are needed for the development of fission product source term models applicable to the upper temperature limit for a hypothetical controlled LOCA, 1200°C. The fuel rod segment used in test HBU-7 (ruptured at 900°C and held at 900°C for only 1 min) was employed. It was maintained at a temperature of 1200°C in a steam atmosphere for the equivalent of 27 min. A resistance heater was used to uniformly heat the entire segment.

The posttest distributions of  $^{134}\text{Cs}$  and total cesium,  $^{129}\text{I}$  and total iodine, and  $^{125}\text{Sb}$  and total antimony in the experimental apparatus are summarized in Tables 31-33. These data indicate that 0.031% (142  $\mu\text{g}$ ) of

Table 30. Distribution of  $^{129}\text{I}$  in High Burnup Fuel Test 10<sup>a</sup>

Location	Temperature (°C)	Amount of $^{129}\text{I}$ found in each location			Total iodine ( $\mu\text{g}$ )
		$\mu\text{g}^{\text{b}}$	Percent of total <sup>c</sup>	Percent of released	
Fuel rod	900-1200	$(3.316 \times 10^4)^{\text{d}}$			$(4.209 \times 10^4)^{\text{d}}$
Furnace tube	~200-900				
Quartz liner		$0.175 \pm 0.003$	$5.28 \times 10^{-4}$	1.60	0.22
Quartz fuel-rod holder		$0.14 \pm 0.009$	$4.22 \times 10^{-4}$	1.28	0.18
Thermal gradient tube	700-225	$2.576 \pm 6.1$	$7.77 \times 10^{-3}$	23.50	3.27
Filter pack components	130				
Stainless-steel inlet fitting		$1.30 \pm 0.12$	$3.92 \times 10^{-3}$	11.86	1.65
First filter paper		$1.92 \pm 0.3$	$5.79 \times 10^{-3}$	17.51	2.44
Second and third filter papers		$0.13 \pm 0.002$	$3.92 \times 10^{-4}$	1.19	0.16
Charcoal No. 1a		$4.722 \pm 0.1$	$1.42 \times 10^{-2}$	43.07	5.99
Charcoal No. 1b		0.0	0.0	0.0	0.0
Charcoal No. 1c		0.0	0.0	0.0	0.0
Charcoal No. 2a		0.0	0.0	0.0	0.0
Charcoal No. 2b <sup>e</sup>		0.0	0.0	0.0	0.0
Charcoal No. 3 <sup>e</sup>		0.0	0.0	0.0	0.0
AgX <sup>e</sup>		0.0	0.0	0.0	0.0
Condenser <sup>e</sup>	0	0.0	0.0	0.0	0.0
Freeze trap <sup>e</sup>	-78	0.0	0.0	0.0	0.0
Cold charcoal traps (two) <sup>e</sup>	-78	0.0	0.0	0.0	0.0
Total		$10.963 \pm 0.63$	$3.31 \times 10^{-2}$	100.00	13.91

<sup>a</sup>Steam flow rate, 1246 cm<sup>3</sup>/min (STP); helium flow rate, 368 cm<sup>3</sup>/min (STP); system pressure, 760 torr. Decay time, 911 days (to Nov. 2, 1976).

<sup>b</sup>Amounts less than  $1.0 \times 10^{-2}$   $\mu\text{g}$  are given as 0.0.

<sup>c</sup>Percentage of radioactive nuclide in fuel rod.

<sup>d</sup>Calculated for burnup of 30,580 MWd per MT of original uranium originally in 12-in. segment, and 911 days of decay.

<sup>e</sup>Not analyzed for  $^{129}\text{I}$  content in any of the High Burnup Series Tests; amount assumed to be 0.0.

Table 31. Distribution of  $^{134}\text{Cs}$  in High Burnup Fuel Test 11<sup>a</sup>

Location	Temperature (°C)	Amount of $^{134}\text{Cs}$ found in each location			Total cesium ( $\mu\text{g}$ )
		( $\mu\text{g}$ )	Percent of total <sup>c</sup>	Percent of released	
Fuel rod	1200	(8685) <sup>d</sup>			( $4.572 \times 10^5$ ) <sup>d</sup>
Furnace tube	1200				
Quartz liner		0.393	$4.53 \times 10^{-3}$	14.57	20.69
Quartz fuel-rod holder		0.400	$4.61 \times 10^{-3}$	14.82	21.06
Thermal gradient tube	1050-200	1.068	$1.23 \times 10^{-2}$	39.58	56.22
Filter pack components	125				
Stainless-steel inlet fitting		0.052	$5.99 \times 10^{-4}$	1.93	2.74
Other housing components		0.0	0.0	0.0	0.0
First filter paper		0.785	$9.04 \times 10^{-3}$	29.10	41.32
Second filter paper		$2.23 \times 10^{-5}$	$2.57 \times 10^{-7}$	$8.27 \times 10^{-4}$	$1.17 \times 10^{-3}$
Third filter paper		$1.10 \times 10^{-5}$	$1.27 \times 10^{-7}$	$4.08 \times 10^{-4}$	$5.79 \times 10^{-4}$
Charcoal No. 1a		0.0	0.0	0.0	0.0
Charcoal No. 1b		0.0	0.0	0.0	0.0
Charcoal No. 1c		0.0	0.0	0.0	0.0
Charcoal No. 2a		0.0	0.0	0.0	0.0
Charcoal No. 3		0.0	0.0	0.0	0.0
AgX		0.0	0.0	0.0	0.0
Condenser		0.0	0.0	0.0	0.0
Freeze trap	-78	0.0	0.0	0.0	0.0
Cold charcoal traps (two)	-78	0.0	0.0	0.0	0.0
Total released		2.698	$3.11 \times 10^{-2}$	100.0	142.03

<sup>a</sup>Steam flow rate, 1323 cm<sup>3</sup>/min (STP); helium flow rate, 344 cm<sup>3</sup>/min (STP); pressure, 760 torr. Decay time, 911 days (to Nov. 2, 1976).

<sup>b</sup>Amounts less than  $1.0 \times 10^{-5}$   $\mu\text{g}$  are given as 0.0.

<sup>c</sup>Percent of radioactive nuclide in fuel rod.

<sup>d</sup>Calculated for burnup of 30,580 MWd/per MT of original uranium, 183.3 g of uranium originally in 12-in. segments, and 911 days of decay.

Table 32. Distribution of  $^{129}\text{I}$  in High Burnup Fuel Test 11<sup>a</sup>

Location	Temperature (°C)	Amount of $^{129}\text{I}$ found in each location			Total iodine ( $\mu\text{g}$ )
		$\mu\text{g}$ <sup>b</sup>	Percent of total <sup>c</sup>	Percent of released	
Fuel rod	1200	(3.316 x 10 <sup>4</sup> ) <sup>d</sup>			(4.208 x 10 <sup>4</sup> ) <sup>d</sup>
Furnace tube	1200				
Quartz liner		<0.02	6.03 x 10 <sup>-5</sup>	0.13	< 0.03
Quartz fuel-rod holder		<0.02	6.03 x 10 <sup>-5</sup>	0.13	< 0.03
Thermal gradient tube	1050-200	5.33 ± 0.60	1.61 x 10 <sup>-2</sup>	33.45	6.76
Filter pack components	125				
Stainless-steel inlet fitting		1.74 ± 0.13	5.25 x 10 <sup>-3</sup>	10.91	2.21
First filter paper		7.82 ± 0.24	2.36 x 10 <sup>-2</sup>	49.07	9.92
Second and third filter papers		0.275 ± 0.003	8.29 x 10 <sup>-4</sup>	1.73	0.35
Charcoal No. 1a		0.69	2.08 x 10 <sup>-3</sup>	4.33	0.88
Charcoal No. 1b		0.04	0.0	0.25	0.0
Charcoal No. 1c		0.0	0.0	0.0	0.0
Charcoal No. 2a		0.0	0.0	0.0	0.0
Charcoal No. 2b <sup>e</sup>		0.0	0.0	0.0	0.0
Charcoal No. 3 <sup>e</sup>		0.0	0.0	0.0	0.0
AgX <sup>e</sup>		0.0	0.0	0.0	0.0
Condenser <sup>e</sup>	0	0.0	0.0	0.0	0.0
Freeze trap <sup>e</sup>	-78	0.0	0.0	0.0	0.0
Cold charcoal traps (two) <sup>e</sup>	-78	0.0	0.0	0.0	0.0
Total released		15.93 ± 0.60	4.80 x 10 <sup>-2</sup>	100.0	20.2

<sup>a</sup>Steam flow rate, 1323 cm<sup>3</sup>/min (STP); helium flow rate, 344 cm<sup>3</sup>/min (STP); pressure, 760 torr. Decay time, 911 days (to Nov. 2, 1976).

<sup>b</sup>Amounts less than 0.03  $\mu\text{g}$  are given as 0.0.

<sup>c</sup>Percent of radioactive nuclide in fuel rod.

<sup>d</sup>Calculated for burnup of 30,580 MWd per MT of original uranium, 183.3 g of uranium originally in 12-in. segments, and 911 days of decay.

<sup>e</sup>Not analyzed for  $^{129}\text{I}$  content in any of the High Burnup Series Tests; amount assumed to be 0.0.

Table 33. Distribution of  $^{125}\text{Sb}$  in High Burnup Fuel Test 11<sup>a</sup>

Location	Temperature (°C)	Amount of $^{125}\text{Sb}$ found in each location			Total antimony ( $\mu\text{g}$ )
		$\mu\text{g}^b$	Percent of total <sup>c</sup>	Percent of released	
Fuel rod	1200	(965) <sup>d</sup>			(2523) <sup>d</sup>
Furnace tube	1200				
Quartz liner		$1.98 \times 10^{-2}$	$2.05 \times 10^{-3}$	4.73	$5.18 \times 10^{-2}$
Quartz fuel-rod holder	1050-200	$5.18 \times 10^{-3}$	$5.37 \times 10^{-4}$	1.24	$1.35 \times 10^{-2}$
Thermal gradient tube	1050-200	$3.83 \times 10^{-1}$	$3.97 \times 10^{-2}$	91.47	1.001
Filter pack components	125				
Stainless-steel inlet fitting		$1.33 \times 10^{-3}$	$1.38 \times 10^{-4}$	0.32	$3.48 \times 10^{-3}$
Other housing components		0.0	0.0	0.0	0.0
First filter paper		$9.35 \times 10^{-3}$	$9.69 \times 10^{-4}$	2.23	$2.44 \times 10^{-2}$
Second filter paper		$1.12 \times 10^{-5}$	$1.16 \times 10^{-6}$	$2.67 \times 10^{-3}$	$2.93 \times 10^{-5}$
Third filter paper		$6.00 \times 10^{-6}$	$6.22 \times 10^{-7}$	$1.43 \times 10^{-3}$	$1.57 \times 10^{-5}$
Charcoal No. 1a		$3.47 \times 10^{-6}$	$3.60 \times 10^{-7}$	$8.29 \times 10^{-4}$	$9.07 \times 10^{-6}$
Charcoal No. 1b		$3.34 \times 10^{-6}$	$3.46 \times 10^{-7}$	$7.98 \times 10^{-4}$	$8.73 \times 10^{-6}$
Charcoal No. 1c		$1.72 \times 10^{-6}$	$1.78 \times 10^{-7}$	$4.11 \times 10^{-4}$	$4.50 \times 10^{-6}$
Charcoal No. 2a		0.0	0.0	0.0	0.0
Charcoal No. 2b		0.0	0.0	0.0	0.0
Charcoal No. 3		0.0	0.0	0.0	0.0
AgX		0.0	0.0	0.0	0.0
Condenser		0.0	0.0	0.0	0.0
Freeze trap	-78	0.0	0.0	0.0	0.0
Cold charcoal traps (two)	-78	0.0	0.0	0.0	0.0
Total released		$4.187 \times 10^{-1}$	$4.34 \times 10^{-2}$	100.00	1.094

<sup>a</sup>Steam flow rate,  $1323 \text{ cm}^3/\text{min}$  (STP); helium flow rate,  $344 \text{ cm}^2/\text{min}$  (STP); pressure, 760 torr.  
Decay time, 911 days (to Nov. 2, 1976).

<sup>b</sup>Amounts less than  $1.0 \times 10^{-6} \mu\text{g}$  are given as 0.0.

<sup>c</sup>Percentage of radioactive nuclide in fuel rod.

<sup>d</sup>Calculated for burnup of 30,580 MWd per MT of original uranium, 183.3 g of uranium originally in 12-in. segments, and 911 days of decay.

the total cesium, 0.048% (20.2  $\mu\text{g}$ ) of the total iodine, and 0.043% (1.09  $\mu\text{g}$ ) of the total antimony inventories of the irradiated fuel rod segment were released during the test.

As seen in Table 31, approximately 71% of the released cesium was transported out of the furnace tube; similarly, almost all of the iodine (>99%) and antimony (>99%) were found beyond the furnace tube. A comparison of the distribution summaries for cesium and iodine (Tables 31 and 32) shows that more cesium (mass) than iodine was present in most of the apparatus components, except for the charcoal which contained no cesium. Approximately 4.5% of the iodine released was collected as elemental iodine on the charcoal. Based on the collection behavior, the iodine was apparently collected primarily as CsI. We estimate that only 6% of the released iodine was collected as elemental iodine. Table 32 shows that most (91%) of the released antimony was deposited in the gold thermal-gradient tube.

Concentration profiles for  $^{134}\text{Cs}$  along the furnace tube liner and fuel rod holder, and for  $^{134}\text{Cs}$ ,  $^{125}\text{Sb}$ , and  $^{129}\text{I}$  along the gold thermal-gradient tube are presented in Fig. 31. The cesium that deposited in the furnace tube was found at the cooler outlet end. The temperature at that location is estimated to have been in the 1000 to 1150°C range. In previous tests with steam, the quartz surfaces near the cladding defect reacted with the cesium so efficiently that only 4 to 16% of the released cesium was transported beyond the furnace tube (even less was transported beyond the furnace tube in tests at lower-sweep-stream flow rates). However, the temperature of the quartz in the previous tests never exceeded 900°C. (With induction heating, the temperature of the quartz remains less than that of the fuel rod.) At higher temperatures, quartz apparently becomes considerably less effective at "gettering" cesium.

On the other hand, there is no apparent attraction of the released antimony for the quartz; in addition, the deposition profile of  $^{125}\text{Sb}$  in the gold thermal-gradient tube (see Fig. 31) reveals that about 70% of the  $^{125}\text{Sb}$  deposited in the temperature range 800 to 1050°C. Most of the  $^{129}\text{I}$  that deposited in the thermal gradient tube was located in the 300

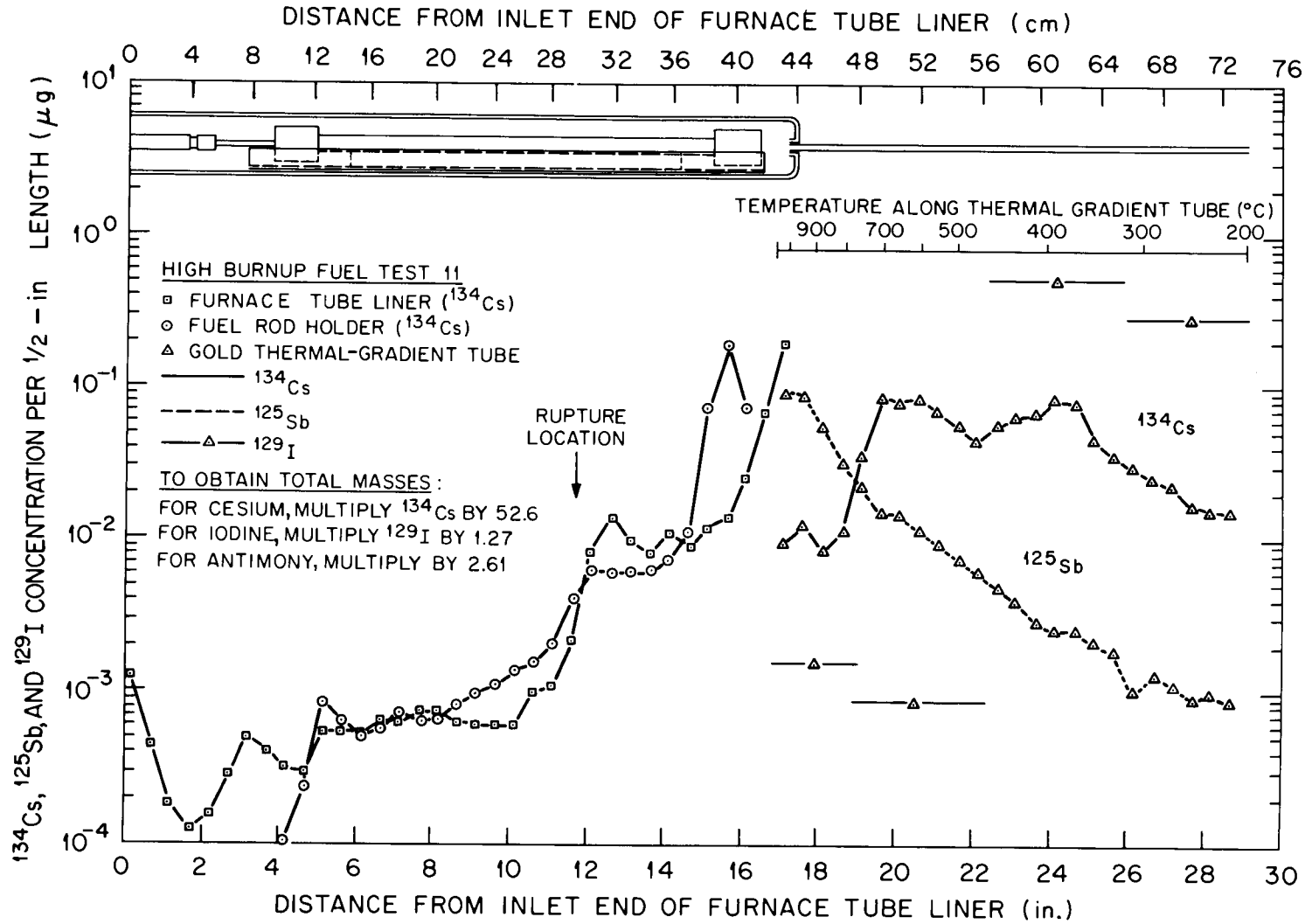


Fig. 31. Concentration profiles of  $^{134}\text{Cs}$ ,  $^{125}\text{Sb}$ , and  $^{129}\text{I}$  in apparatus components in test HBU-11.

to 450°C range. In the Implant Test Series,<sup>2</sup> it was observed that CsI deposited primarily in the 300 to 600°C range.

Continuous monitoring of the thermal gradient tube and filter pack (Fig. 32) indicates that the <sup>134</sup>Cs deposition rate was linear while the fuel rod segment was at the test temperature. From the data displayed in Fig. 32 and those presented in Table 31, we estimate that the rate of diffusional release was about 0.01 µg of the <sup>134</sup>Cs per min (0.53 µg of total cesium per min).

Data for <sup>85</sup>Kr, which was released from the fuel rod segment and collected in solid carbon dioxide-cooled charcoal traps, are also presented in Fig. 32. These data indicate that 0.47% (6.3 mCi) of the original <sup>85</sup>Kr inventory in the segment was released. One-half of this quantity was released in a 2-hr period during which the test rod was held at approximately 300°C in flowing helium.

At variance with the results obtained in previous steam tests, no ruthenium was released in this test. The ruthenium species that is primarily released in steam was possibly depleted from the segment during test HBU-7.

Tests HBU-7 and -11 provided separate measurements of burst release and diffusional release from a ruptured fuel rod at 900 and 1200°C respectively. It is of interest to compare the combined release from these two experiments with the results of test HBU-10, a single experiment in which the test rod was ruptured at 900°C and the temperature was immediately raised to 1200°C and maintained for 10 min. Results from the individual experiments, estimates for test HBU-11 scaled to 10 min, and the sum of the HBU-7 and the adjusted HBU-11 release value are presented in Table 34. The sums of the individual release components compare quite well with the results from test HBU-10, the combined experiment. This lends credence to the assumption that the burst and diffusional release components of the release models are additive.

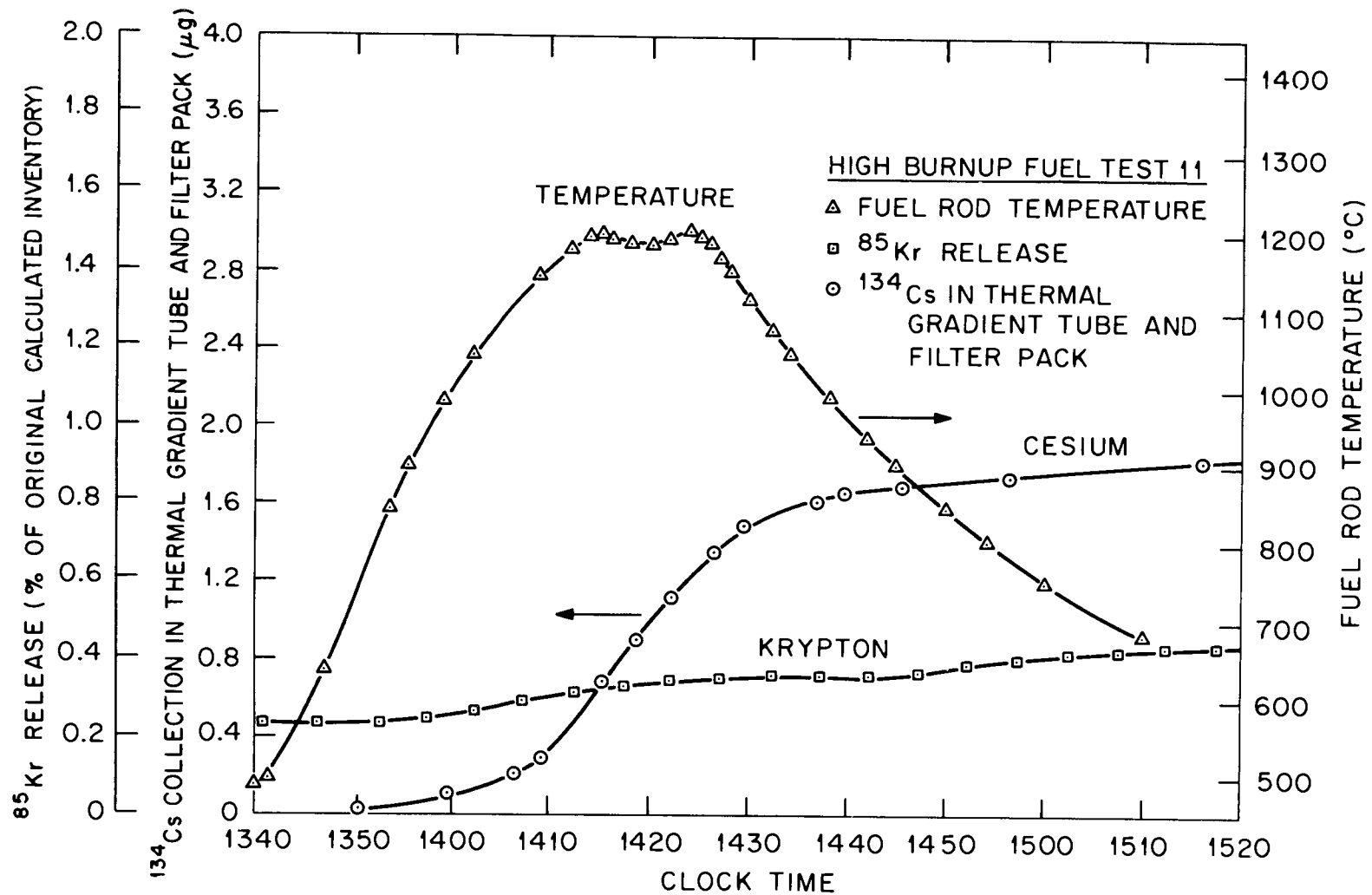


Fig. 32. Collection of <sup>134</sup>Cs in the thermal gradient tube and filter pack, and of <sup>85</sup>Kr in the cold charcoal traps during test HBU-11.

Table 34. Burst release at 900°C followed by diffusional release at 1200°C

Test	Temperature	Test period (min)	Percent of total inventory released				
			$^{85}\text{Kr}$	$^{134}\text{Cs}$	$^{129}\text{I}$	$^{125}\text{Sb}$	$\text{UO}_2$ fuel as dust
HBU-7 <sup>a</sup>	Ruptured at 900	1	0.97	0.029	0.035	b	0.016
HBU-11 <sup>a</sup>	1200	27 <sup>c</sup>	0.47	0.031	0.048	0.043	0.0
HBU-11 (adj) <sup>d</sup>	1200	10	0.33	0.011	0.018		0.0
Sum of HBU-7 + HBU-11 (adj)			1.30	0.040	0.053		0.016
HBU-10 <sup>e</sup>	Ruptured at 900	1.8 <sup>f</sup>	1.69	0.061	0.033	b	0.022
	at 1200	10.0					

<sup>a</sup>Fuel rod segment B-6 from H. B. Robinson rod H-15 was used in both tests.

<sup>b</sup> $^{125}\text{Sb}$  obscured by fuel dust radioactivity.

<sup>c</sup>Actual time at 1200°C was 10 min. Slow heatup and cooldown resulted in a calculated equivalent time of 27 min for cesium diffusional release.

<sup>d</sup>HBU-11 release adjusted for a 10-min period. The releases of cesium and iodine were assumed to be linear with time.

<sup>e</sup>Fuel rod segment A-6 from H. B. Robinson rod D-12.

<sup>f</sup>Time between rupture and heatup to 1200°C.

#### 4.11 High Burnup Fuel Test 12 (Gap Purge Test)

##### 4.11.1 Experimental results

Test HBU-12 was conducted in an attempt to quantitatively determine the amounts of fission products that are readily available for release from the high-burnup H. B. Robinson fuel rod segments that were tested in this experimental series. These quantities are the fractions of the total inventories that would be present in the pellet-to-clad interface and in other void spaces in the fuel, such as cracks and pores that are openly connected to the surface. They constitute the so-called gap inventories. In time-temperature regimes for controlled LOCAs and SFTAs, additional fission product migration to the gap from the fuel matrix would be small. Consequently, the fission product gap inventory is one of the primary controlling determinants of fission product release under LOCA and SFTA conditions.

In this test, a stainless-steel Swagelok fitting on the downstream end of the fuel rod specimen (B-7) was replaced with one fabricated from Zircaloy. In addition, a 0.0625-in. (0.159 cm)-ID Zircaloy tube was attached to provide an outlet for the fission products, and a platinum cone was positioned at the downstream end of the quartz furnace-tube liner to prevent interaction of the fission products with the quartz components (see Fig. 33). In the experiment, performed in a helium atmosphere, purified helium was employed to purge volatilized fission products from the gap space. The purge helium was purified by passing the gas stream through a stainless-steel cylinder that contained zirconium chips and was maintained at 800°C. The test was conducted in the following time-temperature sequence: 52 min at 700°C, 65 min at 900°C, 260 min at 1100°C, and 40 min at 1200°C.

The posttest distributions of cesium and iodine in the experimental apparatus are summarized in Tables 35 and 36 respectively. These data indicate that 0.46% (1996  $\mu\text{g}$ ) of the total cesium and 0.44% (189  $\mu\text{g}$ ) of the total iodine inventories were released. As was anticipated, most of the released cesium (90%) and iodine (91%) deposited in the thermal gradient tube. Only 0.2% of the released iodine was found on the impregnated charcoal.

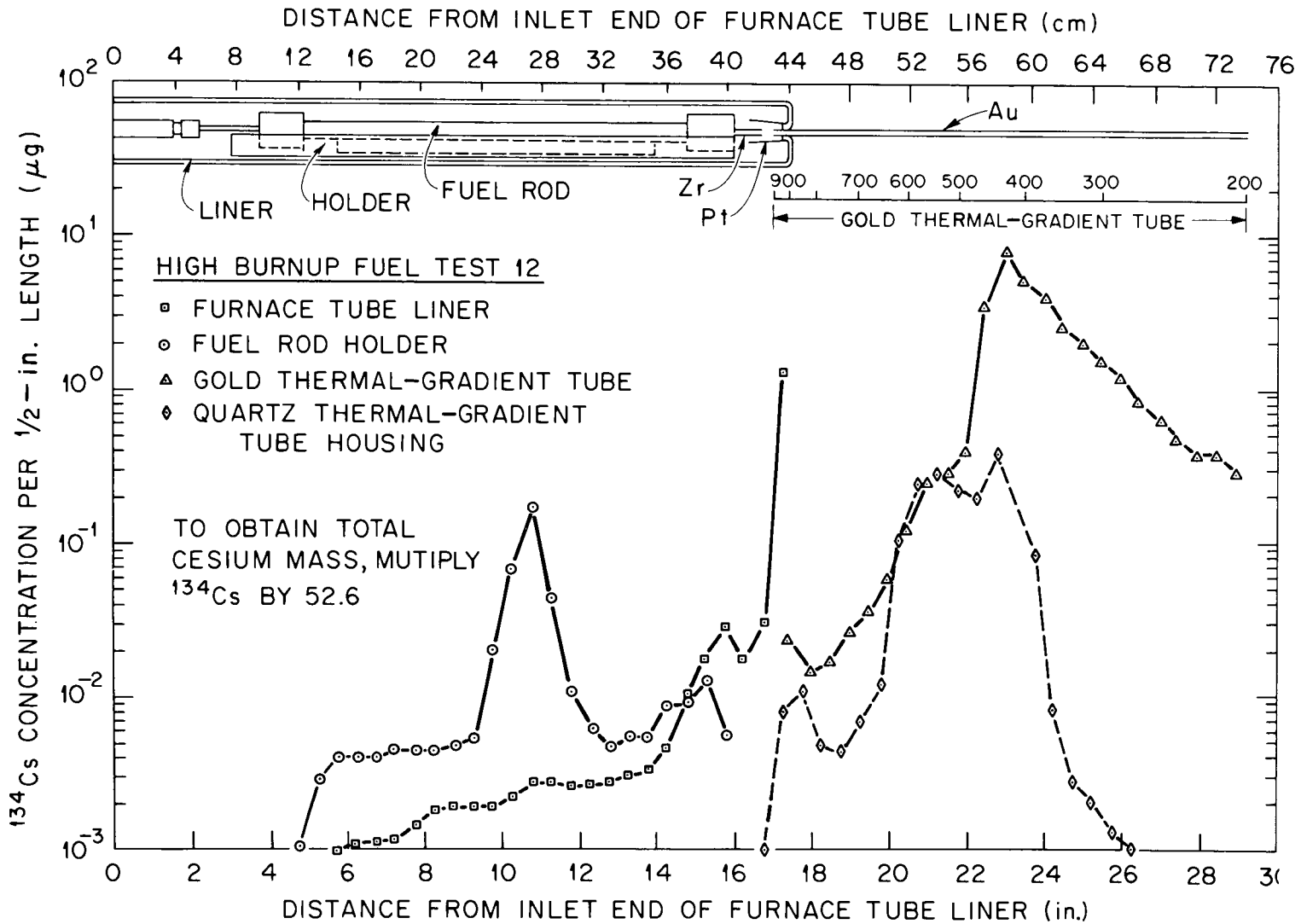


Fig. 33. Concentration of <sup>134</sup>Cs in apparatus components in test HBU-12.

Table 35. Distribution of  $^{134}\text{Cs}$  in High Burnup Fuel Test 12<sup>a</sup>

Location	Temperature (°C)	Amount of $^{134}\text{Cs}$ found in each location			Total cesium ( $\mu\text{g}$ )
		$\mu\text{g}^{\text{b}}$	Percent of total <sup>c</sup>	Percent of released	
Fuel rod	d	(8537) <sup>e</sup>			(4.494 x 10 <sup>5</sup> ) <sup>e</sup>
Furnace tube	d				
Quartz liner		1.468	1.72 x 10 <sup>-2</sup>	3.87	77.273
Quartz holder		0.419	4.91 x 10 <sup>-3</sup>	1.10	22.055
Thermal gradient tube	950-200				
Quartz housing		1.819	2.13 x 10 <sup>-2</sup>	4.80	95.75
Gold liner		32.324	3.79 x 10 <sup>-1</sup>	85.25	1701.47
Filter pack components	125				
Stainless-steel inlet fitting		0.235	2.75 x 10 <sup>-3</sup>	0.62	12.370
First filter paper		1.653	1.94 x 10 <sup>-2</sup>	4.36	87.011
Second and third filter papers		1.06 x 10 <sup>-6</sup>	1.24 x 10 <sup>-8</sup>	2.80 x 10 <sup>-6</sup>	5.5 x 10 <sup>-5</sup>
Charcoal No. 1a		0.0	0.0	0.0	0.0
Charcoal No. 1b		0.0	0.0	0.0	0.0
Charcoal No. 1c		0.0	0.0	0.0	0.0
Charcoal No. 2a		0.0	0.0	0.0	0.0
Charcoal No. 2b		0.0	0.0	0.0	0.0
Charcoal No. 3		0.0	0.0	0.0	0.0
AgX		0.0	0.0	0.0	0.0
Condenser	0	0.0	0.0	0.0	0.0
Freeze trap	-78	0.0	0.0	0.0	0.0
Cold charcoal traps (two)	-78	0.0	0.0	0.0	0.0
Total release		37.918	4.45 x 10 <sup>-1</sup>	100.0	1995.93

<sup>a</sup>Combined rod gap, ferrule leak, and furnace tube helium flow: 700 cm<sup>3</sup> (STP)/min at 700°C, 960 cm<sup>3</sup> (STP)/min at 900°C, and 1700 cm<sup>3</sup> (STP)/min at 1100 to 1200°C. System pressure, 760 to 800 torr. Decay time, 911 days (to Nov. 2, 1976).

<sup>b</sup>Amounts less than 1.0 x 10<sup>-7</sup>  $\mu\text{g}$  are given as 0.0.

<sup>c</sup>Percent of radioactive nuclide in fuel rod segment.

<sup>d</sup>The temperature-time sequence was conducted as follows: 700°C for 52 min, 900°C for 65 min, 1100°C for 260 min, and 1200°C for 40 min.

<sup>e</sup>Calculated for burnup of 31,360 MWd per MT of original uranium, 175.5 g of uranium originally in 11.5-in. segment, and 911 days of decay.

Table 36. Distribution of  $^{129}\text{I}$  in High Burnup Fuel Test 12<sup>a</sup>

Location	Temperature (°C)	Amount of $^{129}\text{I}$ found in each location			Total iodine ( $\mu\text{g}$ )
		$\mu\text{g}^b$	Percent of total <sup>c</sup>	Percent of released	
Fuel rod	d	( $3.40 \times 10^4$ ) <sup>e</sup>			( $4.315 \times 10^4$ ) <sup>e</sup>
Furnace tube	d				
Quartz liner		0.10	$2.94 \times 10^{-4}$	0.07	0.13
Quartz fuel-rod holder		$0.0075 \pm 0.0004$	$2.21 \times 10^{-5}$	0.01	0.01
Thermal gradient tube	950-200	$135.3 \pm 28$	0.40	91.10	171.73
Filter pack components	125				
Stainless-steel inlet fitting		$1.8 \pm 0.2$	$5.29 \times 10^{-3}$	1.21	2.28
First filter paper		$11.0 \pm 0.6$	$3.24 \times 10^{-2}$	7.41	13.96
Second and third filter papers		$0.066 \pm 0.002$	$1.94 \times 10^{-4}$	0.04	0.08
Charcoal No. 1a		$0.243 \pm 0.02$	$7.15 \times 10^{-4}$	0.16	0.31
Charcoal No. 1b		0.0	0.0	0.0	0.0
Charcoal No. 1c		0.0	0.0	0.0	0.0
Charcoal No. 2a		0.0	0.0	0.0	0.0
Charcoal No. 2b <sup>f</sup>		0.0	0.0	0.0	0.0
Charcoal No. 3 <sup>f</sup>		0.0	0.0	0.0	0.0
AgX <sup>f</sup>		0.0	0.0	0.0	0.0
Condenser <sup>f</sup>	0	0.0	0.0	0.0	0.0
Freeze trap <sup>f</sup>	-78	0.0	0.0	0.0	0.0
Cold charcoal traps (two)	-78	0.0	0.0	0.0	0.0
Total		$148.52 \pm 28$	0.437	100.00	188.50

<sup>a</sup>Combined rod gap, ferrule leak, and furnace tube helium flow:  $700 \text{ cm}^3$  (STP)/min at  $700^\circ\text{C}$ ,  $960 \text{ cm}^3$  (STP)/min at  $900^\circ\text{C}$ , and  $1700 \text{ cm}^3$  (STP)/min at  $1100$  to  $1200^\circ\text{C}$ . System pressure, 760 to 800 torr. Decay time, 911 days (to Nov. 2, 1976).

<sup>b</sup>Amounts less than  $1.0 \times 10^{-7} \mu\text{g}$  are given as 0.0.

<sup>c</sup>Percentage of radioactive nuclide in fuel rod segment.

<sup>d</sup>The temperature-time sequence was conducted as follows:  $700^\circ\text{C}$  for 52 min,  $900^\circ\text{C}$  for 65 min,  $1100^\circ\text{C}$  for 260 min, and  $1200^\circ\text{C}$  for 40 min.

<sup>e</sup>Calculated for burnup of 31,360 MWd per MT of original uranium, 175.7 g of uranium originally in 11.5-in. segment, and 911 days of decay.

<sup>f</sup>Not analyzed for  $^{129}\text{I}$  content; amount assumed to be 0.0.

Distribution of the  $^{134}\text{Cs}$  along the furnace tube liner, fuel rod holder, and thermal gradient tube is shown in Fig. 33. The principal deposition occurred at the 300 to 500°C location in the thermal gradient tube. Although not shown in the figure, it was determined that the iodine deposition in the thermal gradient tube also occurred at the 300 to 500°C location. Apparently the iodine was released and deposited as CsI. In addition to CsI, a vapor species of cesium other than elemental cesium (possibly  $\text{Cs}_2\text{O}$ ) was collected.

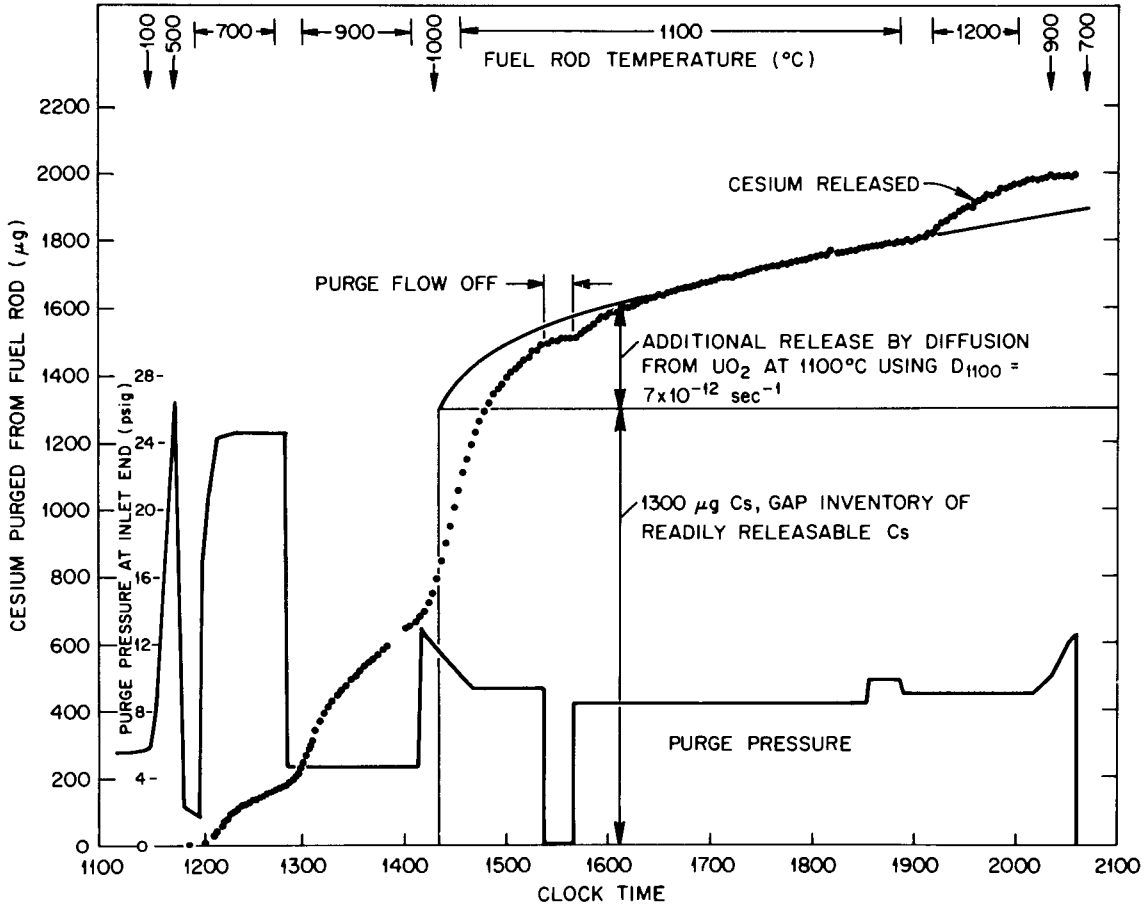
The pressure of the purified helium purge as applied to the inlet end of the pellet-to-clad gap is depicted graphically in Fig. 34 along with a fuel rod temperature and cumulative release of cesium. The radioactive isotopes  $^{134}\text{Cs}$  and  $^{137}\text{Cs}$  were monitored with a single-channel analyzer, and the concentrations were subsequently normalized to the total mass of cesium released after the fuel rod was heated above 500°C. Because of a leak that developed in the inlet-end stainless-steel ferrule fitting as a result of thermal expansion, the flow rate of the helium could not be measured directly. It is believed that the leak was insignificant during the heatup to 500°C, so that all of the measured purge flow passed through the pellet-to-clad gap space. For this period of operation, it was possible to calculate values of gap width from the purge flow data according to a method<sup>13,14</sup> discussed in Appendix A. The results given in Table 37, indicate that the radial gap width remained unchanged at about 40  $\mu\text{m}$ . This is somewhat larger than was determined with other segments of H. B. Robinson fuel which were taken from bundle B05.

Table 37. Calculated width of radial gap, test HBU-12

Fuel rod temperature (°C)	Inlet end pressure <sup>a</sup> (atm)	Helium flow rate (cm <sup>3</sup> , STP/min)	Helium viscosity (10 <sup>6</sup> g/cm·sec)	Calculated gap width (μm)
70	1.38	63.5	220	43
200	1.73	76.3	267	41
300	2.10	90.2	305	41
400	2.49	104.3	342	41
500	2.76	124.2	376	43

<sup>a</sup>Outlet end pressure, 1.02 atm.

ORNL DWG 78-13931



PURGE PRESSURE AND CESIUM RELEASE DURING TEST HBU-12

Fig. 34. Purge pressure and cesium release during test HBU-12.

By using the measured purge pressure and assuming that the gap size remained constant at higher temperatures, the purge flow rate was calculated for several test periods, as listed in Table 38. The cesium purge rate was obtained from the data displayed in Fig. 34; the purge data were then used to calculate corresponding values of cesium concentration. These concentrations are only approximate because the helium purge rate was not measured directly. However, it is clear that, as a given temperature was attained, the initial cesium concentration was greater than the later "stabilized" value. See Sect. 5.3.2 for comparison of concentrations of cesium and iodine in the gas release at rupture.

Data for  $^{85}\text{Kr}$  collection in the charcoal traps and for the deposition of  $^{134}\text{Cs}$  in the thermal gradient tube are presented in Fig. 35. The krypton data indicate that 1.36% (17.8 mCi) of the original  $^{85}\text{Kr}$  inventory was released. Approximately 90% of the  $^{85}\text{Kr}$  was collected while the segment was being heated to  $700^\circ\text{C}$  and during the subsequent time period (52 min) at that temperature. The remainder occurred during the next heatup period of the rod segment (to  $900^\circ\text{C}$ ) and the first 10 min at which this temperature was maintained.

No release of  $^{125}\text{Sb}$  was detected in this test, which is at variance with the results obtained in test HBU-11, conducted at  $1200^\circ\text{C}$  in steam and discussed earlier in this report, nor was ruthenium released.

#### 4.11.2 Diffusion of cesium from the $\text{UO}_2$ pellet matrix

In test HBU-12, the concentration of cesium in the purge stream at  $1100^\circ\text{C}$  gradually decreased to a value less than that at  $900^\circ\text{C}$ , which suggests that the gap inventory of cesium was being depleted. Based on previous tests<sup>15</sup> with irradiated  $\text{UO}_2$ , additional cesium should diffuse from the  $\text{UO}_2$  matrix at a slow but measurable rate.

Equations were derived<sup>16</sup> for diffusion from sintered  $\text{UO}_2$  by assuming the pellets were composed of an agglomeration of independent spheres.<sup>16</sup> For uniform initial concentration of the diffusing species, the fraction released when the pellet was heated to a given temperature was estimated by

$$f = \frac{6}{(\pi)^{1/2}} (D't)^{1/2}, \quad (1)$$

Table 38. Cesium purge rates during test HBU-12<sup>a</sup>

Time interval (clock time)	Temperature (°C)	Inlet pressure <sup>b</sup> (atm)	Helium flow rate <sup>b</sup> (cm <sup>3</sup> /min, STP)	Cesium purge rate (µg Cs/min)	Cesium concentration <sup>c</sup> (µg Cs/cm <sup>3</sup> He)	Comments
1210-1220	700	2.66	69.7	6.0	0.086 <sup>d</sup>	Maximum rate at 700°C
1230-1246	700	2.67	70.1	2.1	0.030	Stabilized rate at 700°C
1300-1310	900	1.31	5.05	14.0	2.77	Maximum rate at 900°C
1330-1405	900	1.31	5.05	4.7	0.93	Stabilized rate at 900°C
1420-1430	1060	1.74	12.4	21.0	1.69	Maximum release rate
1430-1440	1100	1.67	10.2	19.0	1.86	Maximum rate at 1100°C
1750-1850	1100	1.61	8.66	0.83	0.096	Stabilized rate at 1100°C
1910-1930	1200	1.61	7.67	3.4	0.44	Maximum rate at 1200°C

<sup>a</sup>Assumes constant radial gap width of 41 µm.

<sup>b</sup>Outlet pressure ranged from 1.02 atm at 700°C to 1.14 atm at 1100°C (initial)

<sup>c</sup>Helium flow rate and cesium concentration are only approximate because helium flow rate could not be measured directly.

<sup>d</sup>This is equivalent to a partial pressure of  $1.46 \times 10^{-6}$  MPa.

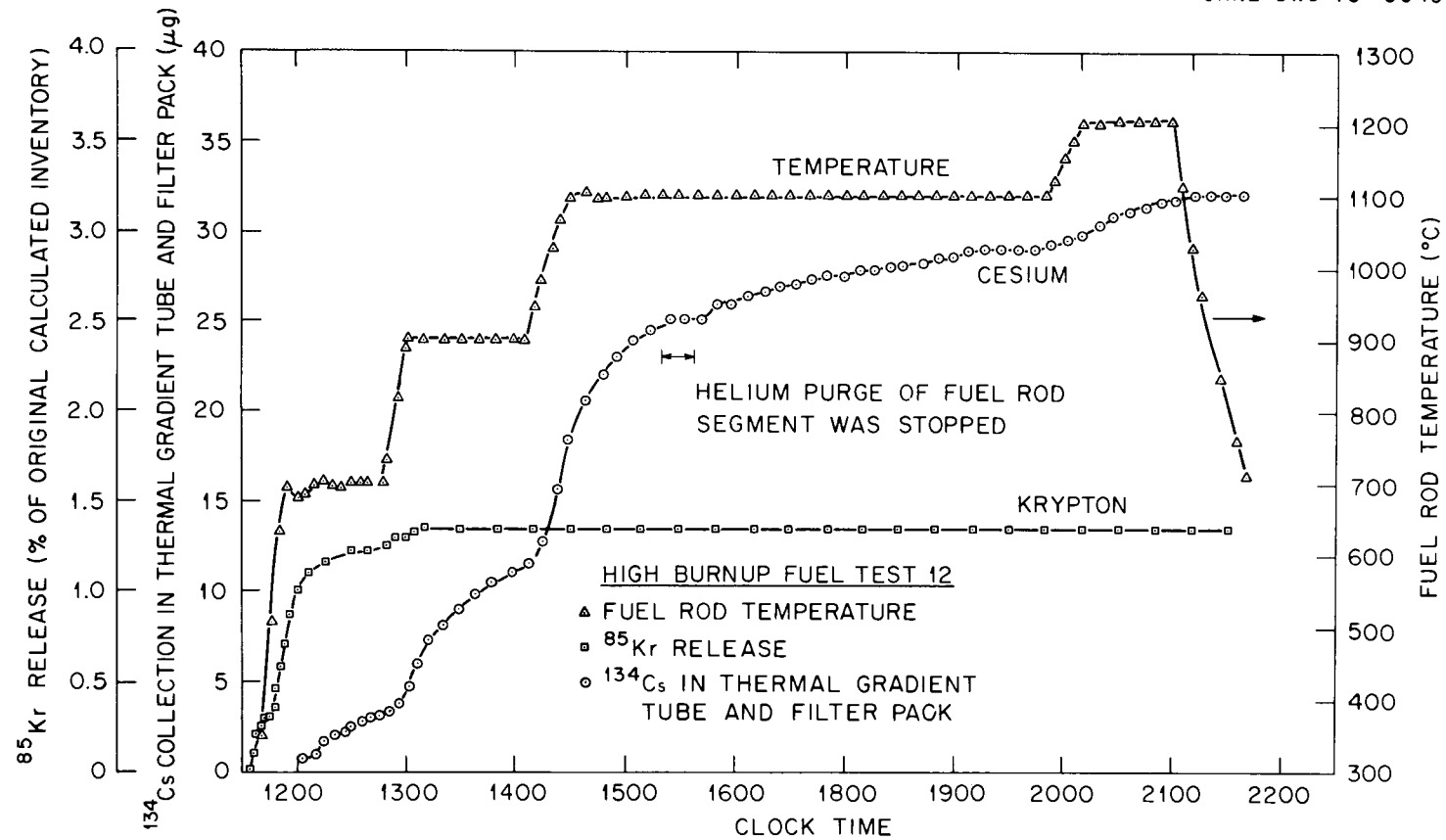


Fig. 35. Collection of  $^{134}\text{Cs}$  in the thermal gradient tube and filter pack, and of  $^{85}\text{Kr}$  in the cold charcoal traps during test HBU-12.

where

- f = fraction released by diffusion at time t (only for  $f \leq 0.1$ ),  
 D' = diffusion parameter,  $D/a^2$ ,  $\text{sec}^{-1}$ ,  
 D = diffusion coefficient,  $\text{cm}^2/\text{sec}$ ,  
 a = radius of equivalent sphere, cm, and  
 t = time at temperature, sec.

During the 4.5-hr period at  $1100^\circ\text{C}$ , some of the cesium purged from the gap space may represent diffusional release from the  $\text{UO}_2$  matrix. By trial and error, a diffusion parameter (D') value of  $7.0 \times 10^{-12} \text{ sec}^{-1}$  was found to fit the observed release curve reasonably well if the initial gap inventory of cesium was assumed to be 1300  $\mu\text{g}$ .

The calculated amounts released by diffusion from the  $\text{UO}_2$  matrix are listed in Table 39. The sum of the amount diffused and the initial gap inventory plotted in Fig. 34, along with the measured release amounts, assumes that all of the cesium was released at the same rate that the  $^{134}\text{Cs}$  and  $^{137}\text{Cs}$  collected in the thermal gradient tube and filter pack. Clock time 1420 (fuel rod temperature,  $1025^\circ\text{C}$ ) was chosen as the starting time for diffusional release. Obviously, the gap inventory (i.e., 1300  $\mu\text{g}$  of cesium) was not completely released by clock time 1420.

Table 39. Calculated amount of cesium released by diffusion at  $1100^\circ\text{C}$

Time at $1100^\circ\text{C}$		Amount of cesium released <sup>a</sup>	
		Fraction of total inventory, f	Mass ( $\mu\text{g}$ )
sec	hr		
600	0.167	$2.194 \times 10^{-4}$	96
3,600	1	$5.374 \times 10^{-4}$	235
7,200	2	$7.599 \times 10^{-4}$	333
10,800	3	$9.307 \times 10^{-4}$	408
14,400	4	$1.075 \times 10^{-3}$	471
18,000	5	$1.202 \times 10^{-3}$	526
21,600	6	$1.316 \times 10^{-3}$	577

<sup>a</sup>Calculated for  $D' = 7.0 \times 10^{-12}/\text{sec}$ .

According to this simple, two-component release model, the initial gap inventory of cesium was 1300  $\mu\text{g}$ , which was equivalent to about 0.30% of the total cesium inventory in the segment. This can be compared with the in-reactor xenon release to the fuel rod voids and plenum of 0.25% that was measured at room temperature. (Heating to 1200°C during the HBU-12 test released an additional 1.36% of the fission gas.)

The best-fit diffusion parameter for cesium also compares reasonably well with that for fission gas release. A xenon  $D'$  value of  $2.1 \times 10^{-12}/\text{sec}$  at 1100°C was determined for trace-irradiated fuel; for fuel irradiated in the 1000-4000 MWd/MT burnup range, the  $D'$  value was  $\sim 1.2 \times 10^{-11}/\text{sec}$ .<sup>15</sup> The ANS-5.4 subcommittee<sup>17</sup> observed that  $D'$  at 1100°C for xenon ranged from  $7.5 \times 10^{-12}/\text{sec}$  to  $8.3 \times 10^{-11}/\text{sec}$  for LWR fuel irradiated mainly to burnups of 1000 to 10,000 MWd/MT. The relative rates of release of cesium and xenon from  $\text{UO}_2$  have been observed to vary widely,<sup>17</sup> whereas postirradiation annealing studies<sup>15</sup> indicate that the release of iodine from  $\text{UO}_2$ , as compared with xenon release, averages approximately 2.5 times more (i.e.,  $D'$  for iodine is about six times larger than the corresponding value for xenon).

For high-temperature, long-term exposures, the diffusion of cesium and iodine from the  $\text{UO}_2$  matrix should probably be treated as a replenishment of the gap inventory and not as being directly released from the rod. This effect was demonstrated in test HBU-12 between clock times 1522 and 1539, when shutoff of the purge flow resulted in a large decrease in the rate of cesium escape from the test fuel rod segment.

#### 4.12 Summary of Release Data

Fission product and fuel release during the High Burnup Fuel Tests are summarized in Table 40. The release values from the Low Burnup Test Series are included for comparison. In Appendix B, the releases for cesium and iodine that were obtained with the low burnup fuel are compared with releases obtained in similarly conducted high burnup fuel tests.

Table 40. Summary of fission product and fuel release from irradiated fuel

Test No.	Type of test	Temperature (°C)	Diffusional release time (hr)	Percent of total inventory in test segment released				$^{85}\text{Kr}$	$\text{UO}_2$
				Cesium	Iodine	Antimony	Ruthenium		
HBU-4	Steam, diffusion, drilled hole	500	20	$3.62 \times 10^{-6}$	$2.24 \times 10^{-4}$	— <sup>a</sup>	$1.5 \times 10^{-7}$	0.63	—
HBU-1	Steam, diffusion, drilled hole	700	5	$2.62 \times 10^{-5}$	$2.14 \times 10^{-3}$	—	$3.6 \times 10^{-8}$	≈1.0	—
HBU-2	Steam, diffusion, drilled hole	900	2	$6.16 \times 10^{-4}$	$4.17 \times 10^{-3}$	$2.0 \times 10^{-3}$	$7.0 \times 10^{-9}$	1.10	—
HBU-11 <sup>b</sup>	Steam, diffusion, drilled hole	1200	0.45	0.0311	0.0480	0.0434	—	0.47 <sup>b</sup>	—
HBU-5 <sup>c</sup>	Air, diffusion, drilled hole	500	20	$5.13 \times 10^{-7}$	0.0140	—	$9.04 \times 10^{-5}$	0.53 <sup>c</sup>	—
HBU-6	Air, diffusion, drilled hole	700	5	$1.43 \times 10^{-3}$	0.0479	—	$7.27 \times 10^{-4}$	1.24	—
HBU-7 <sup>d</sup>	Steam, rupture, and diffusion	900-900	0.017	0.0286	0.0265	—	$8.3 \times 10^{-6}$	0.97	0.016
HBU-8 <sup>d</sup>	Steam, rupture, and diffusion	900-900	1.0	0.0087	0.0322	—	$8.8 \times 10^{-6}$	1.26	0.0408
HBU-9 <sup>d</sup>	Steam, rupture, and diffusion	900-1100	0.140	0.0240	0.0392	—	$1.1 \times 10^{-6}$	1.47	0.018
HBU-10 <sup>d</sup>	Steam, rupture, and diffusion	900-1200	0.167	0.0611	0.0331	—	$9.2 \times 10^{-7}$	1.69	0.022
HBU-12	Gap purge	700-1200	9.0	0.455	0.437	—	—	1.36	—
LBU-1 <sup>e</sup>	Steam, diffusion, drilled hole	700	5	$3.02 \times 10^{-4}$	0.021	—	—	—	—
LBU-2	Steam, diffusion, drilled hole	900	2	0.123	2.56	—	—	—	—

<sup>a</sup>— means not detected.

<sup>b</sup>Test segment used previously in HBU-7. The  $^{85}\text{Kr}$  release is in addition to the 0.97% obtained in HBU-7.

<sup>c</sup>Test segment used previously in HBU-4. The  $^{85}\text{Kr}$  release is in addition to the 0.63% obtained in HBU-4.

<sup>d</sup>Only ~55% of the test segment length was heated to temperatures shown. Percentages given are based on entire segment length. First temperature is for rupture; second is for diffusional release time.

<sup>e</sup>See Appendix B for description of tests with low burnup (LBU) fuel tests.

#### 4.12.1 Cesium, iodine, antimony, and ruthenium release in steam

The releases of cesium, iodine, and antimony are shown graphically in Fig. 36. Diffusional release quantities were reduced to a 10-min basis assuming linear release rates. For the diffusional release tests, the difference between iodine and cesium release percentages was much greater at the lower temperatures. No direct comparison can be made between diffusion from the test segments with drilled holes and those with rupture-formed holes and expanded cladding. If gas-phase diffusion is assumed to occur along the pellet-clad gap space and out the hole, the initial release rate should be proportional to the available cross-sectional area. We have estimated that the diffusional release rates from pressure-ruptured cladding, which occurs in our induction-heated tests, is approximately ten times greater than from the test segments with drilled holes and unexpanded cladding.

One to two hundred times more cesium and iodine were released when the test segments were pressure ruptured at 900°C, as compared with the amounts released in 10 min by diffusion from the test segments with pre-drilled holes and unexpanded cladding. The two tests in which rupture occurred at 900°C, followed by diffusional release at either 1100 or 1200°C, did not release much more cesium and iodine than those that remained at 900°C following rupture.

Only a trace amount of ruthenium was released in each of the tests conducted in steam, which was less than  $10^{-5}$ % of the segment inventory (Table 40). In each case, the ruthenium was primarily collected downstream on the charcoal, which suggests a very volatile form of ruthenium. A more detailed discussion is presented in Sect. 5.1.4.

Antimony release could only be quantitatively measured in two diffusion release tests, HBU-2 and HBU-11. The data in Table 40 revealed that the antimony releases were comparable with the cesium releases in those tests.

ORNL DWG 78-21510RA

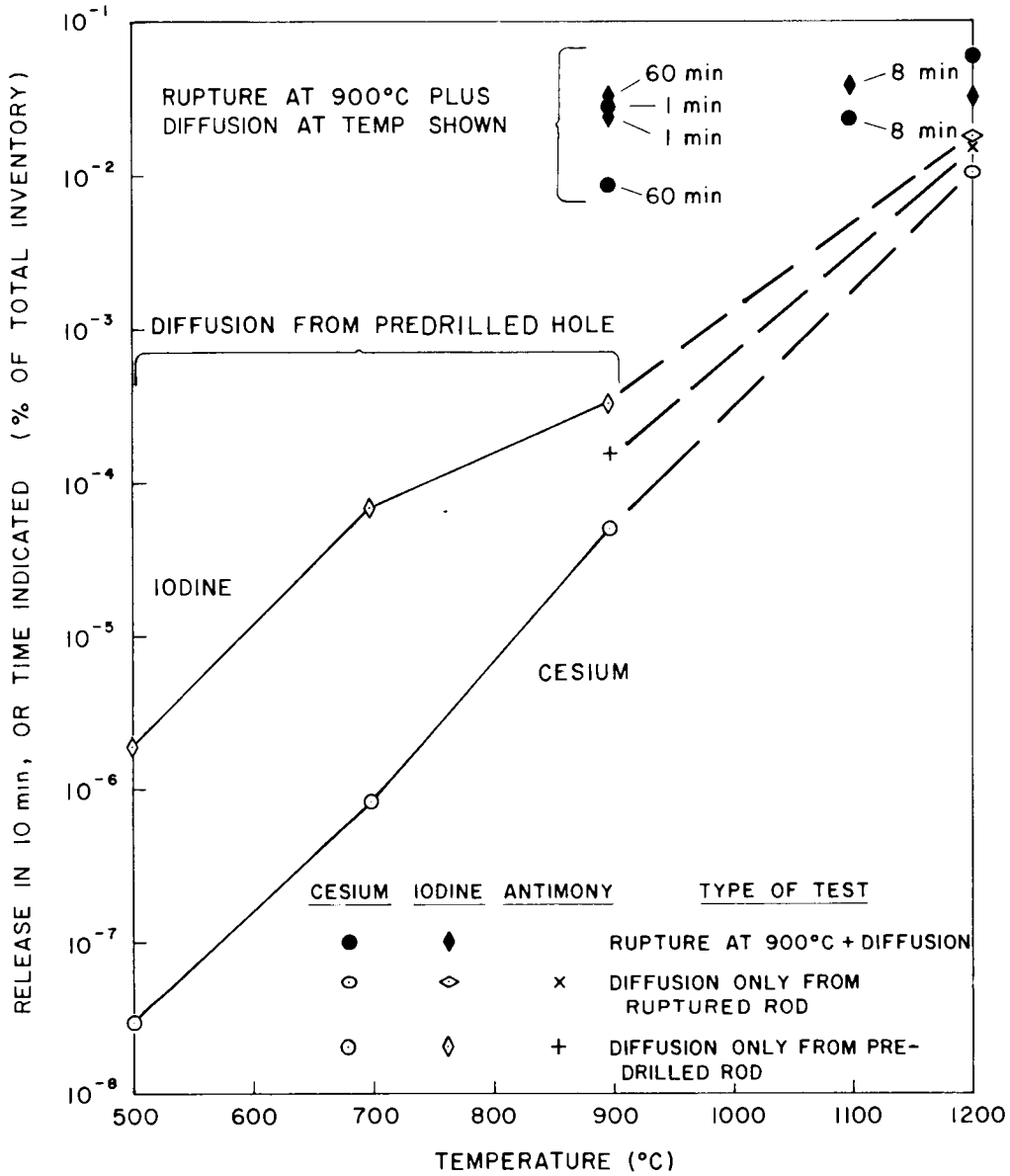


Fig. 36. Summary of fission product release in steam: high burnup fuel.

4.12.2 Cesium, iodine, and ruthenium releases in dry air compared with those obtained in steam

In this experimental series, only two tests (HBU-5 and -6) were conducted with flowing dry-air atmospheres. A 0.159-cm-diam hole was drilled into each of the two rod segments at the midpoint to simulate a defect. As was expected, the fuel in the vicinity of the defects became oxidized and there was visible expansion of the cladding. Collection data for cesium and krypton (Sects. 4.4 and 4.5) suggested that the cesium releases in both tests were linear with time.

The most notable result in these tests was the relatively large releases of ruthenium. In Table 41, the data indicate that 3290 times more ruthenium was released in test HBU-5 (500°C), a dry air test, than was released in HBU-4 (500°C), a steam test. The difference was even more dramatic in comparing the 700°C tests, HBU-6 (dry air) and HBU-1 (steam); about 21,400 times more ruthenium was released in dry air. In all of the steam tests, regardless of temperature, the ruthenium releases were about the same (Table 40).

Table 41. Release data for similarly conducted dry air and steam tests

Test No.	Type test	Temperature (°C)	Percent of total inventory released per hour		
			Cesium	Iodine	Ruthenium
HBU-4	Steam	500	$0.18 \times 10^{-6}$	$12.1 \times 10^{-6}$	$0.007 \times 10^{-6}$
HBU-5 <sup>a</sup>	Dry air	500	$0.13 \times 10^{-6}$	$3500.0 \times 10^{-6}$	$23.0 \times 10^{-6}$
HBU-1	Steam	700	$5.2 \times 10^{-6}$	$428.0 \times 10^{-6}$	$0.007 \times 10^{-6}$
HBU-6	Dry air	700	$286.0 \times 10^{-6}$	$9580.0 \times 10^{-6}$	$150.0 \times 10^{-6}$

<sup>a</sup>In this test, the drilled defect hole became plugged by expanding oxidized fuel (according to the release of <sup>85</sup>Kr), the fission product release was assumed to have stopped after 4 hr of testing (see Sect. 4.4).

The cesium releases for both the dry air and steam tests at 500°C were almost identical (Table 41); however, about 290 times more iodine was released in the dry air test HBU-5 than the steam test HBU-4; at 700°C,

approximately 55 times more cesium and 22 times more iodine were released in the dry air test HBU-6 than in the steam test HBU-1.

The release data in Table 41 show that iodine and ruthenium releases in dry air were considerably more significant than those in steam. This was also true for cesium at 700°C.

#### 4.12.3 Fuel particles ejected at time of rupture

Particles of  $UO_2$  fuel were ejected at the time of rupture (Table 42); a small fraction (0.8 to 2.9%) of the ejected fuel was carried out of the furnace tube into the thermal gradient tube and filter pack. At the time of rupture, the velocity of steam flowing through the furnace tube was approximately 15 cm/sec, so that particles would have to fall at a rate of about 3 cm/sec in order to settle out before reaching the thermal gradient tube. Fuel particles 12 to 15  $\mu m$  in diameter or larger would fall at this rate. The scanning electron microscope (SEM) was used to measure the size of fuel particles; those found in the furnace tube were typically 150  $\mu m$  diam, and those found on the filter papers or inlet fitting were typically 10  $\mu m$  diam. Details of particle measurement are given in Appendix C.

Table 42. Mass of  $UO_2$  found in each location (mg)

Test No.	H. B. Robinson fuel rod No.	Furnace tube and fuel rod holder	Thermal gradient tube	Filter Pack		Total
				Inlet fitting	First filter paper	
HBU-7	D-12	32.49	a	0.17	0.55	33.21
HBU-8	D-12	84.06	0.007	0.093	0.589	84.75
HBU-9	D-12	36.96	0.056	0.079	0.257	37.35
HBU-10	H-15	44.68	0.22	0.12	1.01	46.03

<sup>a</sup>Not detected.

#### 4.12.4 Fission gas release

As detailed in Sect. 2.4, approximately 0.25% of the fission gas was released to the plenum and void spaces during operation of the H. B. Robinson reactor. During heatup of the segments in our test series, an additional amount of fission gas was released, as is shown in Fig. 37. Although the precise mechanism for retention and release of this portion of the fission gas is not known, it is believed to be similar to "attached gas."<sup>18</sup> Swanson et al.<sup>19</sup> and Kryger<sup>20</sup> made use of the thermal release characteristics of the attached fission gas to estimate the in-reactor operating temperatures of type 316 stainless steel cladding.

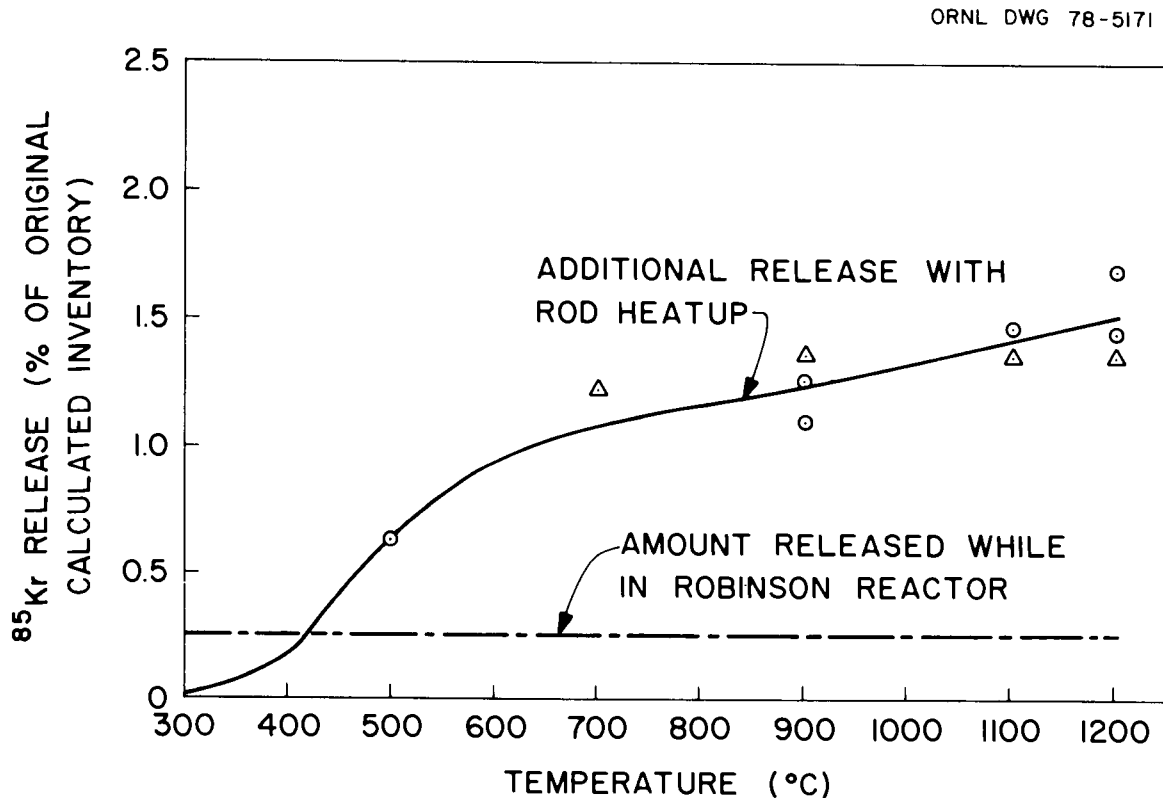


Fig. 37. Amount of  $^{85}\text{Kr}$  released from high burnup fuel.

According to Fig. 37, significant amounts of the attached fission gas will be released in almost any accident reaching 500°C. No data could be found to indicate whether the amounts of gas shown in Fig. 37 are reproducible in other LWR fuels. No  $^{85}\text{Kr}$  release was detected in the low burnup tests, but the small charcoal traps employed at that time, combined with smaller amounts of  $^{85}\text{Kr}$  and long purging times at -78°C, would have allowed loss of  $^{85}\text{Kr}$  from the traps without detection during the course of the tests.

## 5. DISCUSSION OF FACTORS AFFECTING FISSION PRODUCT RELEASE

In the following subsections, the effects of several factors, including fission product chemistry on fission product release, are discussed. A preliminary quantitative model for cesium and iodine release in steam under LOCA conditions has been formulated based on these factors. Details of the model have been published separately.<sup>21</sup>

### 5.1 Chemical Behavior of Releasable Fission Products

The chemical behavior of a fission product in the pellet-clad gap of LWR fuel rods under LOCA and SFTA conditions is dependent on its chemical form. (Only fission products in the gap are releasable under these conditions.) The chemical form is important because it dictates whether or not the fission product will interact with the fuel, cladding, or other fission products and, more importantly, the extent of the release. In a controlled LOCA, the core would experience a temperature excursion (max, 1200°C) and some of the rods would rupture. Some ingress of steam into those rods would occur, which could alter the chemical form of certain fission products. Ingression of a steam and air mixture is a possibility that would present a different chemical behavior scenario in the fuel-clad gap under severe SFTA conditions.

Observed chemical behavior of cesium and iodine in the Control,<sup>1</sup> Implant,<sup>2</sup> and Low Burnup Fuel Test Series<sup>22</sup> proved to be an invaluable aid in the analysis and interpretation of results in this series.

In a recent report,<sup>23</sup> equilibrium thermodynamic calculations were performed on the Cs-U-Zr-H-I-O system that is assumed to exist in the fuel-clad gap of LWR fuel under in-reactor, steam, and 50% steam--50% air conditions. The predictions of chemical behavior of fission products in that system have been fairly consistent with our experimental findings. These calculations suggested that:

1. The chemical potential of oxygen (oxygen potential) is a parameter that defines many of the equilibrium species.
2. The oxygen potential in the pellet-clad gap is probably controlled by  $\text{UO}_{2+x} + \text{Cs}_2\text{UO}_4$ .
3. In an intact rod, the important condensed phases are  $\text{UO}_{2+x}$ ,  $\text{Cs}_2\text{UO}_4$ , and CsI; in the gas phase, Cs and CsI are the major species of cesium and iodine.
4. The presence of steam does not alter the condensed phases, but CsOH becomes a major species in the gas phase in addition to Cs and CsI.
5. In a 50% steam--50% air system, the equilibrium condensed phases are  $\text{U}_3\text{O}_8$  or  $\text{UO}_3$  and  $\text{Cs}_2\text{U}_{15}\text{O}_{46}$ , and the primary cesium species in the gas phase would be CsOH. Elemental iodine rather than CsI would be the major iodine species.

Oxygen potential is probably one of the main determinants of chemical behavior of fission products in the pellet-clad gap. Measurements with an emf probe have been taken over radial cross sections of pellets from low and high burnup LWR fuel rods.<sup>24</sup> It was determined that the oxygen potential of the fuel at the pellet surface was about 450 kJ/mole at 750°C for one of the rods that was similar to the H. B. Robinson fuel that we used. It had a burnup of 18,900 MWd/MT and an average heat rating of 7 kW/ft, as compared with 30,000 MWd/MT and 6 kW/ft for the H. B. Robinson fuel. According to Blackburn's model,<sup>25</sup> which gives the stoichiometry of the fuel as a function of oxygen potential, urania with an oxygen potential of 450 kJ/mole at 750°C would have an oxygen-to-uranium ratio in the range 2.000 and 2.001 (near stoichiometric). Oxygen balance calculations to determine oxygen potential for irradiated LWR fuel<sup>26</sup> show fairly good agreement with the measured values.<sup>24</sup>

### 5.1.1 Behavior of iodine

The release data in these experiments demonstrated that the test atmosphere and the surfaces of the apparatus were very influential in determining the final chemical state of iodine as it was found in the apparatus after testing. Measurable quantities of iodine were released in each test. As in the Implant Test Series,<sup>2</sup> difficulty was encountered in some of the tests in identifying the chemical state of the iodine while it was escaping from the fuel rod segments. This was caused by the tendency of CsI in the presence of steam to react with the hot (>600°C) surfaces of the quartz furnace tube to form cesium silicate and elemental iodine.<sup>1</sup>

Table 43 indicates the distributions of cesium and iodine for each of the HBU tests. Table 44 shows the percentages of released iodine that were found as elemental iodine in the collection system for each experiment. The values were obtained by assuming that cesium detected on a collection component was present as CsI and that any excess iodine was elemental iodine. A purified helium purge gas was employed in test HBU-12 to minimize the possibility of "tramp" oxygen altering the pellet-clad gap chemistry by increasing the oxygen potential or oxygen/uranium ratio at the surface of the pellets. The apparatus was also modified (see Sect. 4.11) to lessen the chance of released species making contact with hot quartz. Only 0.2% (0.39 µg) of the released iodine was collected as elemental iodine. [Because elemental iodine is very volatile (bp, 183°C), it has typically been found downstream on the charcoal in the filter pack with a fraction sorbed on the filter papers.] Most of the released iodine in test HBU-12 was found in the gold thermal gradient tube at the 280 to 430°C location where most of the cesium was detected (Fig. 33). These data, although inferential, indicate that CsI was the primary iodine species released, which agrees with the prediction of Besmann and Lindemer.<sup>23</sup>

Test HBU-7 was conducted to determine the fission product release that would occur at the time of rupture. The segment was ruptured at 900°C in steam, and the induction heater was turned off 1 min later. It can be seen in Table 44 that only 3.6% (0.4 µg) of the released iodine

Table 43. Distribution of cesium and iodine in high burnup fuel tests

Test No. <sup>a</sup>	Test temp (°C)	Test time (min)	Test atmosphere	Furnace tube		Thermal gradient tube		Filter pack inlet fitting		First filter paper		Second and third filter papers		Charcoal No. 1a	
				Cesium (µg)	Iodine (µg)	Cesium (µg)	Iodine (µg)	Cesium (µg)	Iodine (µg)	Cesium (µg)	Iodine (µg)	Cesium (µg)	Iodine (µg)	Cesium (µg)	Iodine (µg)
HBU-4	500	1200	Steam-Ar	0.017	0.040	0.00001	0.003	0.000002	0.003	0.000001	0.018	0.00001	0.005	0.000006	0.036
HBU-1	700	300	Steam-Ar	0.123	0.019	0.00009	0.143	0.000005	0.003	0.0	0.194	0.0	0.203	0.00002	0.362
HBU-2	900	120	Steam-Ar	2.816	0.055	0.0007	0.145	0.00001	0.051	0.000005	0.405	0.0	0.381	0.00001	0.673
HBU-11	1200	27	Steam-He	41.75	0.06	56.22	6.76	2.74	2.21	41.32	9.92	0.001	0.35	0.0006	0.88
HBU-7	900	1	Steam-He	113.52	3.95	8.74	3.92	0.47	0.34	7.84	2.52	0.005	0.04	0.0	0.36
HBU-8	900	60	Steam-He	33.41	0.25	3.72	0.25	0.29	3.18	2.8	1.89	0.00002	1.42	0.00001	6.54
HBU-9	900-1100	8.4	Steam-He	108.34	0.13	2.23	0.87	0.17	2.66	1.57	1.69	0.0	1.40	0.0	10.17
HBU-10	900-1200	10	Steam-He	236.77	0.40	17.16	3.27	1.0	1.65	14.53	2.44	0.0	0.16	0.00001	5.99
HBU-5	500	1200	Dry air	0.002	0.213	0.0003	0.441	0.00007	0.008	0.0002	0.038	0.000001	0.038	0.000001	5.29
HBU-6	700	300	Dry air	1.834	0.025	4.195	0.277	0.004	0.014	0.097	0.119	0.0	0.119	0.0	18.431
HBU-12	700-1200 <sup>b</sup>	b	Helium	99.33	0.14	1797.22	171.73	12.37	2.28	87.01	13.96	0.00006	0.08	0.0	0.31

<sup>a</sup>In tests HBU-1, -2, -4, -5, and -6, the fuel rod segments were predrilled to cause simulated defects. The ruptured segment used in test HBU-7 was also used in test HBU-11. These tests were diffusional release tests. In tests HBU-8, -9, and -10, the segments were pressure-ruptured at 900°C and subsequently heated at the shown temperatures. In test HBU-12 a special Zircaloy ferrule fitting at the outlet end provided the opening through which the fission products were purged with purified helium.

<sup>b</sup>See Fig. 35 for time-temperature sequence.

Table 44. Distribution of cesium and iodine in High Burnup Fuel tests

Test No. <sup>a</sup>	Test temp (°C)	Test time (min)	Test atmosphere	Total cesium found (μg)	Total iodine found (μg)	Cesium/iodine (μg Cs/μg I)	Estimated mass of elemental iodine (μg)	Percentage of released iodine found as elemental iodine (μg)
HBU-4	500	1200	Steam-Ar	0.017	0.105	0.162	0.089	84.7
HBU-1	700	300	Steam-Ar	0.123	0.925	0.133	0.905	97.8
HBU-2	900	120	Steam-Ar	2.818	1.755	1.606	1.655	94.3
HBU-11	1200	27	Steam-He	142.03	20.20	7.031	1.23	6.1
HBU-7	900	1	Steam-He	130.577	11.13	11.73	0.40	3.6
HBU-8	900	60	Steam-He	39.60	13.53	2.927	10.86	80.3
HBU-9	900-1100	8.4	Steam-He	112.31	16.92	6.638	14.26	84.3
HBU-10	900-1200	10	Steam-He	279.46	13.91	20.091	6.85	49.2
HBU-5	500	1200	Dry air	0.0024	6.03	0.0004	6.02	99.9
HBU-6	700	300	Dry air	6.164	19.02	0.324	18.59	97.7
HBU-12	700-1200 <sup>b</sup>	b	Helium	1995.93	188.5	10.589	0.39	0.2

<sup>a</sup>In tests HBU-1, -2, -4, -5, and -6, the fuel rod segments were predrilled to cause the simulated defects. The ruptured segment used in test HBU-7 was also used in test HBU-11. These tests were diffusional release tests. In tests HBU-8, -9, and -10, the segments were pressure-ruptured at 900°C and subsequently heated at the shown temperatures. In test HBU-12 a special Zircaloy ferrule fitting at the outlet end provided the release opening, through which fission products were purged from the segment with purified helium.

<sup>b</sup>See Fig. 35 for time-temperature sequence.

was collected as elemental iodine. The results of this test, as well as test HBU-12, indicate that CsI was the primary iodine species released.

The fuel rod segments in tests HBU-8 to -10 were ruptured at 900°C into flowing steam-helium atmospheres and subsequently heated at the temperatures and for the time periods shown in Table 44. In those tests, 49 to 84% of the released iodine was found as elemental iodine. Our data (Sect. 4.12.1) indicate that the largest portion of the released iodine in each of those tests occurred at the time of rupture. Because the iodine species released in tests HBU-7 and -12 was observed to be CsI, we maintain that CsI was also the primary iodine species released in tests HBU-8 to -10, and that the large percentages of elemental iodine found in these tests resulted from the reaction of the CsI with the hot quartz surfaces of the furnace tube.

It has been experimentally observed that the reactivity of CsI with urania is dependent on the oxygen content (or stoichiometry) of the urania. Epstein<sup>27</sup> reported that CsI does not interact chemically with fuel in hypostoichiometric fast-reactor fuel pins. In tests HBU-7, -11, and -12, in which the fuel in the pellet-clad gap was probably near stoichiometric ( $O/U \approx 2.000$  to  $2.001$ ),<sup>23,25</sup> we observed that CsI was stable and was the major iodine species released. It has been determined<sup>28</sup> that when CsI was mixed with urania in the stoichiometry range  $UO_{2.0}$  to  $UO_{2.67}$ , greater yields of elemental iodine per given amount of CsI were obtained as higher oxygen/uranium ratios of urania were used. We also found that CsI reacted with hyperstoichiometric urania in Implant Tests<sup>2</sup> 1 and 2.

Elemental iodine was the major iodine species released in tests HBU-5 and -6, which were conducted in dry air atmospheres at 500 and 700°C respectively (see Table 44). Approximately 2500 times more iodine mass than cesium was released in test HBU-5; only 3 times more was released in test HBU-6. These results are consistent with the equilibrium predictions<sup>23</sup> and with the results obtained in two implant tests that were conducted in dry air.<sup>2</sup>

For tests HBU-4 (500°C, 20 hr) and HBU-1 (700°C, 5 hr), Table 44 shows the ratios of iodine (mass) to cesium that were released were 6.0 and 7.5,

respectively, and that the deposition behavior of iodine was that of elemental iodine. Both tests were performed in a steam-argon atmosphere. One plausible explanation for the iodine not being released as CsI is that any CsI that might have been released possibly reacted with partially oxidized fuel at the surface of the pellets in the vicinity of the defect opening, forming stable cesium uranate and elemental iodine. The fuel could have become oxidized by tramp oxygen ( $\sim 2$  ppm) that was in the argon carrier gas. This is credible because the attraction of uranium for oxygen at 500 and 700°C is significant.<sup>29</sup> The gettering attraction of Zircaloy cladding covered with a thin oxide layer would not be expected to greatly diminish the number of oxygen molecules that could get to the exposed fuel at those temperatures.

The silicates of cesium are not very stable at temperatures above 1000°C,<sup>30</sup> which is confirmed by deposition behavior of CsI in test HBU-11. The data in Table 44 show that 94% of the released iodine behaved like CsI rather than elemental iodine. The temperature of the quartz furnace tube surrounding the fuel rod segment was 1200°C, and we estimate that the temperature was between 1000 and 1050°C at the cooler outlet end. The instability of cesium silicate above 1000°C enabled the released CsI to transport through the furnace tube with negligible reaction with the quartz. Most importantly, this test also demonstrated that CsI was the probable major iodine species in the pellet-clad gap at the temperature of release (700 to 1200°C).

#### 5.1.2 Behavior of cesium

The important condensed phases of cesium in the pellet-clad gap of an intact LWR fuel rod should be CsI and  $\text{Cs}_2\text{UO}_4$ , and elemental cesium and CsI should be the major species in the gas phase.<sup>23</sup> In steam, the only difference would be that CsOH as well as elemental cesium would be present in the gas phase.<sup>23</sup> The calculated predictions appear consistent with the experimental results that were obtained in the Implant,<sup>2</sup> Low Burnup Fuel,<sup>22</sup> and High Burnup Fuel Test Series, and in the Knudsen cell--mass spectrometer<sup>3</sup> experiments.

Experiments that were conducted in the Implant Test Series<sup>2</sup> indicated that at test temperatures of  $\leq 900^\circ\text{C}$ , the implanted cesium (as CsOH) was considerably stabilized by both the fuel and cladding, which probably suggest the formation of cesium uranate and zirconate.<sup>31</sup> This stabilizing behavior was also noted when we tested mixtures of CsOH-UO<sub>2</sub> and Cs<sub>2</sub>CO<sub>3</sub>-UO<sub>2</sub> in a Knudsen cell--mass spectrometer;<sup>3</sup> in those tests, a detectable cesium ion current could only be measured at temperatures  $\geq 925^\circ\text{C}$ . By comparison, in an experiment with pure Cs<sub>2</sub>CO<sub>3</sub>, cesium was first measured under identical test conditions at  $650^\circ\text{C}$ . In tests conducted with the above, no uranium-containing species were detected in the vapor phase over the mixtures; this agrees with other Knudsen cell--mass spectrometer observations of vapor species over Cs<sub>2</sub>UO<sub>4</sub> in which cesium was the major species in the vapor.<sup>32</sup>

Thermodynamic calculations<sup>23</sup> show that the partial pressure of cesium vapor in equilibrium with Cs<sub>2</sub>UO<sub>4</sub> should increase with lower oxygen potential. This may explain the difference in Cs/I ratio of material released from burst-type tests compared with diffusional release tests in steam. Burst releases originate from sealed fuel rods in which the oxygen potential in the pellet-to-cladding gap space should be lower than during diffusional release tests when the gap is exposed to steam. The Cs/I mass ratios of released material listed in Table 44 show higher values in the burst tests (HBU-7, -8, -9, and -10) than in the diffusional release tests conducted in steam. The same difference was noted with the Implant Test Series results (see Sect. 8 of ref. 2). The scatter in results and the fact that most of the burst release tests included significant time for diffusional release in steam make it difficult to quantify the effect. As discussed in more detail in Sect. 5.3.2, the effective partial pressures of the cesium and iodine species released with rupture at  $900^\circ\text{C}$  are considerably lower than the vapor pressure of CsI ( $2.7 \times 10^{-3}$  MPa at  $900^\circ\text{C}$ ).<sup>33</sup>

In each experiment (except test HBU-11) where the defected fuel rod segments were tested in steam, cesium was primarily found on the quartz surfaces of the furnace tube in the region of the defect openings. This suggests that the venting cesium species was very reactive with the quartz. Other than CsI, the chemical species of cesium that could be present in

the gas phase of an intact fuel rod are elemental cesium and the cesium chalcogenides ( $\text{Cs}_2\text{O}$ ,  $\text{Cs}_2\text{Se}$ , and  $\text{Cs}_2\text{Te}$ ). Cesium reacts directly with selenium and tellurium to form  $\text{Cs}_2\text{Te}$  and  $\text{Cs}_2\text{Se}$ . When exposed to steam, any of these species would form cesium hydroxide.<sup>1,2</sup> ( $\text{Cs}_2\text{Te}$  and  $\text{Cs}_2\text{Se}$  hydrolyze readily, releasing  $\text{H}_2\text{Te}$  and  $\text{H}_2\text{Se}$ , which oxidize to form elemental Te and Se.)<sup>34</sup> Furthermore, since cesium monotelluride melts with decomposition at  $680^\circ\text{C}$ ,<sup>35</sup> its presence in the gas phase in tests  $\geq 700^\circ\text{C}$  would be questionable. Cesium hydroxide reacts vigorously with quartz to form less-volatile silicates<sup>2,30</sup> that are stable at temperatures below  $1000^\circ\text{C}$ . Cs and CsI are believed to react with quartz in a similar manner, but at a much slower rate. In test HBU-11, which was conducted at  $1200^\circ\text{C}$  in steam, the surface temperature of the quartz furnace tube exceeded  $1000^\circ\text{C}$  even at the cooler outlet end near the entrance to the gold thermal gradient tube. Consequently, most of the released cesium ( $\sim 71\%$ ) transported downstream. The cesium that was found in the furnace tube ( $\sim 29\%$ ) was found at the cooler outlet end rather than near the defect opening (Fig. 31).

A flowing dry-air atmosphere was employed in tests HBU-5 and -6. Any cesium released in those tests other than CsI should have been cesium monoxide. The higher oxides of cesium ( $\text{Cs}_2\text{O}_2$  and  $\text{CsO}_2$ ) are not stable above  $400^\circ\text{C}$ .<sup>36</sup> In test HBU-6, which was conducted at  $700^\circ\text{C}$  for 5 hr, the released cesium (probably forming an oxide) behaved somewhat differently than it did in steam; it was considerably less reactive with the quartz surfaces of the furnace tube (Sect. 4.6). In the first hour of the test, the cesium apparently reacted with the hot quartz in a manner that passivated it. Thereafter most of the released cesium transported and condensed downstream in the gold thermal-gradient tube. The peak occurred at  $430^\circ\text{C}$  (Fig. 14).

Table 44 shows that in test HBU-12, which was conducted in a purified helium atmosphere, about 90% of the released cesium deposited in the gold thermal-gradient tube at a peak location of  $430^\circ\text{C}$  (Fig. 33). The deposition profile was similar to that observed for the cesium (probably  $\text{Cs}_2\text{O}$ ) in the thermal gradient tube in test HBU-6 (a dry-air test) except for amounts. Because elemental cesium is much more volatile than  $\text{Cs}_2\text{O}$ , it would have transported further downstream. Unfortunately, this experiment

does not prove that  $\text{Cs}_2\text{O}$  was the major species (other than  $\text{CsI}$ ) that was purged from the segment. It is possible that enough tramp oxygen in the untreated helium carrier gas ( $\sim 2$  ppm) that was being supplied to the furnace tube (not to be confused with the purified helium gas that was used to purge the segment) was able to pass through to the gold thermal-gradient tube and react with purged elemental cesium, if that were the case, to form the oxide. However, the Zircaloy cladding of the segment itself would have served as a "getter" to somewhat remove this oxygen impurity.

### 5.1.3 Behavior of ruthenium

Ruthenium is a member of the platinum metals family and like the other elements in that family (platinum, iridium, osmium, palladium, and rhodium) it is known for its chemical inactivity. It is refractory, with a melting point of  $2310^\circ\text{C}$ . In  $\text{UO}_2$  fuels that have experienced high linear heat ratings, metallic inclusions are found that contain ruthenium as well as other noble metals (molybdenum, tellurium, and rhodium).<sup>37</sup> Ruthenium is resistant to oxidation in air at moderate temperatures.

It has been observed that oxidation of finely divided ruthenium powder to the dioxide ( $\text{RuO}_2$ ) started at about  $500^\circ\text{C}$  when it was heated in a stream of oxygen, and the oxidation rate rapidly increased with temperature.<sup>38</sup> The formation and vaporization of ruthenium tetroxide ( $\text{RuO}_4$ ) began at about  $600^\circ\text{C}$  and increased considerably with temperature; the rate of vaporization was about 4000 times faster at  $1200^\circ\text{C}$  than at  $700^\circ\text{C}$ . Below  $600^\circ\text{C}$ , the tetroxide decomposed back to the dioxide.

To verify the chemical behavior of ruthenium, several side experiments were conducted. Finely divided ruthenium metal was heated at  $500^\circ\text{C}$  in a flowing oxygen atmosphere for 2 hr. The grayish-white metal appeared to have been completely oxidized to the black dioxide. Furthermore, a small amount of ruthenium vaporized (probably as  $\text{RuO}_4$ ), transported downstream, and deposited (ring-shaped) on the cooler quartz surface at the outlet end of the furnace. Subsequently, the dioxide was heated for 2-hr periods at  $700$  and  $900^\circ\text{C}$  and for 10 min at  $1200^\circ\text{C}$ . Prior to increasing the temperature each time, the quartz furnace tube was repositioned to allow the deposition to occur at a different location so that it could easily be

compared with the previous one. With each jump in temperature, the resulting ring deposit became heavier, darker, and somewhat wider. These deposits occurred in the temperature range 400 to 200°C. The results obtained in this experiment are similar to those obtained in ref. 38; however, we observed vapor transport of ruthenium at 500°C.

Considering the oxygen potential that probably existed in the gap of the H. B. Robinson fuel rod segments prior to testing,  $\sim 450$  kJ/mole (Sect. 6.1), and based on thermodynamic calculations,<sup>26,37</sup> it is probable that elemental ruthenium rather than ruthenium dioxide was the major species in the condensed phase. Our experimental results support this contention. In test HBU-12, which was conducted in the time and temperature sequence given in Fig. 35, no ruthenium was released. Had the dioxide been the major condensed-phase species, measurable quantities of ruthenium would have been released as tetroxide. Elemental ruthenium in an inert atmosphere is very refractory and would not be expected to be released, as was the case.

Significant amounts of ruthenium were released in tests HBU-5 and -6, which were conducted in a flowing dry-air atmosphere at 500 and 700°C (see Table 45). The released ruthenium was primarily found downstream at the cool end of the thermal gradient tube, on the inner surfaces of the stainless steel inlet to the filter pack, and on the first HEPA filter paper. The deposition occurred in the temperature range 300 to 150°C. When  $\text{RuO}_2$  was heated in the side experiments, the vaporized ruthenium deposited in approximately the same temperature range. The release values obtained in tests HBU-5 and -6 (Table 45) indicate that the rate of release was temperature dependent; six times more ruthenium (mass) was released per min at 700 than at 500°C; and the rate of decomposition of  $\text{RuO}_2$  (or the rate of formation of  $\text{RuO}_4$ ) increased with temperature.

Trace amounts of ruthenium were released in the steam atmosphere tests, with the exception of test HBU-11, as shown in Table 45. In the diffusional release tests HBU-1, -2, -4, and -11, no difficulty was encountered in measuring the released ruthenium. However, in the burst tests HBU-7 to -10, the ruthenium that transported and deposited in the

Table 45. Distribution of ruthenium in high burnup tests

Test No. <sup>a</sup>	Test temp (°C)	Test time (min)	Test atmosphere	Thermal gradient tube (μg)	Filter pack inlet fitting (μg)	First filter paper (μg)	Second filter paper (μg)	Third filter paper (μg)	First charcoal (μg)	Rate of release (μg/min)	First charcoal deposition (μg/min)
HBU-5	500	1200	Dry air	0.166	0.085	0.121	$2.26 \times 10^{-4}$	$1.02 \times 10^{-4}$	$160.0 \times 10^{-6}$	0.0016	$6.7 \times 10^{-7}$
HBU-6	700	300	Dry air	0.205	1.12	1.46	$3.52 \times 10^{-4}$	$0.41 \times 10^{-6}$	$81.0 \times 10^{-6}$	0.0093	$2.7 \times 10^{-7}$
HBU-4	500	1200	Steam-Ar	$8.6 \times 10^{-6}$	$1.6 \times 10^{-5}$	$2.8 \times 10^{-5}$	0.0	0.0	$560.0 \times 10^{-6}$	$5.1 \times 10^{-7}$	$4.7 \times 10^{-7}$
HBU-1	700	300	Steam-Ar	0.0 <sup>b</sup>	$0.9 \times 10^{-5}$	$1.9 \times 10^{-5}$	0.0	0.0	$120.0 \times 10^{-6}$	$4.9 \times 10^{-7}$	$4.0 \times 10^{-7}$
HBU-2	900	120	Steam-Ar	0.0	0.0	0.0	0.0	0.0	$33.0 \times 10^{-6}$	$2.7 \times 10^{-7}$	$2.7 \times 10^{-7}$
HBU-11	1200	27	Steam-Ar	0.0	0.0	0.0	0.0	0.0	0.0	0.0	0.0
HBU-7	900	1	Steam-He	- <sup>c</sup>	-	-	0.0	0.0	$8.3 \times 10^{-6}$	-	$83.0 \times 10^{-7}$
HBU-8	900	60	Steam-He	-	-	-	0.0	0.0	$8.8 \times 10^{-6}$	-	$1.5 \times 10^{-7}$
HBU-9	900-1100	8.4	Steam-He	-	-	-	0.0	0.0	$1.1 \times 10^{-6}$	-	$1.3 \times 10^{-7}$
HBU-10	900-1200	10	Steam-He	-	-	-	0.0	0.0	$0.9 \times 10^{-6}$	-	$0.9 \times 10^{-7}$
HBU-12	700-1200 <sup>d</sup>	d	Helium	0.0	0.0	0.0	0.0	0.0	0.0	-	0.0

<sup>a</sup>In tests HBU-1, -2, -4, -5, and -6 the fuel rod segments were predrilled to cause the simulated defects. The ruptured segment used in test HBU-7 was also used in test HBU-11. These tests were diffusional release tests. In tests HBU-8 to -10, the segments were pressure-ruptured at 900°C and subsequently heated at the shown temperatures. In test HBU-12, a special Zircaloy ferrule fitting at the outlet end provided the release opening through which the fission products were purged from the segment with purified helium.

<sup>b</sup>Amounts less than  $10^{-8}$  are given as 0.0.

<sup>c</sup>The dash signifies our inability to measure ruthenium because of the presence of fuel dust.

<sup>d</sup>See Fig. 35 for time-temperature sequence.

thermal gradient tube, stainless steel inlet to the filter pack, and first filter paper could not be determined because of the presence of ejected fuel dust. (The gamma activity of vaporized ruthenium was negligible compared to the ruthenium activity in the fuel dust). Nonetheless, ruthenium could be determined on components beyond the first filter paper. Since the largest portions of the released ruthenium were found on the charcoal in tests HBU-1, -2, -4 (>80%), we believe that was probably also the case in the burst tests.

Only a fraction of a percent of the released ruthenium in each of the air tests penetrated to the charcoal, but the amount that did ( $<10^{-4}$   $\mu\text{g}$ ) was about the same as was found on the charcoal in the steam tests that were conducted at the same temperatures. This might indicate that another volatile and penetrating chemical form of ruthenium was also released. In Table 45, it is seen that the rate of collection for most of the tests was about  $10^{-7}$   $\mu\text{g}/\text{min}$ ; note that no ruthenium was released in test HBU-11. The fuel rod segment employed in that test was also used in test HBU-7, a 1-min rupture test. The total mass of ruthenium released in test HBU-7 was identical to the amount released in test HBU-8. In test HBU-8, the segment was ruptured at  $900^\circ\text{C}$  but was heated for an additional 60 min at  $900^\circ\text{C}$ . These data suggest that most of the ruthenium released in the burst tests was released at the time of rupture.

In steam tests HBU-1 ( $700^\circ\text{C}$ ) and -4 ( $500^\circ\text{C}$ ),  $\text{RuO}_4$  was apparently also collected. This is inferred by the presence of ruthenium on upstream surfaces. In these lower-temperature tests that were conducted for long periods of time, the tramp oxygen ( $\sim 2$  ppm) in the argon carrier gas might have altered the oxygen/uranium ratio of the fuel at the surface of the pellets near the defect opening. A localized increase in oxygen potential could have allowed  $\text{RuO}_2$  to form.<sup>26,37</sup> At higher test temperatures, the hydrogen atmosphere produced by the reaction of steam with the cladding would inhibit fuel oxidation and  $\text{RuO}_2$  formation. This possibly accounted for the lack of  $\text{RuO}_2$  deposition in test HBU-2, a  $900^\circ\text{C}$  steam test.

#### 5.1.4 Behavior of antimony

Before discussing the chemical behavior of antimony as it was observed in the experiments, it is appropriate to provide some background information about this element. According to thermodynamic calculations,<sup>26,37</sup> it should be present in LWR fuel rods as elemental antimony rather than the oxide, but the possibility of it forming compounds with other fission products cannot be excluded.

Antimony is a member of the nitrogen family (Group VA) of the periodic table. It has a melting point of 630.7°C and a boiling point of 1440°C. The vapor pressure is given in the following table as a function of temperature.

Temperature (°C)	Vapor pressure (mm)
886	1
1033	10
1141	40
1223	100
1364	400
1440	760

It is not affected by oxygen at ordinary temperatures; however, if it is given the right oxygen potential at elevated temperatures (>400°C), it can form the sesquioxide,  $Sb_2O_3$ . In a hydrogen atmosphere, the oxides of antimony are readily reduced to the metal. The vapor pressure table given below for the trioxide shows that it is more volatile than elemental antimony.<sup>39</sup>

Temperature (°C)	Vapor pressure (mm)
574	1
666	10
812	40
957	100
1242	400
1425	760

Antimony, which is a borderline element (metalloid), can exhibit both metallic and nonmetallic properties; the compounds antimony triiodide

( $\text{SbI}_3$ ) and cesium antimonide ( $\text{CsSb}$ ) are examples. Such compounds are readily oxidized in air.

To help explain some of the observed behavior of antimony in this experimental series, a group of side experiments was conducted with elemental antimony and antimony sesquioxide to determine the reactivity of each with Zircaloy cladding surfaces (oxidized and nonoxidized) and with gold surfaces at 500, 700, 900, and 1200°C. In the first experiment, finely divided antimony was placed on pieces of nonoxidized Zircaloy cladding and heated at those temperatures in an atmosphere of flowing argon. A growing cladding discoloration was observed at 700 and 900°C that extended beyond the liquid antimony, which probably meant that some reaction or alloying occurred at those temperatures. As the temperature was being raised from 900 to 1200°C, there was a considerable reaction of the cladding with the remaining unvolatilized antimony causing the cladding to become extensively pitted. However, when antimony was placed on Zircaloy cladding that was oxidized and tested in a similar fashion, there was no visible evidence of reaction. During each of these experiments, a metallic ring-like deposit occurred downstream on the cooler surfaces of the quartz furnace tube.

Tests with antimony sesquioxide ( $\text{Sb}_2\text{O}_3$ ) revealed that it did not noticeably react with either oxidized or nonoxidized Zircaloy cladding surfaces at temperatures up to 900°C in flowing argon, but rapidly volatilized and condensed downstream on the cooler surfaces of the quartz furnace tube.

When elemental antimony powder was placed on gold foil and heated in flowing argon, it readily reacted and formed a binary liquid solution at a temperature below 500°C. Antimony sesquioxide did not react with gold when tested. It is reported that for the gold-antimony binary system,<sup>40</sup> a eutectic occurs at 360°C, where the mass ratio of antimony to gold is about 0.25.

Quantitative measurements of released antimony could only be made in two experiments with high burnup fuel, HBU-2 (Sect. 4.2) and HBU-11 (Sect. 4.10). Each test was a diffusional release test conducted in steam. The test temperatures were 900°C for test HBU-2 and 1200°C for test HBU-11.

Uniquely, the released antimony (>99%) in each test was found on gold apparatus surfaces. Furthermore, the deposition profiles for those components (Figs. 7 and 31) indicate that the released antimony preferentially deposited on the gold surfaces. In the side experiments, it was seen that elemental antimony alloyed with gold and formed a less volatile compound while antimony trioxide did not. Based upon these data, it appears that elemental antimony was probably the major species released.

It is interesting that no antimony was released in the purified-helium test HBU-12. In that test, a stainless steel fitting on the downstream end of the fuel rod segment was replaced with one fabricated from Zircaloy. A 0.0625-in. (0.159-cm)-ID Zircaloy tube was attached to it to provide an outlet for the fission products being purged. The results obtained in the side experiments and in tests HBU-2 and -11 offer a credible explanation for the lack of antimony release. Remembering that elemental antimony did not react with oxidized Zircaloy cladding but did react with nonoxidized Zircaloy, and that elemental antimony was probably the species released in tests HBU-2 and -11, elemental antimony probably transported down the gap of the segment during the test and reacted with the fresh metal surfaces of the Zircaloy fitting and outlet tube; therefore, there was no release. The inner cladding surface would be expected to have an oxide layer of >1  $\mu\text{m}$ .<sup>24</sup>

## 5.2 Hydrogen Formation and Removal of Oxidizing Contaminants by Steam-Zircaloy Reaction

As steam flows along the length of the fuel rod, hydrogen is produced as a result of the steam-Zircaloy reaction. When the steam reaches the location of the rupture opening, it contains a significant amount of hydrogen; parabolic rate constants<sup>41,42</sup> were used to estimate the amount. The concentration of hydrogen in the steam-He(Ar) mixture at the defect location and the total calculated amount of hydrogen produced are listed in Table 46. The presence of hydrogen that diffuses with the steam into the defect opening can influence the oxygen potential at the fuel and cladding surfaces within the gap space and thereby affect the release rate of susceptible fission product species.<sup>23</sup> Much higher concentrations of hydrogen (and lower concentration of steam) would be expected further

Table 46. Hydrogen formation from steam-Zircaloy reaction

Test No.	Temperature (°C)	Nominal steam + He(Ar) flow rate (cm <sup>3</sup> /min, STP)	Fraction of H <sub>2</sub> in steam-He at fuel rod midpoint <sup>a</sup>			Total H <sub>2</sub> formed <sup>b</sup>	
			10	100	1000	cm <sup>3</sup> , STP	time
HBU -4	500	372	0.00738	0.00233	0.00074	155	20 hr
HBU-1	700	372	0.0313	0.00990	0.00313	483	5 hr
HBU-2	900	372	0.182	0.0576	0.0182	1215	2 hr
HBU-8	900	1800	0.0376	0.0119	0.00376	859	60 min
HBU-9	1100	1800	0.131	0.0414	0.00131	1119	8.4 min
HBU-10, 11	1200	1800	0.216	0.0683	0.0216	2007 <sup>c</sup>	10 min

<sup>a</sup>Calculations based on parabolic rate constants. Data for 500 and 700°C from ref. 41, and data for 900 to 1100°C from ref. 42.

<sup>b</sup>Calculated for entire outside surface area of cladding; does not include oxidation of interior surface.

<sup>c</sup>Half of a typical size core reacting in this manner would produce 9050 l(320 ft<sup>3</sup>) of hydrogen measured at 150°C and 1000 psi.

within the interior of the ruptured fuel rod because of the long residence time and continued steam-Zircaloy reaction.

Traces of oxidizing contaminants were probably present in the steam-He(Ar) mixture. The helium and argon were not purified beyond the several parts-per-million level of oxygen concentration in the supply tanks, and the steam generator tank may not have been purged completely of air following replacement of the water. Both the oxidizing contaminants and the steam probably react with Zircaloy at approximately the same rate so that the ratio of contaminants to steam remains nearly constant. The net result of most tests conducted is that significant amounts of hydrogen were produced, but the reduction in steam and oxidizing contaminants was insignificant except for the first few seconds at higher temperatures. Again, within the gap space at some distance from the defect opening, essentially complete reaction of the steam and oxidizing contaminants with the Zircaloy cladding would be anticipated.

Some evidence exists that the gaseous oxidizing impurities caused conversion of CsI to  $I_2$  either within the fuel rod (thus contributing to enhanced release of total iodine) or on the surfaces of the containment and collection system components (thus causing only a change of iodine species after the initial deposition of the released CsI). The highest percentages of released iodine collected in the elemental form ( $I_2$ ) were found in the tests conducted for the longest times and at the lowest temperatures (test HBU-1, -2, -4, and -8).

### 5.3 Discussion of Blowdown (Burst) Release

#### 5.3.1 Mechanism of release

After the instant of rupture, the plenum gas flows along the pellet-to-clad gap space (and through large cracks within the pellets) and becomes saturated with fission product vapors. Saturation is never precisely reached because of mass transfer limitations and the fact that the fuel rod temperature increases (and therefore the fission product partial pressures increase) as the gas flows toward the rupture location. We have observed that the fraction of the gap inventory released by a typical

burst is relatively small so that the concentration of vaporized fission products in the vented gas is essentially constant. Our model<sup>21</sup> for burst release is therefore:

Mass released at burst = (volume of vented gas) x (concentration of each species in the vented gas).

The volume of vented gas is relatively simple to calculate for almost any postulated accident, but the volume must be calculated at the pressure existing at the location where "saturation" occurs, probably just inside of the rupture opening.

### 5.3.2 Concentration of cesium and iodine in the vented gas

Test data must be used to determine the concentration of species in the vented gas. At first approximation we would be tempted to calculate concentrations from the vapor pressures of probable species (e.g., CsI or CsOH), but we have discovered that the experimentally observed concentrations are much lower.

The concentrations of cesium and iodine in the gas vented at the time of rupture in tests HBU-7 through -10 were calculated by dividing the measured mass released at rupture by the volume of gas vented. Some uncertainty exists in distinguishing the amount released at the time of rupture from that which was released later by diffusion from the opened hole. Continuous monitoring of radioactive cesium transported to the thermal gradient tube and filter pack was not suitable for this determination, because most of the cesium (typically 95% of the released cesium) was held up on the quartz furnace-tube surfaces by reaction, sorption, or condensation. Some of that amount was later returned to the gas phase and transported out of the furnace tube as flow continued and the quartz surface increased in temperature (when induction heating was used).

The method used to determine the amount released at rupture was to estimate the amount released by diffusion (using the diffusional release tests as a guide) and to subtract this from the total release. The reference tests and the results of this determination are listed in Table 47. The calculated cesium and iodine concentrations in the vented gas of the high burnup experiments are listed in Table 47 along with concentrations

Table 47. Summary of fission product release tests

Test No.	Temperature		Diffusion time (hr)	Volume of gas vented (cm <sup>3</sup> , 0°C, 1 atm)	Radial gap width <sup>a</sup> (μm)	Initial gap inventory (cladding)		Mass released with rupture <sup>b</sup>		Mass released by diffusion <sup>b</sup>	
	Rupture (°C)	Diffusion (°C)				μg Cs/cm <sup>2</sup>	μg I/cm <sup>2</sup>	μg cesium	μg iodine	μg cesium	μg iodine
Implant-1 <sup>c</sup>	700	700	1.0	229	127	23.1	22.0	179.5	356	0.54	6.8
Implant-2	700	700	1.5	229	127	0.47	0.45	2.45	4.9	0.036	0.41
Implant-3	900	900	2.0	172	200	87.1	8.66	290	64.6	196	96.9
Implant-4		1100	0.8	0	127	67.6	6.05			1237	145
Implant-5	700	700	2.0	348	127	96.9	8.38	378	103	3.38	5.9
Implant-6		500	20.0	0	127	141.1	12.37			≤43	5.8
Implant-8	900	1100	0.96	293	200	126.7	8.38	1918	240	1393	161
Implant-10		700	5.0	0	127	97.2	9.07			4.84	12
Implant-11		1300	0.25	0	127	113.9	7.97			2320	26
Implant-12	900	900	2.0	172	200	14.6	0.69	217	23.3	47	6.9
LBU-1 <sup>d</sup>		700	5.0	0	26 <sup>c</sup>	68.8	3.40			0.046	0.17
LBU-2		900	2.0	0	27	106.7	5.27			19.4	20.0
HBU-1 <sup>f</sup>		700	5	0	20	13.1	1.20			0.123	0.93
HBU-2		900	2	0	20	12.7	1.17			2.82	1.76
HBU-4		500	20	0	20	13.1	1.20			0.017	0.105
HBU-7	900	900	0.02	96	200	12.7	1.17	130.4	11.1	0.22	0.018
HBU-8	900	900	1.0	97	200	12.7	1.17	26.6	9.1	13.0	4.44
HBU-9	900	1100	0.14	96	200	13.1	1.20	94.1	14.2	18.2	2.74
HBU-10	900	1200	0.17	98	200	11.2	1.03	223.3	11.1	56.2	2.80
HBU-11		1200	0.45	0	200	11.3	1.05			142.0	20.2

<sup>a</sup>For pressure-ruptured test segments, a value of 200 μ represented the combined gap width and hole size.

<sup>b</sup>For pressure-ruptured tests, the fraction released by diffusion was estimated using the diffusion test data as a guide.

<sup>c</sup>Implant Test Series cladding 0.965 cm ID, 24-cm length of pellets coated with simulated fission products.

<sup>d</sup>Low Burnup Fuel Test Series cladding 1.27 cm ID; fuel length, 15.24 cm; in-reactor fission gas release, 11.6% (LBU-1) and 18.9% (LBU-2).

<sup>e</sup>The unusually low cesium and iodine release values suggest that the hole drilled through the cladding might have been at a location where the gap width was much less than the average value of 26 μm.

<sup>f</sup>High Burnup Fuel Test Series cladding, 0.948 cm ID; fuel length, 30.48 cm; in-reactor fission gas release 0.25%.

obtained from Implant Test 12 of the Implant Test Series.<sup>2</sup> The gap inventory of the Implant Test 12 was chosen to be close to that of the H. B. Robinson fuel rods used in the High Burnup Tests Series.

In Fig. 75 of the Implant Test Series final report,<sup>2</sup> it was shown that the measured cesium and iodine concentrations in the vented gas were one to two orders of magnitude less than would prevail in equilibrium with bulk CsI and CsOH. This is also true of the High Burnup Test Series concentrations (Table 48) because they agree with those from Implant Test 12. The reason for the low observed values is probably a combination of different species existing (see Sect. 5.1) and the effect of sorption by fuel and cladding surfaces, especially at low gap inventories--low surface concentration. As shown in Table 38, the calculated cesium concentrations in the purge gas at 900°C agreed with those listed in Table 48.

Table 48. Concentration of cesium and iodine in the vented gas at 900°C

Test No.	Concentration		Partial pressure	
	Cesium ( $\mu\text{g}/\text{cm}^3$ , STP)	Iodine ( $\mu\text{g}/\text{cm}^3$ , STP)	Cesium (MPa)	Iodine (MPa)
HBU-7	1.36	0.116	$2.3 \times 10^{-5}$	$2.03 \times 10^{-6}$
HBU-8	0.27	0.094	$0.46 \times 10^{-5}$	$1.65 \times 10^{-6}$
HBU-9	0.98	0.148	$1.67 \times 10^{-5}$	$2.60 \times 10^{-6}$
HBU-10	2.28	0.113	$3.88 \times 10^{-5}$	$1.98 \times 10^{-6}$
Implant-12	1.32	0.14	$2.25 \times 10^{-5}$	$2.46 \times 10^{-6}$

### 5.3.3 Effect of gap inventory on burst release

In the High Burnup Test Series, all of the test segments had essentially identical concentrations of cesium and iodine in the gap space. This assertion is based on the fact that all test segments experienced similar power histories and total burnup. In Fig. 73 of the Implant Test Series final report,<sup>2</sup> it was shown that the concentrations of cesium and iodine in the vented gas increased with the gap inventory. We presume this effect would also hold for high burnup fuel because agreement has been demonstrated with the H. B. Robinson test segment gap inventories (Table 47).

#### 5.3.4 Effect of temperature on burst release

All of the ruptures in the High Burnup Fuel Test Series occurred at 900°C; therefore, the effect of temperature was not determined. Agreement with Implant Test Series results was demonstrated (Table 47) at that temperature. Data were obtained in the Implant Test Series<sup>2</sup> at both 700 and 900°C.

#### 5.3.5 Rupture characteristics and the rate of blowdown

Parameters regarding heatup, rupture, and blowdown of the fuel rod segments are listed in Table 49. These parameters are presented to allow comparison with rupture characteristics resulting when other methods of heating are employed. The volume and diametral expansions cannot be compared directly with those experiments designed for fuel rod rupture studies because (1) the combination of short rod, flowing steam, and coil spacing results in a slight but definite temperature peak toward the outlet end; (2) induction heating tends to cause localized concentration of heating once swelling has begun; and (3) the quartz fuel-rod holder restricts expansion of the bottom third of the rod.

In spite of these deviations from the ideal, the swelling appears to be similar to that obtained in single-rod tests designed specifically for fuel rod rupture studies in steam, but the rupture opening is smaller in our experiments.

The rate of blowdown of plenum gas when rupture occurs is controlled primarily by the pellet-to-clad gap width. In a full-length fuel rod undergoing a LOCA transient, expansion of the cladding near the ends may be minimal. Minor expansion should be expected over a considerable length depending on the axial temperature gradient.<sup>43,44</sup> In our test arrangement, some restriction, at least for the later stage of the blowdown, was provided by the tubing and fittings that composed our plenum. The pressure measured near the junction between the plenum tubing and the fuel rod segment is plotted in Fig. 38 for the four high-burnup rupture tests. The time needed to vent 75% of the helium pressurizing gas is listed in Table 49.

Table 49. Fuel rod rupture parameters

Experiment No.	Heatup rate <sup>a</sup> (°C/sec)	Conditions at maximum pressure			Conditions at rupture			Pressure decrease, maximum to rupture <sup>d</sup> (psig)	Calculated cladding expansion <sup>e</sup> (cm <sup>3</sup> )	Volume of gas vented at rupture (cm <sup>3</sup> , STP)	Time to vent 75% of gas (sec)
		Pressure (psig)	Pressure (MPa)	Temperature (°C)	Pressure (psig)	Pressure (MPa)	Temperature (°C)				
HBU-7	2.7	302	2.07	825	275	1.89	908	27	1.9	95.7	2.9 ± 0.4
HBU-8	2.4	307	2.11	833	269	1.84	895	38	2.7	97.3	4.3 ± 0.2
HBU-9	2.5	302	2.07	850	264	1.81	910	38	2.7	95.7	4.5 ± 0.2
HBU-10	5.1 <sup>f</sup>	308	2.12	863	291	2.00	898	18	1.1	97.6	2.4 ± 0.2

<sup>a</sup>Average between 750 and 895°C.

<sup>b</sup>Temperature at center of fuel rod; temperature at location of rupture approximately 10°C higher.

<sup>c</sup>Temperature at center of fuel rod; temperature at location of rupture approximately 15°C higher.

<sup>d</sup>Times between maximum pressure and rupture were 37, 39, 30, and 7.5 for the four tests.

<sup>e</sup>Expansion calculated using gas law.

<sup>f</sup>Heatup rate was increased to look for nonuniform heat transfer between cladding and pellets; no irregularities were observed.

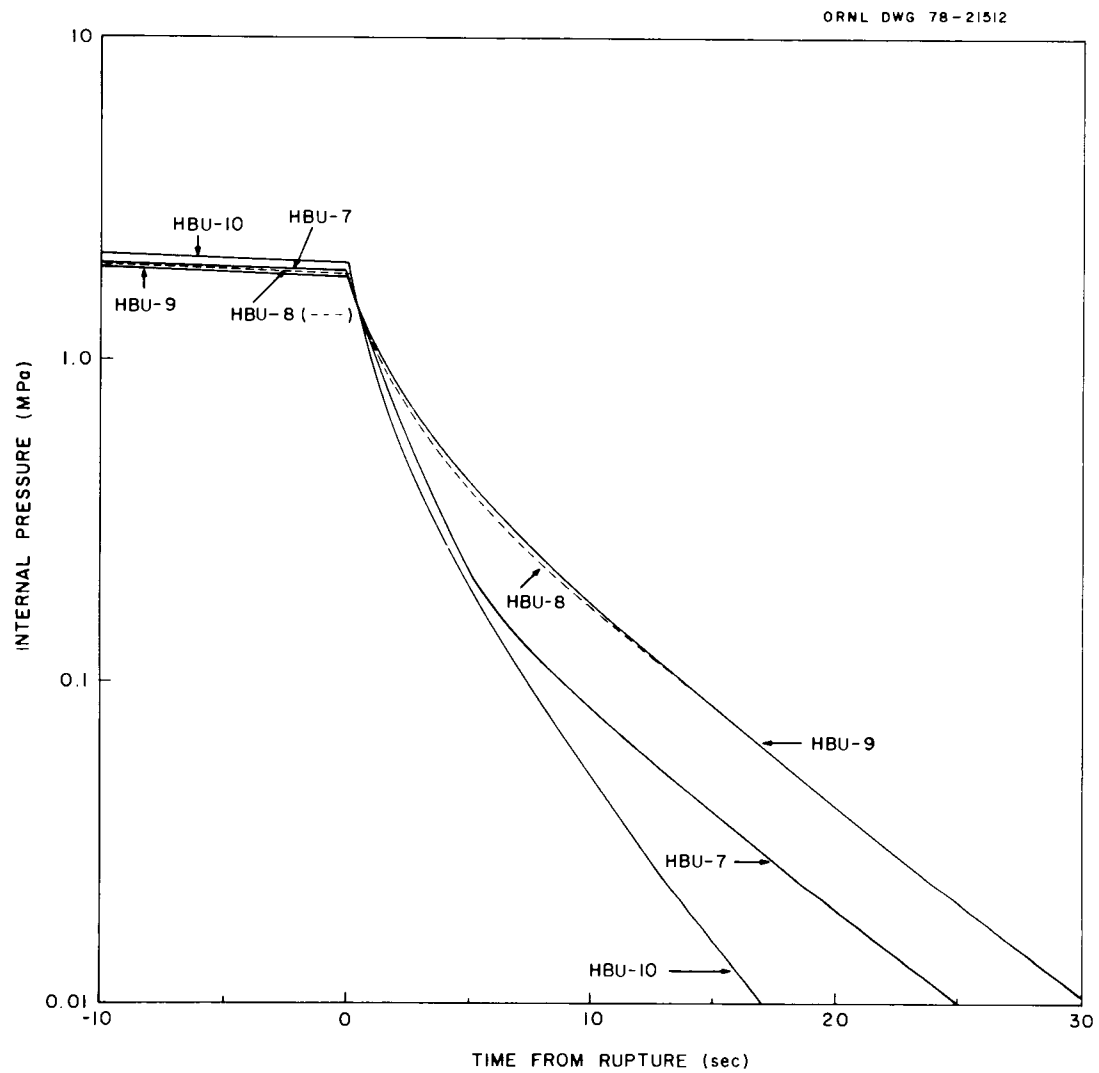


Fig. 38. Pressure drops following rupture of High Burnup Test fuel rods.

The rate of gas flow along the gap space of full-length H. B. Robinson fuel rods with unexpanded cladding was measured by Dagbjartsson et al.<sup>13</sup> Blowdown time for their conditions and the same fractional escape was 5 to 10 times longer for a fuel rod ruptured at midlength. Calculations showed that the maximum cladding strain (balloon diam) would be reduced with small gap spaces. Similar results were obtained<sup>45</sup> by assuming that a check valve or flow restrictor was built into the plenum to minimize gas flow from the plenum into the region of expanding cladding. Gap size measurements for our test segments are described in Appendix A.

The rate of blowdown following rupture could have an influence on the amount of fuel dust ejected and on the amount of vaporized fission products carried out with the venting gas. In the Implant Test Series,<sup>2</sup> the amount of tellurium released appeared to increase with pressure at the time of rupture. No effect of pressure on cesium or iodine release was observed. The High Burnup Tests with the shortest blowdown times (HBU-7 and -10) showed somewhat higher cesium releases but no consistent effect on fuel-dust release. There is not sufficient evidence to warrant the assumption that fission product release is systematically affected by either pressure at time of rupture or the plenum-gas blowdown rate.

#### 5.3.6 Size of hole formed at rupture

A 2-mm<sup>2</sup> hole was formed in our tests with high burnup fuel. This was on the low end of a previously determined range in which a trend toward larger hole sizes was shown with increased initial pressure;<sup>46</sup> however, the scatter was so great that it is clear that initial pressure is not the sole determinant of hole size. It has been suggested that the stored energy in the gas prior to rupture (pressure x volume) determines the hole size.<sup>47</sup> In our experiments, the localized bulging and small gap size, which restrict immediate inflow of plenum gas, tended to inhibit enlargement of the rupture opening.

The size of the opening should have no effect on fission product release at blowdown as long as the gap size controls the flow rate of plenum gas during the blowdown. Following blowdown, it is possible that extremes in hole sizes could affect the diffusional release of fission products (see Sect. 5.4).

### 5.3.7 Amount of cladding expansion (ballooning)

The volume increase as the cladding expanded prior to rupture is listed in Table 49. As mentioned previously, both the induction heating and our method of fuel rod support tend to promote localized swelling. The pressure and temperature changes between peak pressure and rupture were used in the ideal-gas-law equation to calculate the volume increase. For these calculations, we assumed that the plenum volume of  $4.33 \text{ cm}^3$  (within the tubing and the pressure transducer) remained at  $30^\circ\text{C}$ , that the center portion of the rod contained  $0.6 \text{ cm}^3$  at the temperature of the midpoint of the rod, and that the rod ends and pressurizing "pigtail" contained  $0.8 \text{ cm}^3$  at a temperature midway between  $30^\circ\text{C}$  and the rod midpoint. Some of the observed pressure decreases may have resulted from slow leaks because some  $^{85}\text{Kr}$  release was usually observed before rupture. The increase in pressure between pressurization at  $\sim 850^\circ\text{C}$  was typically very small.

The same technique was employed to calculate volume increases of 7 and  $11 \text{ cm}^3$  in two BWR-diameter rods, with heated lengths of 24 in., which ruptured at approximately  $930^\circ\text{C}$  during fuel rod failure test FRF-1.<sup>43</sup> These rods were part of a six-rod bundle heated in the TREAT reactor. The apparently more uniform temperature environment permitted more generalized swelling along the heated lengths of these rods.

## 5.4 Discussion of Diffusional Release from the Gap Space

Following rupture and blowdown of the plenum gas, vaporized fission products can diffuse along the gap space and out the rupture opening. According to the gas-phase diffusion mechanism, the rate of release should be directly proportional to the distance diffused, and inversely proportional to the absolute pressure. Details of modeling are presented elsewhere.<sup>21</sup>

### 5.4.1 Effect of gap width

During the effort to correlate diffusional release from the gap space of test rods with drilled-hole defects (Implant, Low Burnup, and High Burnup Test Series), a rigorous mathematical model was followed

that included the effect of hole size, gap width, and distance diffused along the gap and within the hole. This thorough analysis did not correlate the data any better than the single parameter of gap width. The measured gap width was used for unexpanded cladding (drilled hole defect), but for pressure-ruptured cladding, a 200- $\mu\text{m}$  gap width was found to adequately describe the combined effect of ballooned cladding (providing a locally very large gap width) and the size of the hole.

#### 5.4.2 Effect of hole size

As described in Sect. 5.4.1, the variation in hole size encountered in our test series was not sufficient to warrant a separate correlating term within the scatter of experimental data. It is possible that extremes in hole sizes could affect the diffusional release rates either as a physical barrier or by secondary chemical effects. The hole size affects the rate of steam diffusion into the gap space; this, along with the rod temperature, determines the rate of hydrogen production by the steam-Zircaloy reaction. Hydrogen in the gap space decreases the oxygen potential, one of the controlling factors in fission product release, especially for cesium (see Sect. 5.1). The vapor pressure of cesium species in equilibrium with  $\text{UO}_{2+x}$  increases with decreasing oxygen potential.<sup>23</sup> Such an effect caused by a small hole size was not detected in our three test series, but a small rupture opening in the irradiated rod of fuel rod failure test FRF-2<sup>44</sup> was credited with reducing the amount of released tellurium and other fission products with low volatility.

#### 5.4.3 Effect of gap inventory

The gap inventory was not a variable in the High Burnup Test Series. In the Implant Test Series final report,<sup>2</sup> Figs. 73 and 74 display the observed effect of gap inventory affecting cesium and iodine release during both burst and diffusional release. The preliminary source-term model<sup>21</sup> uses this relationship.

#### 5.4.4 Effect of fuel rod length

For most of the tests conducted in the three test series, the quantities of cesium and iodine released did not significantly deplete the gap inventory of the 30-cm-long test segments. Possible exceptions were the 10-min diffusional release tests at 1100 and 1200°C where the induction-heated length was 16 or 17 cm and the fractional releases were highest. Since our test conditions included time and temperature regimes for the more severe SFTA and LOCA conditions, we do not believe that full-length fuel rods would release a significantly different mass of cesium or iodine than was observed in our short-rod tests.

#### 5.4.5 Effect of fragmented cladding

All of our test data are applicable to LWR fuel rods with a single opening. If the rod interior were more exposed because of multiple defects or fragmented cladding, the vaporization of the original gap inventory would be much more rapid, and loss by diffusion from the pellets might also become significant. For example, the rate of loss of cesium and iodine from  $UO_2$  irradiated to 4000 MWd/MT at 1200°C in purified helium was approximately 1% of the total fuel inventory per hour.<sup>15</sup> The rate of escape from the ruptured fuel rod segment used in test HBU-11 at 1200°C was only about 0.1% per hr of the total rod inventory.

## 6. CONCLUSIONS

The primary goals of this experimental series were to quantify and characterize fission product release under postulated, successfully terminated LOCA and SFTA conditions. The release data obtained from the experiments conducted with segments of fully irradiated, commercial fuel rods in this series and the results obtained in the Low Burnup Fuel Test and Implant Test Series have been used to develop semiempirical models for predicting cesium and iodine releases from fuel rods that undergo cladding failure within the temperature range 500 to 1200°C in steam.<sup>21</sup>

Fission product release is the sum of two components: burst release (that fraction carried out with the escaping plenum gas when a rod ruptures), and diffusional release (that fraction which diffuses from the gap space after the plenum gas has vented). The experimental results show that burst release would be more significant than diffusional release in a controlled LOCA. In this type accident the fuel rods could reach a maximum temperature of 1200°C, but the emergency core cooling system (ECSS) would bring the temperature of the rods back down within a relatively short time.

The atmosphere a fuel rod is exposed to during accident conditions can be very influential in affecting fission product release. In the two tests conducted in dry air with predrilled fuel rods, it was determined that the diffusional releases of iodine, cesium, and ruthenium were considerably larger than the releases obtained in similarly conducted steam tests. An air-steam atmosphere could possibly occur in a very severe SFTA, and diffusional release might prove to be equal to or greater than burst release. Diffusional release is time dependent; consequently, the magnitude of the release would depend on the speed with which emergency action is taken to cool the fuel. Ingression of air into the shipping cask would allow exposed fuel to become oxidized at rupture locations and at cracks in the cladding caused by the accident impact. We believe that the larger releases in our dry air tests were partly the result of extensive oxidation of the fuel, which unveiled fission products trapped within the fuel matrix and made them available for release. Radial migration of volatile fission products from the pellets into the gap space would be enhanced because oxidized fuel is considerably more porous than unoxidized fuel. Additional tests in dry air and/or air-steam atmospheres with ruptured fuel rod specimens and segments with more fuel exposed would provide a clearer picture of SFTA releases.

Diffusional releases of cesium and iodine that were obtained in the tests conducted with low burnup fuel were larger than those obtained under identical test conditions with high burnup fuel (Sect. 4.12; Table 40). These data demonstrate that fission product release from the gap is unequivocally dependent on the linear heat rating of the fuel (as it affects temperature buildup of the gap inventory as well as burnup).

In addition to burst release and diffusional release from the gap space, three other release modes were identified. When the test segments were first heated to the temperature range 700 to 1200°C, approximately 1.0 to 1.7% of the fission gas was released rather quickly. We believe this to be the release of embedded gas (see Sect. 4.12.4). Another release mechanism was the ejection of a large-particle-size fuel dust at the time of rupture (see Sect. 4.12.3). The third additional release mechanism was diffusion from the UO<sub>2</sub> matrix. This would only be significant when fuel is heated for long times at temperatures above ~1100°C.

The gap inventories for cesium and iodine in a typical 30.5-cm segment of H. B. Robinson fuel were determined in a gap purge test (Sect. 4.11). It was found that 1355 µg of cesium and 128 µg of iodine were potentially releasable; those amounts represent about 0.30% of the total inventories of cesium and iodine in the segment. This can be compared with the in-reactor xenon release to the fuel rod voids and plenum of 0.25% that was measured at room temperatures. (An additional 1.36% of the fission gas was also released in the gap purge test that was conducted at 1200°C.)

The principle factors that influence fission product release ≤1200°C are summarized in Table 50. A source term model that incorporates most of these elements has been published.<sup>21</sup>

The results obtained in the High Burnup Fuel Test Series, reinforced with experimental observations and evidence from the previous series of tests in this program, suggest the following chemical behavior (see Sect. 5):

1. In tests conducted in steam, CsOH and CsI were the major chemical species of cesium and iodine that were released.
2. In the gap voids of the test specimen, cesium was present (in addition to CsI) in the condensed phase in a form that was less volatile than elemental cesium or cesium oxide, probably as cesium uranate.
3. Antimony was apparently released in the steam test as elemental antimony. There was no evidence of antimony release in the dry air tests.

Table 50. Parameters affecting fission product release  
from the gap space <math><1200^{\circ}\text{C}</math><sup>a</sup>

Burst release	Diffusional release
Temperature <sup>b</sup>	Temperature <sup>c</sup>
Gap inventory <sup>b</sup>	Gap inventory <sup>b</sup>
Oxygen potential in UO <sub>2</sub>	Oxygen potential in UO <sub>2</sub>
Volume of vented gas, <sup>b</sup> at system pressure	Time
	Restriction to gas-phase diffusion:
	Gap width } <sup>b</sup>
	Hole size }
	System pressure
	Fuel rod length
	External atmosphere (steam/dry air) <sup>b</sup>

<sup>a</sup>Some replenishment of the gap inventory will occur in the temperature range 1100 to 1200°C by diffusion from the UO<sub>2</sub> matrix.

<sup>b</sup>Indicates moderate investigation of this parameter during the High Burnup and Implant Test Series.

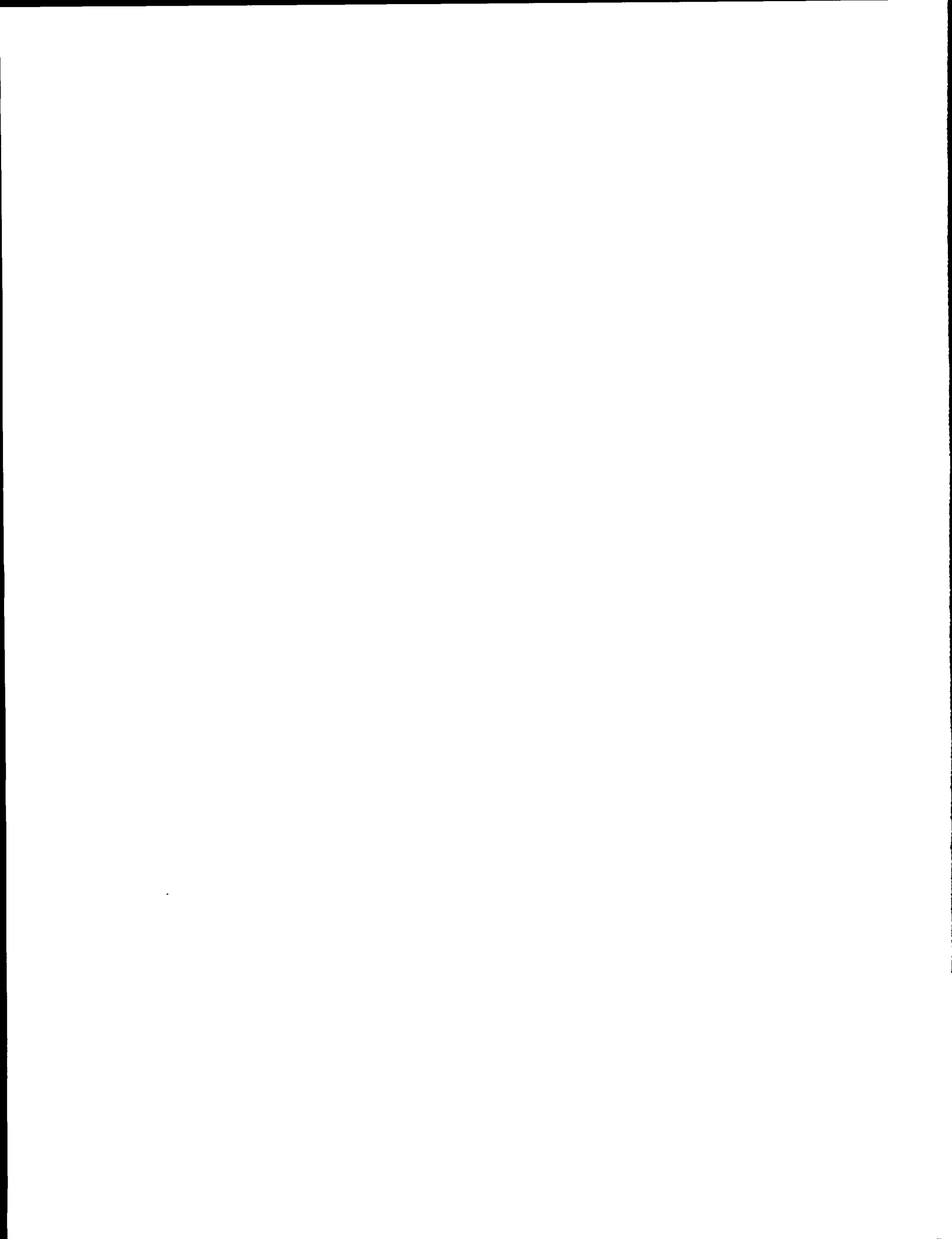
<sup>c</sup>Indicates more thorough investigation of this parameter during the High Burnup and Implant Test Series.

- In the dry air tests, elemental iodine was the major species of iodine that was released. Ingression of air into the fuel segments caused fuel oxidation, swelling of the fuel, and expansion of the cladding. At higher oxygen/uranium fuel ratios, CsI apparently reacts with the fuel to form cesium uranate and elemental iodine.
- Significant amounts of volatile ruthenium were also released in the dry air tests, probably as RuO<sub>4</sub>.

Our test results, which showed that the iodine in the fuel rod gap space was probably present as CsI, were based on the analyses of <sup>129</sup>I, a nearly stable isotope. The possibility exists that isotopes of iodine with short half-lives, and therefore shorter life span in the fuel rod, would not have time to attain the thermodynamically stable form of CsI. A recently published research note provides evidence to support the contention that the 8.05-day <sup>131</sup>I fission product also behaves like CsI.

in LWR fuels. Davies et al.<sup>48</sup> found that  $^{131}\text{I}$  released to the gap space from low-burnup  $\text{UO}_2$  during a power ramp was not in a reactive chemical form (such as  $\text{I}_2$ ), but deposited on surfaces as (or to form) iodides, probably cesium iodide.

7. APPENDIXES



## 7. APPENDIXES

7.1 Appendix A. Gap Size Measurements for High  
Burnup Fuel Test Series

The resistance to flow of argon was employed to obtain an estimate of the pellet-to-cladding gap width in the H. B. Robinson fuel rod segments tested in the High Burnup Test Series. The pressure drop of argon at room temperature and near atmospheric pressure was measured as the gas was made to flow from the inlet end along 15.2 cm (6.0 in.) of the fuel rod length and out the 0.159-cm (0.0625-in.)-diam hole drilled through the cladding.

Figure 39 shows a schematic of the apparatus used in these tests, along with typical data obtained. Beginning with test HBU-2, the system was pressurized to approximately 115 cm (45 in.) of water above hot-cell pressure before the cladding was drilled. Flow was initiated when the drill breached the cladding; 15 min later, the pressure drop across the test rod was compared with that across a length of stainless-steel capillary tubing. Approximately 500 cm<sup>3</sup> of argon was allowed to flow before the test was terminated. (We do not believe that a significant amount of fission products was purged from the fuel rod by this operation.)

So that the relationship between flow resistance and gap size could be validated, we performed similar tests with 0.965-cm (0.380-in.)-ID Zircaloy tubing and steel rods of several sizes to provide known gap clearances.

The rods were centerless ground, and no provision was made to center the rods in the tubing. One set of measurements was made with flow through the annulus vented to the open tubing; a second set was made in which the argon was vented through a drilled hole in the cladding. As is indicated by the data displayed in Fig. 40, in which radial gap size is plotted as a function of resistance to flow that was measured relative to that of the reference capillary, the latter arrangement resulted in higher-flow resistances. Additional tests (not included in the data shown in Fig. 40) indicate that the added restriction created by the drilled-hole exit varied from essentially nothing to twice the increment shown, depending on the

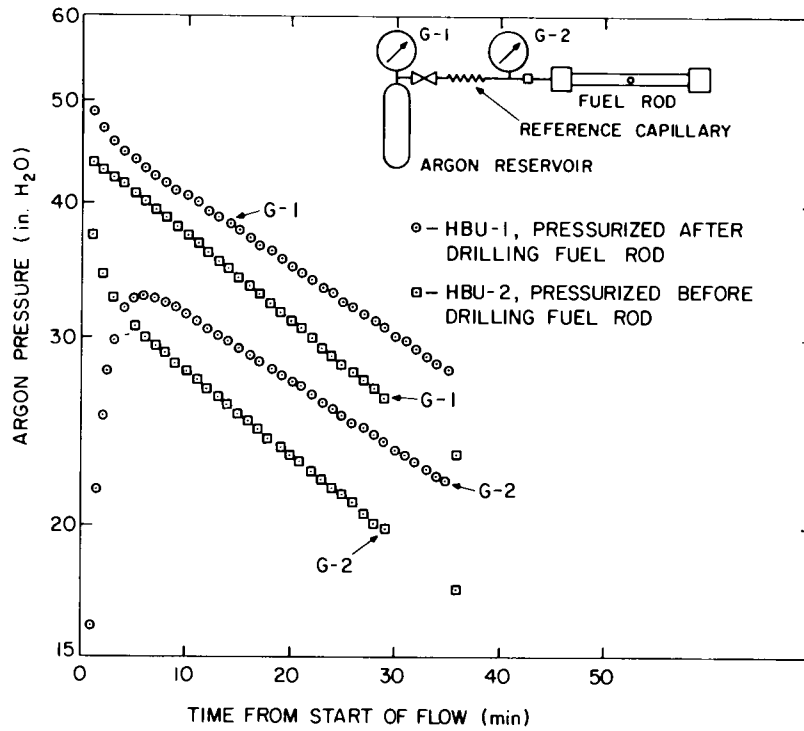


Fig. 39. Apparatus and typical flow data for gap size determinations using a gas flow technique.

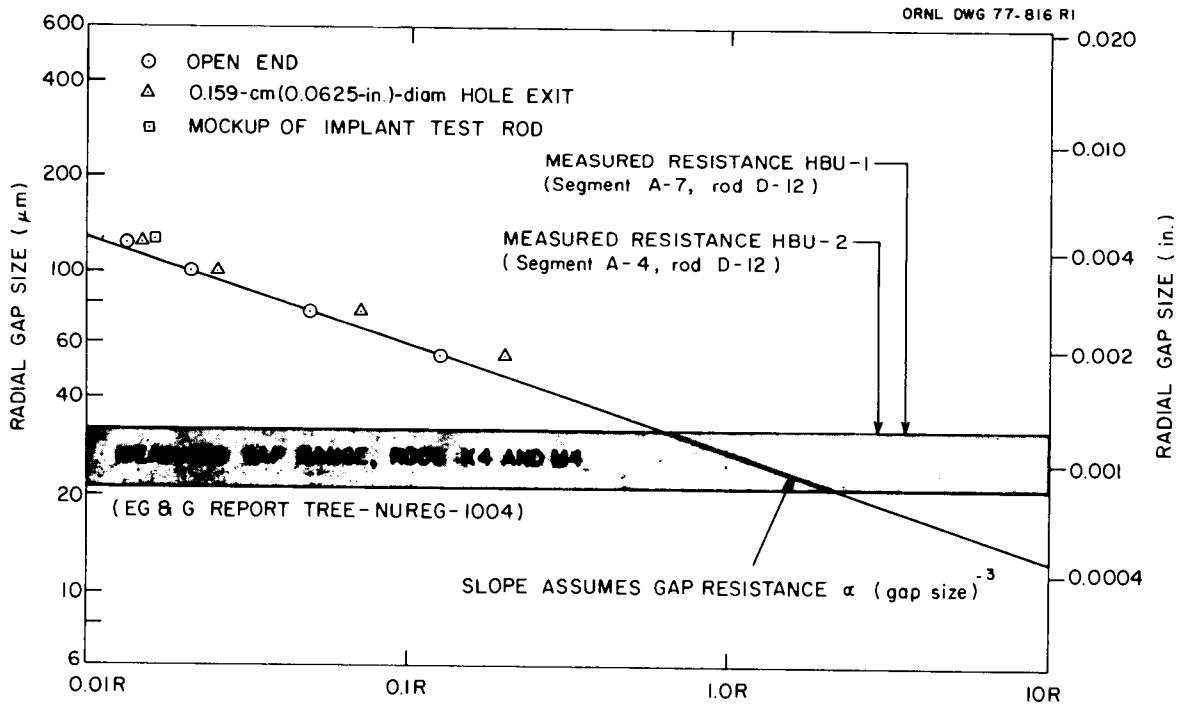


Fig. 40. Dependence of radial gap size on resistance to flow, measured relative to a reference capillary. (Measured gap range is from Ref. 13).

clearance between the pellets (steel rod in our test case) and the drilled hole, as determined by eccentricity at the hole location. The straight line shown in Fig. 40 assumes the conventional relationship between gap width and laminar flow resistance.

Previously measured<sup>13</sup> gap widths in H. B. Robinson fuel rods K-4 and M-4 are indicated in Fig. 40. These results and the following equation were used to calculate  $r_H$ , the effective radial gap:

$$r_H^3 = \frac{Ha}{8\pi} \frac{W\eta RTL}{\bar{r} (P_1^2 - P_2^2)} \quad (A.1)$$

The definitions of these terms, and the values applicable to our test with the fuel rod segment from test HBU-2 (segment A-4, fuel rod D-12), are:

Ha = Hagen number, 96;<sup>13</sup>

W = gas flow rate,  $2.08 \times 10^{-6}$  mole/sec when  $P_1 = 1.0417$  atm;

$\eta$  = gas viscosity,  $2.55 \times 10^{-4}$  g/cm·sec;

R = universal gas constant,  $8.317 \times 10^7$  g·cm<sup>2</sup>/mole·sec<sup>2</sup>·K;

T = absolute temperature, 298 K;

L = length, 15.2 cm;

$\bar{r}$  = mean annulus radius (center of rod to center of annulus),  
0.474 cm;

$P_1$  = pressure at inlet end, 1.0417 atm,  $1.028 \times 10^{-6}$  g/sec<sup>2</sup>·cm;

$P_2$  = pressure at outlet end, 0.9737 atm,  $9.610 \times 10^{-7}$  g/sec<sup>2</sup>·cm.

The gas flow rate W was calculated from the measured system volume of 2475 cm<sup>3</sup> and the observed pressure reduction half-time of 38 min. Using the above values and Eq. (A.1), we calculated the effective radial gap to be 21.6  $\mu$ m ( $8.5 \times 10^{-4}$  in.). Similarly, we calculated that the effective radial gap for HBU-1 was 19.9  $\mu$ m ( $7.8 \times 10^{-4}$  in.), and for HBU-4 it was approximately 17.6  $\mu$ m ( $6.9 \times 10^{-4}$  in.). The latter measurement is less accurate because of a small gas leak. These measurements were probably all affected by added flow resistance where the drilled hole entered the gap region.

Knowledge of the gap width has been helpful in comparing fission product release from rods with greatly differing gap sizes, such as our Implant Test rods (127- $\mu\text{m}$  radial gap) and the H. B. Robinson rods (20- to 30- $\mu\text{m}$  radial gap).

## 7.2 Appendix B. Low Burnup Fuel Test Results and Comparison with Similar HBU Tests

The purpose of this section is to present the unpublished iodine releases that were obtained in the Low Burnup Fuel Test Series, and to compare the releases of both cesium and iodine in that series with those obtained under similar conditions in the High Burnup Fuel Test Series. A complete description of the fuel used in the Low Burnup Fuel Test has already been reported.<sup>22</sup> The calculated inventory of fission products in the low burnup capsules is given in Table 51, and the in-reactor fission gas release data are summarized in Table 52. Key information about the fuel that was tested is also provided in Table 53.

Only two tests were conducted with low burnup fuel and each was in a flowing steam-argon atmosphere. Prior to testing, each capsule was drilled to produce a cladding defect, a 0.159-cm (0.0625-in.)-diam hole. The distributions of cesium and iodine in the experimental apparatus at the conclusions of those tests are summarized in Tables 54 and 55. The data listed for test LBU-1, which was conducted at 700°C for 5 hr, indicate that 0.0003% (0.046  $\mu\text{g}$ ) and 0.02% (0.17  $\mu\text{g}$ ) of the total cesium and iodine inventories, respectively, were released; this is about 3.5 times more iodine (mass) than cesium. The data distribution for cesium and iodine also indicate that about 93% of the released iodine was not associated with cesium. These results are very analogous to those obtained in test HBU-1 (Sect. 4.1), which was also conducted in steam at 700°C for 5 hr. In that test, about 7.5 times more iodine (mass) was released than cesium, and about 98% of the iodine was found without the presence of cesium.

In test LBU-2, which was performed at 900°C for 2 hr, the data in Table 55 show that 0.127% (19.31  $\mu\text{g}$ ) and 2.37% (21  $\mu\text{g}$ ) of the cesium and iodine inventories were released; which are almost equal masses. About

Table 51. Amounts of selected fission products in low burnup fuel capsules<sup>a</sup>

Fission product	g/MT	mg/6 in. <sup>b</sup>	Fission product	g/MT	mg/6 in. <sup>b</sup>
<sup>85</sup> Kr	0.568	0.0964	<sup>129</sup> I	4.148	0.704
Total Kr	14.04	2.384	Total I	5.117	0.869
Total Rb	14.12	2.398	Total Xe	147.2	24.99
<sup>90</sup> Sr	18.35	3.116	<sup>137</sup> Cs	30.17	5.123
Total Sr	32.62	5.539	Total Cs	89.77	15.24
Total Y	18.86	3.202	Total Ba	48.65	8.261
Total Zr	131.7	22.36	Total La	39.77	6.753
Total Mo	105.6	17.93	<sup>144</sup> Ce	0.0114	0.00194
<sup>106</sup> Ru	0.00422	7.17 x 10 <sup>-4</sup>	Total Ce	75.61	12.84
Total Ru	51.05	8.68	Total Pr	36.90	6.266
Total Rh	14.55	2.471	Total Nd	132.4	22.48
Total Pd	8.811	1.496	Total Sm	25.84	4.388
Total Sn	1.192	0.202	Total Eu	1.413	0.240
Total Sb	0.295	0.050	U	9.988 x 10 <sup>5</sup>	1.696 x 10 <sup>5</sup> <sup>b</sup>
Total Te	11.33	1.924	Pu	138.6	23.53

<sup>a</sup>Calculated by ORIGEN computer program (Aug. 9, 1979) for a burnup of 1000 MWd/MT, 30 days of irradiation, 9-year decay. The burnup of capsule 013, test LBU-1, was ~970 MWd/MT.

<sup>b</sup>Initial uranium content of the 6-in.-long capsule was 169.8 g (12% enriched).

Table 52. Fission gas released in-reactor in low burnup capsules

Isotope	Total produced in capsule 012 <sup>a</sup> (g-atoms/MT)	Total found in capsule gap region		Amount released to capsule gap region	
		Capsule 013, LBU-1 (g-atoms/MT)	Capsule 012, LBU-2 (g-atoms/MT)	Capsule 013, LBU-1 (%)	Capsule 012, LBU-2 (%)
<sup>82</sup> Kr	0.0000086				
<sup>83</sup> Kr	0.02383	0.00272	0.00486	11.76	20.39
<sup>84</sup> Kr	0.04573	0.00498	0.00895	11.23	19.57
<sup>85</sup> Kr	0.006677	0.00081	0.00140	12.51	20.97
<sup>86</sup> Kr	0.08896	0.00942	0.01674	10.92	18.82
Total Kr	0.1652	0.01793	0.03195	11.18	19.34
<sup>128</sup> Xe	0.0000022				
<sup>130</sup> Xe	0.0000243				
<sup>131</sup> Xe	0.1286	0.01428	0.02331	11.45	18.12
<sup>132</sup> Xe	0.1934	0.02130	0.03648	11.35	18.86
<sup>134</sup> Xe	0.3411	0.03971	0.06581	12.00	19.29
<sup>136</sup> Xe	0.4346	0.04999	0.08298	11.86	19.10
Total Xe	1.098	0.12528	0.20858	11.76	19.00

<sup>a</sup>Calculated for 30 days of irradiation to 1000 MWd/MT burnup with 9 years of decay. Capsule 013 burnup was 970 MWd/MT.

Table 53. Release data for similarly conducted low and high burnup fuel tests

Test No.	Data concerning fuel specimen <sup>a</sup>				Test conditions			Percent of total inventory released					
	Exposure (Mwd/MT)	Maximum linear power		Irradiation time (days)	Temp (°C)	Test period (hr)	Test atmosphere	Fission gas released to gap space during irradiation		Release from specimen during high temperature test		Mass released	
		kW/ft	W/cm					Krypton	Xenon	Cesium	Iodine	Cesium (µg)	Iodine (µg)
LBU-1	970	17.0	558	20.84	700	5	Steam-argon	11.2	11.8	0.00031	0.020	0.046	0.17
LBU-2	1,000	22.2	728	20.84	900	2	Steam-argon						
HUB-1	30,745	9.95	326	799 <sup>b</sup>	700	5	Steam-argon	0.29	0.22	0.000026	0.002	0.123	0.925
HBU-2	29,987	9.95	326	799 <sup>b</sup>	900	2	Steam-argon	0.29	0.22	0.00062	0.004	2.82	1.75

<sup>a</sup>The low burnup fuel was tested 9 years after irradiation; the high burnup fuel, 3 years. The low burnup capsules were 6 in. long and contained an initial uranium content of 169.8 g (12% enriched). By comparison the high burnup segments were 12-in. long and contained 183.3 g of uranium before irradiation (3% enriched).

<sup>b</sup>EFPDs (effective full power days).

Table 54. Distribution of  $^{137}\text{Cs}$  and  $^{129}\text{I}$  in Low Burnup Test 1<sup>a</sup>

Location	Temperature (°C)	Amount of $^{137}\text{Cs}$ in each location		Amount of $^{129}\text{I}$ in each location		Total cesium ( $\mu\text{g}$ )	Total iodine ( $\mu\text{g}$ )
		$\mu\text{g}$	Percent of released	$\mu\text{g}$ <sup>b</sup>	Percent of released		
Fuel rod	700	4969 <sup>c</sup>		683 <sup>c</sup>		14780 <sup>c</sup>	843 <sup>c</sup>
Quartz furnace tube liner	700	$1.515 \times 10^{-2}$	97.528	$0.0091 \pm 0.001$	6.77	$4.51 \times 10^{-2}$	$1.12 \times 10^{-2}$
Thermal gradient tube	700-105	$2.96 \times 10^{-4}$	1.906	$0.0540 \pm 0.008$	40.18	$8.81 \times 10^{-4}$	$6.67 \times 10^{-2}$
Filter pack components	135						
Stainless-steel inlet fitting		$4.70 \times 10^{-6}$	0.030	$0.0293 \pm 0.002$	21.80	$1.40 \times 10^{-5}$	$3.62 \times 10^{-2}$
First filter paper		$8.82 \times 10^{-5}$	0.533	$0.02^{\text{d}}$	14.88	$2.62 \times 10^{-4}$	$2.72 \times 10^{-2}$
Second filter paper		0.0 <sup>e</sup>	0.0	0.0 <sup>e</sup>	0.0	0.0	0.0
Third filter paper		0.0	0.0	0.0	0.0	0.0	0.0
Charcoal No. 1a		$2.62 \times 10^{-7}$	0.002	0.022	16.37	$7.79 \times 10^{-7}$	0.0
Charcoal No. 1b		0.0	0.0	0.0	0.0	0.0	0.0
Charcoal No. 1c		0.0	0.0	0.0	0.0	0.0	0.0
Charcoal No. 1d		$1.73 \times 10^{-7}$	0.001	0.0	0.0	$0.15 \times 10^{-7}$	0.0
Charcoal No. 2		0.0	0.0	0.0	0.0	0.0	0.0
Charcoal No. 3		0.0	0.0	0.0	0.0	0.0	0.0
AgX		0.0	0.0	0.0	0.0	0.0	0.0
Condenser housing	0	0.0	0.0	0.0	0.0	0.0	0.0
Condensate		0.0	0.0	0.0	0.0	0.0	0.0
Freeze trap	-78	0.0	0.0	0.0	0.0	0.0	0.0
Cold charcoal trap	-78	0.0	0.0	0.0	0.0	0.0	0.0
Total released		$0.0155^{\text{f}}$	100.000	$0.1344 \pm 0.01^{\text{g}}$	100.00	$4.61 \times 10^{-2}$	$0.166 \pm 0.01$

<sup>a</sup>Steam flow rate,  $328 \text{ cm}^3/\text{min}$  (STP); argon flow rate,  $60 \text{ cm}^3/\text{min}$  (STP); system pressure, 750 torr.

<sup>b</sup>Errors listed are  $2 \sigma$  counting errors and do not include other possible errors.

<sup>c</sup>Initial amounts of  $^{137}\text{Cs}$ ,  $^{129}\text{I}$ , cesium, and iodine in capsule. Calculated by making use of ORIGIN data for 169.8 g of 12% enriched uranium irradiated 19 days to 970 MWd/MT (decayed 9.0 years).

<sup>d</sup>An estimated value.

<sup>e</sup>Amounts less than  $1.0 \times 10^{-7} \mu\text{g}$  for cesium and  $1.0 \times 10^{-4} \mu\text{g}$  for iodine are given as 0.0.

<sup>f</sup>This amount is  $3.12 \times 10^{-4}\%$  of the total  $^{137}\text{Cs}$  inventory.

<sup>g</sup>This amount is 0.0197% of the total  $^{129}\text{I}$  inventory.

Table 55. Distribution of  $^{137}\text{Cs}$  and  $^{129}\text{I}$  in Low Burnup Fuel Test 2<sup>a</sup>

Location	Temperature (°C)	Amount of $^{137}\text{Cs}$ in each location		Amount of $^{129}\text{I}$ in each location		Total cesium ( $\mu\text{g}$ )	Total iodine ( $\mu\text{g}$ )
		$\mu\text{g}$	Percent of released	$\mu\text{g}^b$	Percent of released		
Fuel rod	900	5123 <sup>c</sup>		704 <sup>c</sup>		15240	869
Quartz furnace tube liner	900	3.409	52.51	0.0056 ± 0.0090 0.0028	0.03	10.14	0.01
Thermal gradient tube	750-150	2.693	41.48	5.3851 ± 0.2359	32.28	8.01	6.65
Filter pack components	135-105						
Stainless steel inlet fitting		1.06 × 10 <sup>-1</sup>	1.63	3.4201 ± 0.0621	20.50	0.32	4.22
First filter paper		2.83 × 10 <sup>-1</sup>	4.36	0.8651 ± 0.0250	5.19	0.84	1.07
Second filter paper		4.5 × 10 <sup>-7</sup>	0.00001			1.3 × 10 <sup>-6</sup>	
Third filter paper		7.9 × 10 <sup>-5</sup>	0.0012	1.0243 ± 0.0251	6.14	2.4 × 10 <sup>-4</sup>	1.26
Charcoal No. 1a		1.0 × 10 <sup>-7</sup>	0.000002	5.970 ± 0.10	35.79	3.0 × 10 <sup>-7</sup>	7.37
Charcoal No. 1b		0.0 <sup>d</sup>	0.0	0.0	0.0	0.0	0.0
Charcoal No. 1c		0.0	0.0	0.0	0.0	0.0	0.0
Charcoal No. 1d		1.1 × 10 <sup>-6</sup>	0.00002	0.0	0.0	3.3 × 10 <sup>-6</sup>	0.0
Charcoal No. 2		0.0	0.0	0.0	0.0	0.0	0.0
Charcoal No. 3		0.0	0.0	0.0	0.0	0.0	0.0
AgX		0.0	0.0	0.0	0.0	0.0	0.0
Condenser housing	0	2.0 × 10 <sup>-6</sup>	0.00004	0.0	0.0	6.0 × 10 <sup>-6</sup>	0.0
Condensate		0.0	0.0	0.0	0.0	0.0	0.0
Freeze trap	-78	3.0 × 10 <sup>-6</sup>	0.00005	0.0113 ± 0.0015	0.07	9.0 × 10 <sup>-6</sup>	0.01
Total released		6.491 <sup>e</sup>	100.00	16.6815 ± 0.46 <sup>f</sup>	100.00	19.31	20.60

<sup>a</sup>Steam flow rate, 366 cm<sup>3</sup>/min (STP); argon flow rate, 60 cm<sup>3</sup>/min (STP); system pressure, 760 torr (0.101 MPa).

<sup>b</sup>Error shown is 2  $\sigma$  counting error only.

<sup>c</sup>Initial amounts of  $^{137}\text{Cs}$ ,  $^{129}\text{I}$ , cesium, and iodine in capsule. Calculated by making use of ORIGEN data from 169.8 g of 12% enriched uranium irradiated 19 days to 1000 MWd/MT (decayed 9.0 years).

<sup>d</sup>Amounts less than 1.0 × 10<sup>-7</sup>  $\mu\text{g}$  for cesium and 1.0 × 10<sup>-4</sup>  $\mu\text{g}$  for iodine are given as 0.0.

<sup>e</sup>This amount is 0.127% of the total  $^{137}\text{Cs}$  inventory.

<sup>f</sup>This amount is 2.37% of the total  $^{129}\text{I}$  inventory.

62% of the released iodine was found in the elemental form. In test HBU-2, which was conducted under similar conditions, about 1.6 times more cesium (mass) was found than iodine, and most (94%) of the iodine was found at locations different from that of cesium.

In tests LBU-1 (700°C), HBU-1 (700°C), and HBU-2 (900°C), greater than 97% of the cesium was found on the surface of the furnace tube liners near the simulated defect openings. However, in test LBU-2 (900°C), approximately 47.5% of the cesium transported downstream beyond the quartz furnace tube; most of that cesium deposited in the gold thermal-gradient tube (Table 55), and an almost identical amount of iodine was also found there. It was determined that most of the cesium and iodine deposited in the 275 to 400°C temperature range, which suggests that CsI was the species deposited.

Table 52, which gives the cesium and iodine release data for comparable high burnup and low burnup fuel tests, clearly suggests the effect that linear heat rating of irradiated fuel has on fission product release under LOCA conditions; only volatile fission products in the pellet-clad interface and void spaces connected to the interface are potentially releasable under LOCA conditions. Little release from the fuel matrix would occur in short times at temperatures  $\leq 1200^\circ\text{C}$ . In postirradiation examinations of the low burnup fuel by beta-gamma autoradiography,<sup>49</sup> it was determined that both capsules had longitudinal centerline voids and fuel relocation to the pellet interfaces. A concentration profile (Fig. 41) of  $^{137}\text{Cs}$  in the LBU-2 capsule prior to testing (9-year decay period) shows that cesium had migrated to the pellet interfaces during irradiation. Similar scans taken shortly after irradiation also revealed peak concentrations of  $^{131}\text{I}$  and  $^{140}\text{Ba} - ^{140}\text{La}$ . Of the fuel capsules examined,<sup>49</sup> it was determined that only capsules operated at heat ratings of  $\geq 17$  kW/ft had centerline voids and gamma spikes at the pellet interfaces. Those capsules experienced estimated centerline temperatures during irradiation of  $1600^\circ\text{C}$  or greater. By comparison, the H. B. Robinson fuel experienced a maximum linear heat rating of only 9.95 kW/ft and an estimated maximum centerline temperature of  $1300^\circ\text{C}$ . No signs of change in microstructure were observed in post-irradiation examination<sup>3</sup> of similar H. B. Robinson fuel, but large cracks

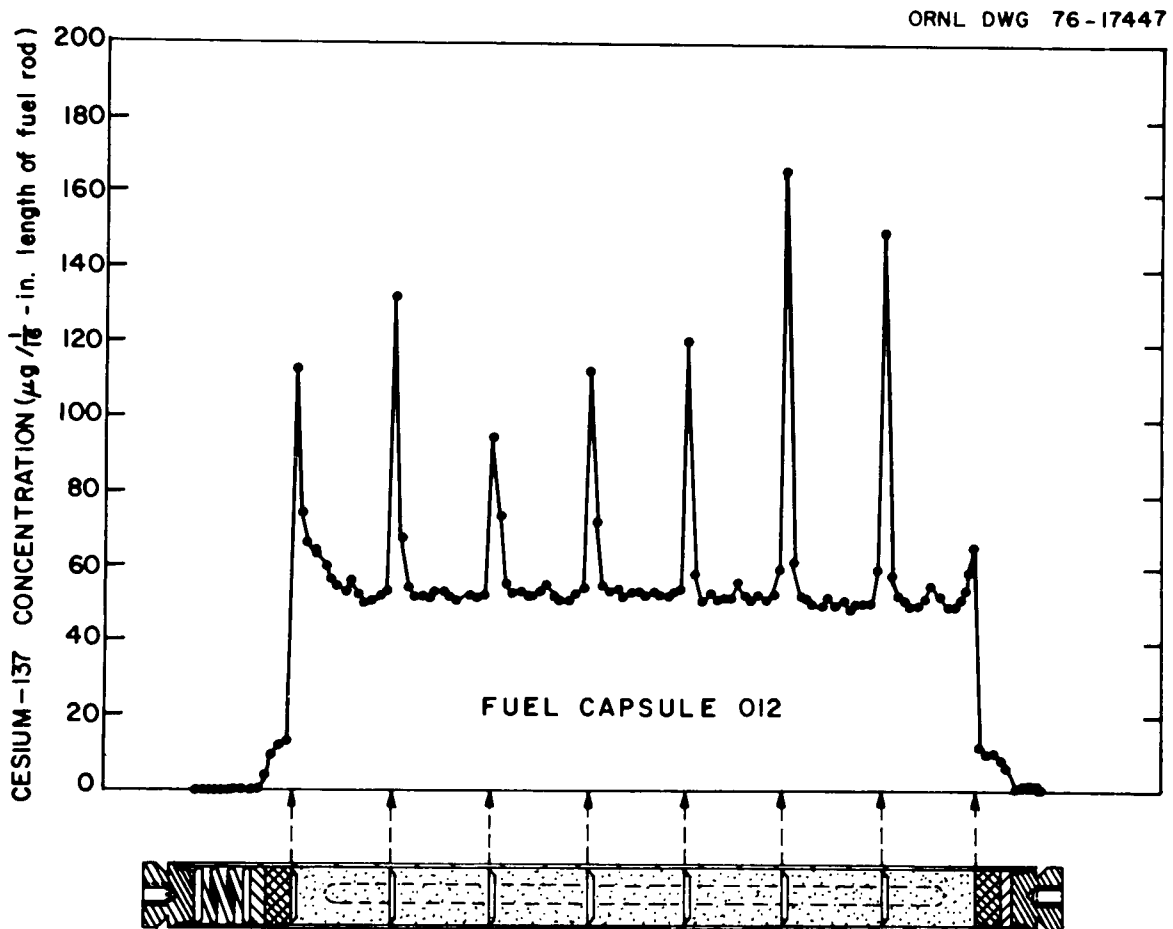


Fig. 41. Cesium-137 concentration profile along fuel rod 012.

were apparent, which were probably caused by thermal shocks that occurred during startup and shutdown periods.

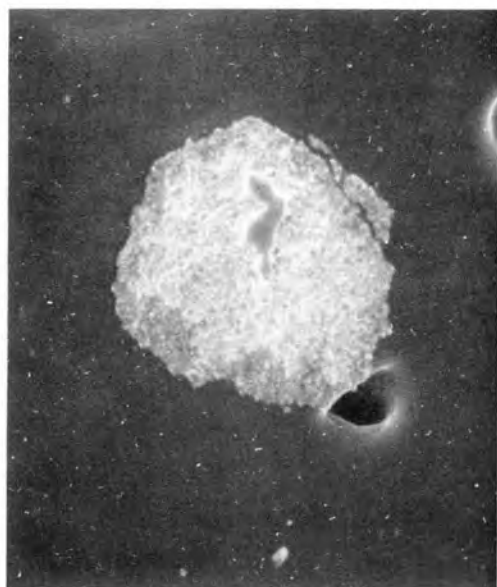
Table 53 shows that the fraction of fission gas released to the gap space during irradiation is very dependent on the linear heat rating. This would also be expected to be true for volatile fission products like cesium and iodine. The mass release data show that 7 times more cesium and 11 times more iodine were released in test LBU-2 (900°C) than in test HBU-2 (900°C), and that the releases for cesium and iodine obtained in tests LBU-1 (700°C) and HBU-1 (700°C) were similar. Considering the difference in total inventories between the two types of fuel (H. B. Robinson, 469 mg Cs and 43.2 mg I vs General Electric Test Reactor, 15.2 mg Cs and 0.87 mg I), the importance of the linear heat rating (as a broad indicator of fission product release to the gap space and subsequent escape following rupture) appears evident. Again, only volatile fission products in the gap are releasable in a LOCA.

### 7.3 Appendix C. Examination of Fuel Particles Ejected from Ruptured Rods

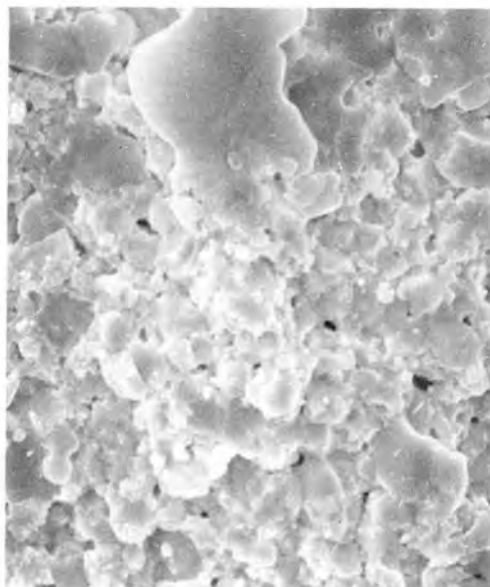
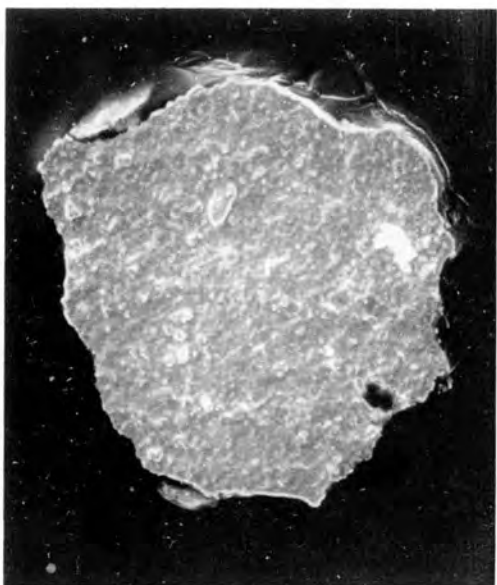
As described in Sect. 5, approximately 0.02% of the UO<sub>2</sub> fuel was ejected when rupture occurred in tests HBU-7 to -10. Samples of the particles were examined by gamma spectrometry and it was found that the measurable gamma emitters (<sup>134</sup>Cs, <sup>137</sup>Cs, <sup>125</sup>Sb, <sup>106</sup>Ru - <sup>106</sup>Rh, <sup>144</sup>Ce, and <sup>154</sup>Eu) were present in the same proportions as in the bulk fuel.

Samples of these particles were examined by the scanning electron microscope, and their composition was measured by energy-dispersive analysis. Typical particles from test HBU-7, identified as mainly uranium in composition (almost certainly UO<sub>2</sub>), are shown in Figs. 42-43. Most of the small particles that were deposited on the filter-pack inlet fitting and the first filter paper were composed mainly of silicon. These are believed to have come from the quartz furnace tube components. We could not distinguish visually between fuel and "quartz" particles, which made it necessary to check each particle of interest for composition. Table 56 summarizes the data for the five particles identified as fuel. Many samples

ORNL DWG 79-1179

100  $\mu\text{m}$  

(a)

10  $\mu\text{m}$  100  $\mu\text{m}$  

(b)

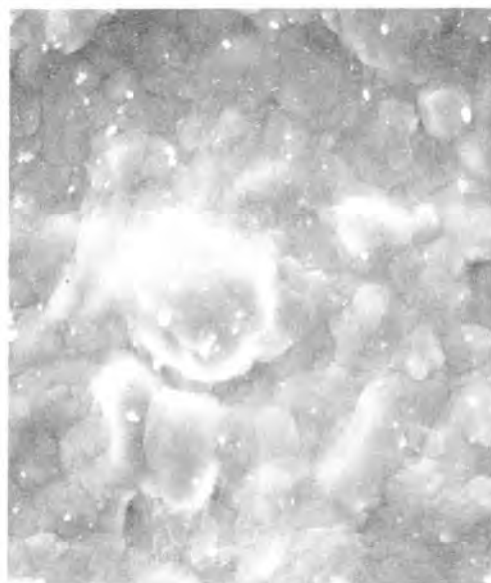
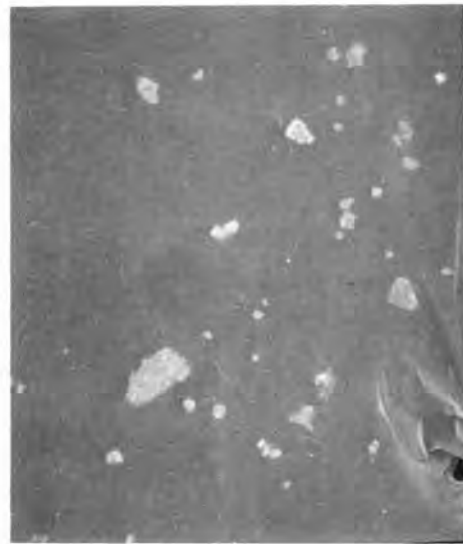
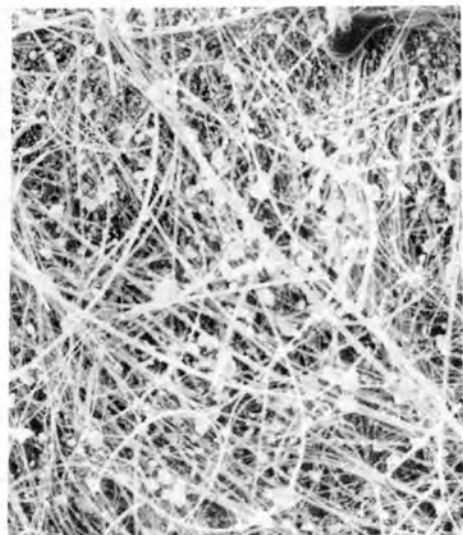
10  $\mu\text{m}$  

Fig. 42. Particle from fuel rod holder of test HBU-7, identified as fuel: (a)  $\sim 140 \mu\text{m}$  diam, (b)  $\sim 210 \mu\text{m}$  diam.



(a)

10  $\mu\text{m}$ 

(b)

10  $\mu\text{m}$ 

Fig. 43. (a) Particles from the stainless-steel inlet fitting to the filter pack test HBU-7; the particle in the center was identified as fuel (average diameter,  $\sim 11 \mu\text{m}$ ). (b) First filter paper from test HBU-7; particle A is primarily composed of silicon, and particle B is  $\text{UO}_2$  (average diameter of particle B,  $\sim 8 \mu\text{m}$ ).

Table 56. Size of particles from test HBU-7 identified as fuel

Location	Identification	Av diam <sup>a</sup> ( $\mu\text{m}$ )
Particles from furnace tube		
Furnace tube	HBU-7-13	150
Fuel rod holder	HBU-7-2a	140
Fuel rod holder	HBU-7-26	210
Filter pack		
Stainless-steel inlet fitting	HBU-7-1	11
Filter paper	HBU-7-11	8

<sup>a</sup>Average of length and width.

especially from the filter pack and first filter paper, were too radioactive for the energy-dispersive analyzer to work properly. Particles smaller than the 8- to 11- $\mu\text{m}$ -diam range probably existed, but it is reasonable to suspect that a discontinuity in the size distribution might occur at the mean  $\text{UO}_2$  grain size, which was 5 to 6  $\mu\text{m}$  diam in the irradiated fuel.

#### 8. ACKNOWLEDGMENTS

The authors wish to thank their colleagues at Oak Ridge National Laboratory who have provided assistance in making this program successful, especially L. L. Fairchild of the Chemical Technology Division for gamma counting of apparatus components after each test; H. A. Parker and J. F. Emery of the Analytical Chemistry Division for neutron activation determination of  $^{129}\text{I}$ ; C. L. Flanary, assisted by B. C. Drake, for preparation of the manuscript; and V. A. Jacobs for editing. Technical reviewers were T. M. Besmann, M. F. Osborne, G. W. Parker, and V. C. A. Vaughen. M. F. Osborne, a vital participant in the early phases of our fission product release program, served as the U.S. Nuclear Regulatory Commission representative at Gesellschaft für Kernforschung m.b.H. Karlsruhe, Germany, at the time that the High Burnup Test Series was performed.

## 9. REFERENCES

1. R. A. Lorenz, M. F. Osborne, J. L. Collins, and S. R. Manning, Behavior of Iodine, Methyl Iodide, Cesium Oxide, and Cesium Iodide in Steam and Argon, ORNL/NUREG/TM-25 (July 1976).
2. R. A. Lorenz, J. L. Collins, and S. R. Manning, Fission Product Release from Simulated LWR Fuel, NUREG/CR-0274, ORNL/NUREG/TM-154 (October 1978).
3. J. L. Collins et al., Knudsen Cell-Mass Spectrometer Studies of Cesium-Urania Interactions, ORNL/NUREG/TM-24 (June 1976).
4. P. E. MacDonald to A. P. Malinauskas, "Transmittal of CPL Assembly B05 Axial Flux Measurements," MacD-67-75 (Sept. 11, 1975).
5. K. R. Perkins to L. B. Thompson, "Thermal Transients of the Carolina Power and Light Fuel Bundle in Air," KRP-4-75 (July 14, 1975).
6. S. M. Gehl et al., Light-Water-Reactor Safety Research Program: Quarterly Progress Report July-September 1975, ANL-75-72 (1975), pp. 42-44.
7. A. A. Bauer, L. M. Lowry, and J. S. Perrin, Progress in Evaluating Strength and Ductility of Irradiated Zircaloy During July Through September 1975, BMI-1938 (September 1975).
8. R. W. Klingensmith, personal communication, Nov. 19, 1975.
9. V. W. Storhok, Battelle Columbus Laboratory, private communication, August 1975.
10. S. M. Gehl and M. G. Seitz, Light Water-Reactor Safety Research Program: Quarterly Progress Report October-December 1975, ANL-76-15 (1976), p. 50.
11. D. O. Campbell, S. R. Buxton, R. L. Beatty, and W. L. Pattison, pp. 26-39 in LWR Fuel Reprocessing and Recycle Program Quarterly Report for Period July 1 to September 30, 1976, ORNL/TM-5660 (November 1976).

12. M. J. Bell, ORIGEN - The ORNL Isotope Generation and Depletion Code, ORNL-4628 (May 1973).
13. S. J. Dagbjartsson, B. A. Murdock, D. E. Owen, and P. E. MacDonald, Axial Gas Flow in Irradiated PWR Fuel Rods, TREE-NUREG-1158 (September 1977).
14. Frank Panisko, Battelle Northwest Laboratories, personal communication, Mar. 9, 1978.
15. G. W. Parker et al., Out-of-Pile Studies of Fission-Product Release from Overheated Reactor Fuels at ORNL, 1955-1965, ORNL-3981 (August 1967), pp. 75-82.
16. A. H. Booth and G. T. Rymer, Determination of the Diffusion Constant of Fission Xenon in UO<sub>2</sub> Crystals and Sintered Compacts, CRDC-720 (August 1958).
17. S. E. Turner et al., Status Report - ANS 5.4 Fuel Plenum Gas Activity (N 218) (Fission Product Release from UO<sub>2</sub> Fuel), personal communication to R. A. Lorenz (April 1977).
18. R. Kelly, "The Diffusion of 'Attached' Inert-Gas Activity," *Canad. J. Chem.* 39, 2411-22 (1961).
19. K. M. Swanson, J. K. Bulter, and D. Clarke, "The Determination of Reactor Fuel Cladding Temperature by Recording Krypton-85 Release During Post-Irradiation Heating," *J. Nucl. Mater.* 33, 302-10 (1969).
20. B. Kryger, "Application de la Methode du Krypton 85 a la Determination des Temperatures de Gaine des Combustibles de Reacteurs a Neutrons Rapides," *J. Nucl. Mater.* 61, 306-12 (1972).
21. R. A. Lorenz, J. L. Collins, and A. P. Malinauskas, Fission Product Source Terms for the LWR Loss-of-Coolant Accident: Summary Report, ORNL/NUREG/TM-206 (June 1978).
22. R. A. Lorenz, J. L. Collins, and O. L. Kirkland, Quarterly Progress Report on Fission Product Release from LWR Fuel for the Period July-September 1976, ORNL/NUREG/TM-73 (December 1976).

23. T. M. Besmann and T. B. Lindemer, "Chemical Thermodynamics of the System Cs-U-Zr-H-I-O in the Light Water Reactor Fuel-Cladding Gap," Nucl. Technol. 40, 297-305 (1978).
24. M. G. Adamson, E. A. Aitken, S. K. Evans, and J. H. Davies, "Oxygen Redistribution and its Measurements in Irradiated Oxide Fuels," p. 59 in Proc. Symp. Thermodynamics of Nuclear Materials 1974, vol. I, Vienna, October 21-25, 1974, International Atomic Energy Agency, Vienna, (1975).
25. P. E. Blackburn, "Oxygen Pressures Over Fast Breeder Reactor Fuel. (1). A Model for  $UO_{2+x}$ ," J. Nucl. Mater. 46, 244 (1973).
26. D. Cubicciotti and J. E. Sanecki, "Characterization of Deposits on Inside Surfaces of LWR Cladding," J. Nucl. Mater. 78, 96-111 (1978).
27. B. D. Epstein, A Review of the Literature Pertinent to Fission-Product Migration and Interaction in Fuel Rods, GA-A13423, p. 13 (June 1975).
28. S. Nicolosi, p. 8 in Reactor Safety Research Program's Quarterly Progress Report October-December 1977, BNL-NUREG-50785, NRC-4, -7, -8 (January 1973).
29. V. J. Tennery, pp. 23-32 in Voloxidation-Removal of Volatile Fission Products from Spent LMFBR Fuels, J. H. Goode (ed.), ORNL-TM-3732 (January 1973).
30. Z. D. Aleckseeva, "The  $Cs_2O-SiO_2$  System," Russ. J. Inorg. Chem. 2(5), 626-29 (1966).
31. S. A. Kutolin and A. E. Sergeeva, "Thermodynamic Study of Formation of Compounds of the Types  $M_2TiO_3$  and  $M_2ZrO_3$  (Titanates and Zirconates)," Zh. Fiz. Khim. 39 (11), 2763-65 (1965) (trans.) Russian J. Phys. Chem., 39 (11), 1475-76 (1965).
32. C. E. Johnson and I. Johnson, p. 5.2 in Reactor Development Program Progress Report, ANL-RDP-33 (October 1974).
33. R. C. Feber, Thermodynamic Data for Selected Gas Impurities in the Primary Coolant of High-Temperature Gas-Cooled Reactors, LA-NUREG-6635 (April 1977).

34. J. C. Bailar, Jr., Comprehensive Inorganic Chemistry, vol. 3, pp. 433-35, Pergamon, New York, 1973.
35. A. Bergman, Z. Anorg. Allg. Chem. 231, 268-80 (1937).
36. S. P. Berardinelli, Sr., and D. L. Kraus, "Thermal Decomposition of the Higher Oxides of Cesium in the Temperature Range 320-500°C," Prog. Inorg. Chem. 13(1), 189-91 (1973).
37. D. R. Olander, Fundamental Aspects of Nuclear Reactor Fuel Elements, TID-26711-P1 (1976), pp. 176-81.
38. O. Maisch, Z. Anorg. Allg. Chem. 96, 186 (1916).
39. C. W. Robert (ed.), Handbook of Chemistry and Physics, 55th Ed., p. D-162, CRC Press (1974),
40. R. Hultgren et al., Selected Values of the Thermodynamic Properties of Binary Alloys, American Society for Metals, pp. 314-16 (1973).
41. R. R. Biederman, W. G. Dobson, and J. K. Jones, A Study of Zircaloy-Steam Oxidation Reaction Kinetics, First Interim Progress Report July 1, 1976 through October 15, 1976, Project No. 249-2, Electric Power Research Institute.
42. J. V. Cathcart et al., Zirconium Metal-Water Oxidation Kinetics IV. Reaction Rate Studies, ORNL/NUREG-17 (August 1977).
43. R. A. Lorenz, D. O. Hobson, and G. W. Parker, Final Report on the First Fuel Rod Failure Transient Test of a Zircaloy-Clad Fuel Rod Cluster in TREAT, ORNL-4635 (March 1971).
44. R. A. Lorenz and G. W. Parker, Final Report on the Second Fuel Rod Failure Transient Test of a Zircaloy-Clad Fuel Rod Cluster in TREAT, ORNL-4710 (January 1972).
45. R. A. Lorenz and G. W. Parker, "The Dynamics and Prevention of Fuel Rod Swelling During a LOCA," Trans. Am. Nucl. Soc. 14(1), 142-43 (1971).

46. R. E. Westerman and G. M. Hesson, Zircaloy Cladding ID/OD Oxidation Studies, EPRI-N-525 (November 1977).
47. A. A. Bauer, W. J. Gallagher, Evaluating Strength and Ductility of Irradiated Zircaloy, Task 5, Quarterly Progress Report October Through December 1977, NUREG/CR-0026, BMI-1992 (January 1978).
48. J. H. Davies, F. T. Frybendo, and M. G. Adamson, "Determination of the Chemical Activity of Fission Product Iodine in Zircaloy Clad  $UO_2$  Fuel Rods," J. Nucl. Mater. 80, 366-70 (1979).
49. T. C. Rowland,  $UO_2$  Irradiation for ORNL Final Report, GEAP-5642 (June 1968), p. 178.

NUREG/CR-0722  
 ORNL/NUREG/TM-287/R2  
 Dist. Category R3

## INTERNAL DISTRIBUTION

- |        |                   |        |                               |
|--------|-------------------|--------|-------------------------------|
| 1.     | T. M. Besmann     | 33.    | M. F. Osborne                 |
| 2.     | W. D. Burch       | 34.    | G. W. Parker                  |
| 3.     | D. O. Campbell    | 35.    | W. A. Pryor                   |
| 4-5.   | J. L. Collins     | 36.    | J. H. Shaffer                 |
| 6.     | W. Davis, Jr.     | 37.    | L. B. Shappert                |
| 7.     | F. F. Dyer        | 38.    | R. G. Stacy                   |
| 8.     | C. L. Fitzgerald  | 39.    | O. K. Tallent                 |
| 9.     | M. H. Fontana     | 40.    | V. C. A. Vaughen              |
| 10.    | J. H. Goode       | 41.    | B. L. Vondra                  |
| 11.    | V. A. Jacobs      | 42.    | S. K. Whatley                 |
| 12.    | G. H. Jenks       | 43.    | R. P. Wichner                 |
| 13.    | O. L. Kirkland    | 44-45. | Central Research Library      |
| 14.    | C. E. Lamb        | 46.    | Document Reference Section    |
| 15.    | T. B. Lindemer    | 47-48. | Laboratory Records Department |
| 16-23. | R. A. Lorenz      | 49.    | Laboratory Records (RC)       |
| 24-30. | A. P. Malinauskas | 50.    | ORNL Patent Section           |
| 31.    | J. R. Marshall    |        |                               |
| 32.    | F. R. Mynatt      |        |                               |

## EXTERNAL DISTRIBUTION

51. Office of Assistant Manager, Energy Research and Development, DOE, ORO
- 52-53. Director, Division of Reactor Safety Research, Nuclear Regulatory Commission, Washington, DC 20555
- 54-80. Special Nuclear Regulatory Commission distribution
- 81-82. Technical Information Center, Oak Ridge
- 83-457. Given distribution as shown in Category R3